UNCLASSIFIED

AD **408 668**

DEFENSE DOCUMENTATION CENTER

FOR

SCIENTIFIC AND TECHNICAL INFORMATION

CAMERON STATION, ALEXANDRIA, VIRGINIA

UNCLASSIFIED

408 668

U. S.   A R M Y
TRANSPORTATION RESEARCH COMMAND
FORT EUSTIS, VIRGINIA

TRECOM TECHNICAL REPORT 63-9

THEORETICAL INVESTIGATION OF THE FLUTTER CHARACTERISTICS OF A JET-FLAP HELICOPTER ROTOR IN HOVERING AND FORWARD FLIGHT

Task 1D121401A14303
(Formerly Task 9R38-13-014-03)

Contract DA 44-177-TC-699

April 1963

prepared by:

CORNELL AERONAUTICAL LABORATORY, INC.
Buffalo 21, New York

DISCLAIMER NOTICE

HEADQUARTERS

U. S. ARMY TRANSPORTATION RESEARCH COMMAND

Fort Eustis, Virginia

This report has been reviewed by the U. S. Army Transportation Research Command and is considered to be technically sound. The report is published for the exchange of information and the stimulation of ideas.

FOR THE COMMANDER:

KENNETH B. ABEL
Captain   TC
Adjutant

APPROVED BY:

JOHN E. YEATES
USATRECOM Project Engineer

Task 1D121401A14303
(Formerly Task 9R38-13-014-03)
Contract DA 44-177-TC-699
April 1963

THEORETICAL INVESTIGATION OF THE
FLUTTER CHARACTERISTICS OF A JET-FLAP
HELICOPTER ROTOR IN HOVERING AND FORWARD FLIGHT

TRECOM TECHNICAL REPORT 63-9

CAL REPORT BB-1493-S-2

Prepared by
Cornell Aeronautical Laboratory, Inc.
Buffalo 21, New York

for
U. S. ARMY TRANSPORTATION RESEARCH COMMAND
FORT EUSTIS, VIRGINIA

FOREWORD

The work described in this report was accomplished by the Cornell
Aeronautical Laboratory, Inc. (CAL), Buffalo, New York for the
U. S. Army Transportation Research Command (USATRECOM),
Fort Eustis, Virginia under Contract No. DA 44-177-TC-699, Task
9R38-13-014-03, "Jet-Flap Rotor Investigations". Messrs. Andrew
R. Trenka and Richard P. White, Jr. of CAL conducted the study,
and Mr. John E. Yeates administrated the project for USATRECOM.
The work was performed during the period November 1961 to
November 1962.

Appreciation is extended by the authors to Mr. Frank A. DuWaldt of
Cornell Aeronautical Laboratory, Inc. for the significant contributions
he made to the investigation. The authors also wish to thank the U. S.
Army Transportation Research Command and the Giravions-Dorand
Company of Paris, France for their cooperation in helping to establish
the physical characteristics of a suitable jet-flap rotor system for use
in the present investigation.

The work reported herein is a continuation of the initial effort under
Contract No. DA 44-177-TC-699 that was reported in TCREC Technical
Report 61-142, "Theoretical Investigation of the Flutter Characteristics
of a Jet-Flap Rotor System in Hovering Flight", November 1961.

TABLE OF CONTENTS

ILLUSTRATIONS

SYMBOLS

C_B Blade Chord on Nontapered Section - ft.

C_f Chord of Control Flap - ft.

C_t Blade Tip Chord - ft.

$\overline{C}_J$ Blowing Coefficient at Blade Tip - Nondimensional

$(CG)_o$ Center-of-gravity Position Over Outer 30% of Blade
Radius - Percent of Chord

$(CG)_R$ Center-of-gravity Position Over Constant Chord Section

$(EA)_R$ Elastic Axis Position Over Constant Chord Section

$(EA)_o$ Elastic Axis Position Over Outer 30% of Blade
Radius - Percent of Chord

g_i Structural Damping Coefficient for i^{th} Degree-of-freedom

m Mass Per Unit Length - Slugs/ft.

U Local Free Stream Velocity - ft/sec.

$\Delta\overline{u}$ Nondimensional Teeter Pin Displacement in X-Direction - ft.

$\Delta\overline{v}$ Nondimensional Teeter Pin Displacement in Y-Direction - ft.

R	Blade Radius - ft.
β_1	Steady-State Flapping Angle - Radians
$\Delta\beta_1$	Perturbation Flapping Angle - Radians
$\Delta\beta_2$	Perturbation Teetering Angle - Radians
δ_V	Vertical Offset of Blade Below the Teetering Axis - ft.
δ_h	Horizontal Offset of the Flapping Hinge from the Axis of Rotation - ft.
ν	Ratio of Flutter Frequency to Rotational Speed, $\dfrac{\omega}{\Omega}$ - Nondimensional
Ω	Rotational Speed - Cycles/sec.
$\overline{\Omega}$	Nondimensionalized Rotor Speed
Ω_0	Rotational Speed of Rotor at Zero Advance Ratio, cps.
ω_f	Flutter Frequency - Cycles/sec.
ω_{β_2}	Natural Frequency of the Teetering Mode - Cycles/sec.
$\overline{\omega}_{\theta_1}$	Nonrotating Torsional Frequency - Cycles/sec.
$\overline{\omega}_{\varphi_1}$	Nonrotating First Bending Frequency - Cycles/sec.

γ Viscous Damping in Control Flap Mode

$\bar{\omega}_{\varphi_2}$ Nonrotating Second Bending Frequency - Cycles/sec.

$\bar{\omega}_{\tau}$ Nonrotating Frequency of Jet-Flap Control - Cycles/sec.

$\Delta\phi_N$ Perturbation Bending Deflection at Blade Tip for n^{th} Mode - ft.

$\Delta\theta_1$ Perturbation Torsional Deflection at Blade Tip for First Mode - Radians

$\Delta\tau$ Perturbation Rotation Angle of Jet-Flap with Respect to Blade Chord Line - Radians

θ_1 Steady-State Torsional Deflection - Radians

τ Steady-State Rotation Angle of Jet-Flap with Respect to Blade Chord Line - Radians

$\bar{\mu}$ Advance Ratio - $= \dfrac{U \cos \alpha_0}{R\Omega}$

x

SUMMARY

The purpose of the theoretical study reported herein was to investigate the aeroelastic characteristics of a jet-flap rotor system in hovering and forward flight. The jet-flap rotor configuration assumed for this study incorporated most of the general characteristics of an experimental jet-flap rotor being developed for USATRECOM by the Giravions-Dorand Company of Paris, France. On the basis of the investigation that was conducted and within the range of operating conditions and parameters considered, the following general conclusions were drawn regarding the aeroelastic characteristics of a jet-flap rotor system in hovering and forward flight.

1. The critical rotor speed associated with the symmetric flutter modes calculated on the basis of the flapping, first flapwise bending, torsion and control flap rotational degrees of freedom was sensitive to changes in the control flap to torsional frequency ratio, blade center-of-gravity position, jet blowing and control flap damping, but was not sensitive to control flap center-of-gravity position located on the control flap chord.

2. The critical rotor speed associated with the antisymmetric flutter modes calculated on the basis of the flapping, first flapwise bending, torsion and teetering degrees of freedom was markedly insensitive to changes in the bending to torsion frequency ratio, blade center-of-gravity position, jet blowing and steady-state jet deflection angle. The addition of the swivel degree of freedom to the antisymmetric flutter modes is markedly destabilizing.

3. In the symmetric modes, the effect of increasing advance ratio is destabilizing. The advance ratio at which destabilization begins and the rate of destabilization with advance ratio are dependent upon control-flap center-of-gravity position, rotor blade center-of-gravity position and the ratio of control flap rotation frequency to blade torsional frequency.

CONCLUSIONS

On the basis of the results obtained and within the range of operating conditions and parameters considered, the following conclusions can be drawn regarding the general aeroelastic characteristics of jet-flap rotor systems in hovering and forward flight.

1. Increasing the ratio of the control flap to torsion frequency ratio is always stabilizing for $\overline{\omega}_\tau/\overline{\omega}_\theta > 0.80$, but the stabilization is dependent upon the blowing coefficient for $\overline{\omega}_\tau/\overline{\omega}_\theta < 0.80$.

2. Aft movement of the blade center-of-gravity position is stabilizing over the range of positions investigated (28% to 38%).

3. In hovering flight, for control flap center-of-gravity positions within the limits of the control flap chord, the critical rotor speed is essentially independent of the center-of-gravity position of the control flap.

4. Mass overbalancing of the control flap can cause a significant increase in the critical rotor speed.

5. The effect of increasing advance ratio on the symmetric mode instabilities is destabilizing. The advance ratio at which destabilization starts to occur and the rate of destabilization with advance ratio are dependent upon control flap center-of-gravity position and control flap rotation frequency to blade torsional frequency.

3

6. The addition of viscous damping in the control flap increases the critical rotor speed at all advance ratios for the range of viscous damping and advance ratios investigated.

7. The instability caused by the symmetric degrees of freedom was found to be primarily torsion-control flap, with flapping, first bending, and higher bending modes having little effect on the flutter mode.

8. The effect of replacing the control flap degree of freedom by the teetering degree of freedom is to cause an antisymmetric flutter mode to occur at a constant value of $\overline{\omega}_{\phi_1}/\Omega$ for all values of $\overline{\omega}_\theta/\overline{\omega}_{\phi_1} > 3.0$.

9. The addition of the swivel degree of freedom to the antisymmetric flutter mode was destabilizing, causing the critical rotor speed to be reduced by approximately 30%.

10. The critical asymmetric flutter boundaries are not sensitive to changes in the center-of-gravity position.

11. A decrease of the vertical offset of the flapping hinge has a stabilizing effect on the asymmetric flutter boundaries.

12. The steady-state deflection angle of the control flap is not a significant parameter of the asymmetric flutter boundary.

13. An increase in jet blowing is destabilizing in the symmetric degrees of freedom but has little or no effect in the asymmetric degree of freedom.

RECOMMENDATIONS

Based on the results that have been obtained during the present investigation, the following recommendations are made:

1. Experimental data should be obtained to test the validity of the oscillatory aerodynamic theories that have been developed.

2. The effects of advance ratio on the aeroelastic characteristics of a jet-flap rotor should be investigated for advance ratios up to 1.0.

3. The effects of advance ratio and control flap on the asymmetric flutter modes should be investigated.

INTRODUCTION

Recently there has been much interest in the development of a helicopter rotor system that applies the jet-flap principle to obtain both cyclic and collective pitch control as well as to provide propulsion (References 1, 2). This interest derives from the gains in performance that may be obtainable through circulation and boundary layer control. In addition, a jet-flap rotor system should delay the adverse effects of blade stall and compressibility losses and provide the many advantages of torque transmission that are inherent in all tip-drive systems. Considerable effort has been applied to the theoretical and experimental study of the flutter of conventional helicopter rotors in hovering flight (e. g., References 3 - 10). These investigations have contributed to the understanding of the blade instabilities that have been encountered and have indicated means for avoiding such difficulties.

In contrast, comparatively little work has been done to determine the effects of forward velocity on rotor flutter. References 11 - 17 present the results of some investigations of the effects of forward velocity on the aeroelastic characteristics of unconventional rotor configurations. References 18 and 19 present the results of a systematic program of combined theoretical and experimental investigations of the effects of forward flight on the aeroelastic characteristics of rotor blades having pitching and flapping degrees of freedom. The results obtained indicate that forward flight can have a serious destabilizing effect on the aeroelastic characteristics of a conventional rotor.

Introduction of the jet-flap to a rotor increases the complexity of the theoretical representation of the flutter problem over that associated with a conventional rotor in that the aerodynamic loads arising from the

jet reaction and supercirculation must also be included. The dynamic interactions of these additional aerodynamic forces with the mass and elastic forces may be different from those associated with the aerodynamic forces of a conventional rotor.

The hovering flutter characteristics of a representative jet-flap rotor having flapping, teetering, bending and torsional degrees of freedom were investigated and discussed in Reference 20. The effects of the chordwise center-of-gravity and elastic-axis position, bending-to-torsion frequency ratio, and the jet-blowing coefficient on the aeroelastic characteristic of the rotor system were determined. In the present investigation, the effect of the dynamic characteristics of the oscillatory control flap on the aeroelastic stability of basically the same representative rotor system was investigated theoretically in both hovering and forward flight. In addition, the control flap degree of freedom was replaced by a weakly restrained swivel degree of freedom and the effects on the aeroelastic characteristics of the rotor system were investigated for the hovering flight condition only.

DESCRIPTION OF THE ROTOR SYSTEM ANALYZED

General Characteristics of the Rotor System

The jet-flap rotor system considered corresponds to one that is under development for the United States Army. The rotor is a two-bladed symmetrical rotor having a teetering hinge on the axis of the rotation and flapping hinges which are symmetrically offset from the axis of rotation and lie beneath the teetering hinge. In addition, the teetering hinge is allowed a restrained swivel motion in the plane of the rotor.

The cyclic and collective pitch control, as well as the rotor torque, are supplied by the jet-flap located over the outer portion of the blade span. It was assumed that the characteristics of the blowing are such that the jet momentum per unit span is constant.

Geometric Characteristics of the Rotor System

Figure 1 presents a sketch of the rotor system that was analyzed. The blade planform had a constant chord from 40% R to 70% R and was tapered in a linear manner to a tip chord of 67.3% of the main blade chord. The chord was also linearly tapered to the root section. The jet-flap was located at the trailing edge over the tapered outer 30% of the blade radius. A "conventional-type" flap over which the jet exhausted was used to deflect the jet with respect to the airfoil. The "conventional-type" flap had a constant chord equal to 12.3% of the blade tip chord and extended from the 70% radius station to the blade tip. For all the investigations reported herein, the elastic axis was a straight line from the blade root to tip and was located at 30% of the blade chord of the untapered portion (40% to 70% radius).

Vibration Characteristics of the Rotor System

On the basis of mass-elastic data calculated for an experimental jet-flap rotor system under development, a set of nonrotating and rotating flapwise bending and torsional mode shapes and frequencies was calculated by the method presented in Reference 21. These mode shapes were used as the deformation modes in the flutter analysis reported herein. Figure 2 shows the variation of the various mode frequencies with rotational speed. Both the rotational speed and mode frequencies have been nondimensionalized with respect to the normal operating rotational speed. It is noted that the nonrotating frequencies of both the bending and torsional modes are much higher than those of the conventional helicopter blade and, therefore, the variation of the various bending and torsional mode frequencies with rotational speed is not as pronounced. It is believed that the primary reason for these different vibratory characteristics is due to the structural efficiency of the assumed jet-flap blade. Since any jet-flap type of rotor blade might be expected to have a similar type of construction, it is reasonable that relatively rigid rotor blades might be an inherent characteristic of jet-flap rotor system.

METHOD OF ANALYSIS

Equation of Motion

The general equations of motion for helicopter rotor configurations, as
derived by a Lagrangian approach, were developed and reported in Refer-
ence 22. These general equations of motion were then used to develop
specific equations of motion for the jet-flap rotor having flapping, bending,
torsion, teetering, swivel and control-flap degrees of freedom. A detailed
presentation of the equations of motion for the jet-flap rotor is given in
Appendix I, as well as expressions for the aerodynamic and mass coefficients.
Figure 3 presents a schematic representation of the rotor system on which
are noted the coordinate system, which rotates with the rotor, and the
generalized coordinates for the various degrees of freedom.

Derivation of Theoretical Expressions for the Aerodynamic Forces and Moments

The investigations reported herein required the use of aerodynamic theories
suitable for describing the oscillatory aerodynamic forces and moments on
the airfoil arising from three sources. The first source was the oscillating
airfoil with a jet-flap fixed relative to the airfoil chord. The second was
oscillations of the jet-flap relative to the airfoil chord and, finally, the
oscillations of the mechanical flap.

At present there is no theory available which predicts the unsteady aero-
dynamic forces and moments on a rotor with a jet-flap comparable in
accuracy to the theory developed for conventional airfoils and rotors. It
was thus necessary to utilize a quasi-steady representation of the flow for

the derivation of the periodic aerodynamic forces and moments developed on the blade as it oscillates. Some justification for the use of such an approximation is obtained from the following considerations. It is anticipated that the inflow velocity, and hence the wake spacing, of a jet-flap rotor will be large. For large wake spacing, the aerodynamic forces on the rotor blade, at least under a strip theory approximation, approach those on an isolated airfoil (Reference 22). It has been found in previous investigations of the flutter characteristic of conventional rotor systems at CAL that, when this condition exists, the critical flutter mode can be adequately predicted by means of a quasi-steady approximation of the periodic aerodynamic forces and moments.

This justification for the use of a quasi-steady approach must be qualified, however, by noting that an implied assumption has been made in the above argument; namely, that the unsteady forces and moments on conventional and jet-flap airfoils will vary in a similar manner. This assumption has not as yet been verified.

For the analyses reported herein, the quasi-steady aerodynamic forces and moments were derived for the jet-flap airfoil using the steady aero-dynamic theory developed by Spence (Reference 23) and extended by Hough (Reference 24) to include the effects of camber. Appendix II presents the derivation of the aerodynamic expression used. It was necessary to use the results for a cambered airfoil so that the effect of pitching rate, which gives rise under the quasi-steady assumption to an effective camber, could be included.

The oscillatory forces and moments on the rotor blade due to the sinu-soidal oscillation of the jet-flap were those developed by Spence (Reference 25). Due to the complex formulation of the expressions for the oscillatory

aerodynamics, Spence could not obtain a general solution. On the basis of some simplifying approximations, however, Spence did obtain solutions for the cases of high and low reduced frequencies. The approximate aerodynamic expressions valid for low reduced frequencies have been utilized in the analyses reported herein.

The oscillatory aerodynamics on the rotor blade associated with oscillation of the mechanical flap were based on Theodorsen's formulation in Reference 26.

PRESENTATION AND DISCUSSION OF RESULTS

In the following sections, the aeroelastic stability characteristics of a jet-flap rotor in both hovering and forward flight are presented. The majority of the investigations were conducted for the rotor having the symmetric degrees of freedom of flapping, first-flapwise bending, torsion and control-flap rotation. The investigation of the stability characteristics of the rotor having these symmetric degrees of freedom was conducted on an analog computer for both the hovering and translatory flight conditions. The aeroelastic characteristics of the rotor having flapping, torsion, first-flapwise bending, teetering and swiveling as degrees of freedom were asymmetric in character and were investigated for the hovering flight condition by means of a digital computing program on an IBM 704.

In general, the instabilities that were determined for the symmetric modes during the analog computer program were "mild" in character in that rapidly divergent motion did not occur as the stability boundary was crossed. Conversely, the rate of convergence in the stable region increased slowly as the operating conditions were changed from neutrally stable to more stable regimes.

The symmetric clutter mode in most cases was primarily composed of the blade torsional and control-flap rotational degrees of freedom, with the flapping and first-flapwise bending modes playing only secondary roles. The critical asymmetric flutter modes were comprised primarily of the torsion and teetering degrees of freedom, with the rest of the modes having only a minor effect. Some of the supercritical asymmetric flutter modes (those which occur at rotor speeds above the critical), however, involved, to a significant extent, the flapping, first-flapwise bending and swiveling modes as well.

In the following, the symmetric and asymmetric flutter results are pre-
sented and discussed independently for reasons of clarity. Most of the
analyses of the symmetric and asymmetric flutter modes were based on
a blowing coefficient $\overline{C_J}$ = 1.0, and the effect on these modes of changing
the blowing coefficient was determined for only one set of representative
parameters.

Symmetric Flutter Modes

1. Effect of the Rotor Blade Center-of-Gravity Position

   a. Hovering Flight; $\overline{\mu}$ = 0

   The results shown in Figure 4 are extremely interesting in that
they indicate that, at least in hovering flight, the effect of a variation in
the chordwise center-of-gravity position is just opposite to that for a
conventional rotor blade. That is, an aft movement of the center-of-
gravity position is stabilizing for the jet-flap rotor system analyzed,
whereas it is usually destabilizing for a conventional rotor system.

   These opposite trends are believed to be the result of the unusual
combination of the spanwise center-of-gravity distribution in relation to
the spanwise distribution of the first-flapwise bending and torsional mode
shapes.

   It can be shown, on the basis of investigations of the aeroelastic
characteristics of conventional wings, that the distance between the center
of pressure and center of gravity is a prime stability parameter of the
system. An increase in this distance has been shown to be destabilizing
and a decrease in the distance, stabilizing (Reference 27). Generally,

flutter is not obtained for a conventional airfoil when the center-of-gravity and center-of-pressure positions are coincident. For small changes in the distance between the center-of-gravity and center-of-pressure positions, when they are nearly coincident, very large changes in the velocity of the instability occur.

For three-dimensional wings which have a spanwise variation of their mass and elastic properties, the distribution of center-of-gravity position is replaced by its effective position which reflects the effects of the spanwise mass distribution and the deformation modes. This effective center-of-gravity position is determined from the mass term that couples the bending and torsional mode shape and is given by the following expression:

$$\int \overline{m} \, \overline{c}_x \, f_{\phi_1} \, f_\theta \, d\xi$$

where

$\overline{m}$ = spanwise mass distribution

$\overline{c}_x$ = nondimensional distance of the sectional center of gravity from the elastic axis (positive aft)

f_{ϕ_1} = spanwise distribution of the first flapwise bending mode

f_θ = spanwise distribution of the first torsional mode

A positive value of this coupling term corresponds to an effective aft location of the center of gravity relative to the elastic axis and a negative value corresponds to an effective nose-heavy ballast condition. Over the inboard sections of the rotor blade where $\overline{c}_x$ is positive, the torsional mode shape is also positive but the first flapwise bending mode has a negative deflection. The integrated mass coupling for the inboard section of the blade, therefore, is negative. Over the outboard sections of the blade where both the bending and torsional mode shapes have a positive deflection,

the $\bar{C}_\chi$ is still positive but smaller due to the ballast weight distribution. The integrated mass coupling for the outboard section of the blade is thus positive. The contribution of the inboard blade section, however, is larger than that of the outboard section and, thus, the effective mass center of the entire blade is forward of the elastic axis for all the center-of-gravity positions that were investigated. For the reference center-of-gravity position at the 33% chord, the effective mass center of the blade is at the 29.5% chord. Due to the dominant roll of the mass coupling over the inboard sections of the blade, an aft movement of the spanwise mass distribution from the 33% chord results in a larger negative coupling term and, thus, shifts the effective mass center forward. This forward shift of the mass center with an aft movement of the center of gravity reduces the distance between the effective mass center and the center of pressure, which is located at approximately the 24% chord. On the basis of the results obtained with wings, therefore, the stabilizing effect that was obtained on the rotor blade due to the shift of the mass distribution is not surprising.

In Reference 20, the symmetric flutter characteristics of essentially the same rotor system were presented and the effect of an aft center-of-gravity movement was stated to be destabilizing. While this seems to contradict the present findings, it, in fact, does not, since in Reference 20 the center of gravity of only the outboard sections was moved aft, thus causing an aft movement of the effective mass center.

b.   Forward Flight; $\bar{\mu} \neq 0$

Figure 5 shows the effect of advance ratio on the aeroelastic stability of the jet-flap rotor for various values of the blade center-of-gravity position. The curve for each center-of-gravity position has been normalized to its value at $\bar{\mu} = 0$. For a center-of-gravity position aft of the elastic

axis, the effect of advance ratio was destabilizing above an advance ratio of approximately 0.25. For a center-of-gravity position ahead of the elastic axis, the destabilizing effect of advance ratio was present throughout the entire range of advance ratios investigated. The amount and rate of destabilization with increasing advance ratio were dependent upon the center-of-gravity location.

2. Effect of Control Flap Frequency

a. Hovering Flight; $\bar{\mu} = 0$

Figure 6 presents the results of the investigation that was conducted to determine the effect of varying the rotational frequency of the control flap on the aeroelastic characteristics of the rotor system.

The results that were obtained on the basis of a four-degree-of-freedom analysis, which included the effects of the flapping, first-flapwise bending, torsion, and control flap rotational modes, showed that the critical flutter mode was primarily a torsion-control flap rotation instability. The absence of the bending mode in the instability is understandable, since for the rotor configuration analyzed the effective mass center is almost coincident with the elastic axis position at the 30% chord and, thus, the mass coupling between the bending and torsional modes is almost zero. (See Section 1.) To check this supposition, a two-degree-of-freedom analysis was conducted using only the torsion and control flap rotational modes as degrees of freedom. The results of this analysis duplicated almost exactly the data presented in Figure 6. Based on these results, therefore, the data presented in Figure 6 must be viewed as showing only the effect of the frequency ratio $\bar{\omega}_\tau / \bar{\omega}_\theta$ on the critical rotor speed. The rotor speed, however, has, for the sake of convenience, been nondimensionalized by the nonrotating first-flapwise bending frequency.

Results are presented for two values of the blowing coefficient, $\overline{C}_J$. These values of $\overline{C}_J = 1.0$ and 0.1 are believed to be the practical limits of this parameter for the rotor system under consideration. The results obtained for both values of the blowing coefficient indicate that the effect of increasing the frequency, $\overline{\omega}_\tau$, is destabilizing below some critical value and stabilizing above the critical value. It is noted that the effect of reducing the blowing coefficient $\overline{C}_J$ is stabilizing and that the critical value of the frequency ratio increases to about 0.8 as the blowing coefficient decreases to 0.1.

The frequency ratio $\overline{\omega}_\tau / \overline{\omega}_\theta$ for the rotor system that has been considered in these investigations is approximately one, so that the effect of increasing the rotational frequency of the control flap is stabilizing regardless of the blowing coefficient. The effect of increasing the control flap frequency depends on the blowing coefficient for rotor systems having a frequency ratio $0.4 < \overline{\omega}_\tau / \overline{\omega}_\theta < 0.80$. For a rotor system having a frequency ratio in this range, an increase of the control flap frequency may be stabilizing at a high blowing coefficient and destabilizing at a lower blowing coefficient.

b. **Forward Flight; $\overline{\mu} \neq 0$**

Figure 7 shows the effect of advance ratio on the aeroelastic stability of the rotor for different values of the ratio of control flap rotational frequency to blade torsional frequency. The curves have been normalized by the critical rotor speed at $\overline{\mu} = 0$ for each value of $\overline{\omega}_\tau / \overline{\omega}_\theta$. For a frequency ratio $\overline{\omega}_\tau / \overline{\omega}_\theta$ of approximately unity, the destabilizing effects of advance ratio begin at a $\overline{\mu}$ of approximately 0.25. For frequency ratios greater or less than unity, the plotted results indicate that the destabilizing effects of advance ratio start at an advance ratio of 0.10. About

a 20% decrease in the critical rotor speed has occurred at an advance ratio of 0. 35 for $\overline{\omega}_\tau/\overline{\omega}_\theta$ = 0. 99 and 1. 65, while only a 10% decrease in rotor speed has occurred for $\overline{\omega}_\tau/\overline{\omega}_\theta$ = 0. 62.

3. Effect of Control Flap Center-of-Gravity Position

a. Hovering Flight; $\overline{\mu}$ = 0

In hovering flight, for control flap center-of-gravity positions within the limits of the control flap chord, the stability characteristics of the rotor system were essentially independent of the center-of-gravity position. To determine if center-of-gravity positions outside the limits of the control flap chord would significantly alter the aeroelastic stability characteristics of the rotor system, a large overbalance condition was assumed for the control flap. Figure 8 presents the results of this investigation. The results shown were obtained on an IBM 704 digital computer and are for the case of the control flap having a center-of-gravity position at the elastic axis of the rotor blade. Comparison of these results with those presented in Figure 6 indicates that the large negative overbalance eliminated the instability that was present in the frequency ratio range $0 \le \overline{\omega}_\tau/\overline{\omega}_\theta \le 2$. On a practical basis, this is an unrealistic center-of-gravity position for the control flap; but the results do indicate that if a flutter instability occurs within the operating speed of the rotor, negative overbalancing of the control flap may eliminate the instability. More realistic values of negative overbalances should be investigated to determine the extent of beneficial effects that can reasonably be expected.

b. **Forward Flight;** $\bar{\mu} \neq 0$

Figure 9 shows the effect of advance ratio on the aeroelastic
stability of the jet-flap rotor for various control flap center-of-gravity
positions. Each curve has again been normalized to its value at $\bar{\mu} = 0$.
It is of interest to note that the fully balanced control flap (flap center of
gravity on flap rotation axis) is the flap configuration that is most strongly
affected by advance ratio. In addition, it is noted that the destabilizing
effects of advance ratio begin to occur at lower advance ratios as the control
flap center-of-gravity position moves aft.

4. Effects of Control Flap Damping

Because of the type of construction used in the rotor being considered,
the viscous damping in the control flap degree of freedom was 50% of
critical. Since not all jet-flap control mechanisms for the rotor blades
will necessarily have this amount of damping, it was of interest to determine
the effect of damping on the aeroelastic stability of the rotor system. Figure
10 presents the results of this investigation. The curves have been non-
dimensionalized with respect to the critical rotor speed at $\bar{\mu} = 0$ for
$\gamma = 0.5$. The results indicate that halving the amount of viscous damping
causes a 28% reduction in the critical rotor speed but does not significantly
alter the destabilizing effects of advance ratio. Since other jet-flap rotor
designs may have significantly lower values of viscous damping than those
investigated herein ($\gamma \leq 0.10$) or may have only structural damping, in-
vestigation of the effects of damping in the control-flap degree of freedom
on the rotor stability characteristics should be extended to include a wider
range of both structural and viscous damping coefficients.

The reasons for the various trends with advance ratio that have been presented in Figures 5, 7, and 9 are not understood as yet; therefore, it cannot be stated what the extrapolation of the results to higher advance ratios might indicate. On the basis of results obtained for the effects of advance ratio on a conventional rotor (References 18, 19), the destabilizing effects of advance ratio tend to change for values of advance ratio higher than those for which results are presented herein. Since the jet-flap rotor system has a great potential for a high-speed rotor system, it is felt that the aeroelastic characteristics of the jet-flap rotor system should be investigated for advance ratios up to about 1.0.

Asymmetric Flutter Modes

The antisymmetric flutter modes were calculated for the rotor system having flapping, first-flapwise bending, torsion and teetering degrees of freedom. The results of the investigation, conducted for the hovering flight regime, are given in Figure 11. The antisymmetric flutter characteristics that are presented in Figure 11 are similar to those that were presented in Reference 20 for the same rotor having a slightly different set of geometric, mass and elastic parameters. The interesting aspects of the results that were obtained are that (1) the critical rotor speed is independent of the frequency ratio $\bar{\omega}_\theta / \bar{\omega}_{\phi_1}$ for $\bar{\omega}_\theta / \bar{\omega}_{\phi_1} > 3$, and (2) the critical flutter mode is primarily a torsion-teetering instability having a frequency of about 75% of the first-flapwise bending mode. Since the instability is characterized by extremely large amounts of teetering and torsion as compared to bending, it is not surprising that the critical rotor speed is insensitive to the frequency ratio $\bar{\omega}_\theta / \bar{\omega}_\phi$. The other flutter boundaries that are presented, marked 1 , 2 , 3 , 5 , and 6 , have no real significance since they are supercritical. The effects of parameter changes,

63-9

however, might cause them to become critical. The flutter mode marked 2 is like the critical mode in that it is primarily a torsion-teetering instability. The flutter modes marked 1, 5, and 6 are primarily asymmetric modes made up of all the degrees of freedom. The flutter mode marked 3 is a mode that is closest to a symmetric instability in that it contained only a small amount of teetering and larger relative amounts of flapping and bending.

1. Effect of the Swivel Degree of Freedom on the Antisymmetric Flutter Modes

The addition of the swivel degree of freedom (restrained motion of the teetering axis in the plane of the rotor) on the antisymmetric flutter modes was investigated and the results are presented in Figure 12. As can be seen by comparing Figures 11 and 12, the effect of adding the swivel degree of freedom is markedly destabilizing. The flutter mode marked 2, previously supercritical, was destabilized to such an extent as to make it the critical flutter mode when the swivel degree of freedom is included. It is noted that the characteristics of the critical flutter mode, i.e., the variation of $\bar{\omega}_{\phi_I}/\Omega$ with $\bar{\omega}_{\theta}/\bar{\omega}_{\phi_I}$, is basically the same as it was before the addition of the swivel degree of freedom, but the frequency of the critical mode was almost doubled.

2. Effect of the Center-of-Gravity Position

To determine if the flutter boundaries were sensitive to the center-of-gravity position, the effect on the asymmetric flutter modes of moving the mass center aft was investigated. The results of these calculations are also shown in Figure 12. The open symbols show the results that were calculated with the center-of-gravity position moved 5% of the chord aft of

the position for which the solid curves were calculated. As can be seen, all but one of the boundaries remained unchanged. The boundary that did change, 3, is the mode that had more bending motion in the flutter motion; therefore, changes in the torsion-bending coupling would be expected to have a significant effect on the flutter mode. Since, however, the critical flutter mode was primarily a teetering-torsion instability, a change in the center-of-gravity position would not be expected to affect the stability boundary.

3. Effect of the Vertical Offset of the Flapping Hinge

To determine if the flutter boundaries could be altered significantly by changing the amount of the vertical offset of the flapping hinge from the teetering axis, the amount of this vertical offset was reduced to one-half its original value and the flutter boundaries recalculated. Figure 13 gives the results of these calculations. As can be seen from a comparison of the results plotted in Figures 12 and 13, the effect of reducing the vertical offset of the flapping hinge is stabilizing. The variation of the various flutter boundaries with the frequency ratio $\bar{\omega}_{\theta}/\bar{\omega}_{\phi_1}$, however, was not significantly altered. The rotor speed at which the critical flutter boundary is crossed was increased about 10% by decreasing the offset by 50%. It is expected, however, that as the vertical offset is decreased further, the amount of stabilization obtained would increase in a nonlinear fashion. This trend is to be expected since, if the vertical offset is reduced to zero, the asymmetric modes should disappear as the modal couplings between the teetering and the other normal modes of the rotor system tend to zero. This fact is shown conclusively in Reference 20, which presented results for a similar rotor in which the vertical offset of the flapping hinge was allowed to approach zero.

4. Effect of the Steady-State Control Flap Deflection Angle

In all previous cases discussed, the control flap steady-state deflection was assumed to be zero. Figure 14 shows the results obtained assuming that the steady-state deflection angle of the control flap was 0.5243 radian (30°). Comparison of Figures 12 and 14 shows that the steady-state deflection angle of the control flap does not significantly affect the asymmetric flutter boundaries.

Discussion of Possible Limitations of the Analyses Conducted and Results Obtained

Any theoretical analysis is usually based on a number of assumptions which may or may not alter the results that are obtained. In the present analyses, several rather basic assumptions had to be made in order to analyze the jet-flap rotor system under consideration. Most of these assumptions were made in regard to the oscillatory aerodynamic forces acting on the rotor system. They were:

1. The quasi-steady aerodynamic forces and moments, as based on Hough's development in Reference 24, are adequate for approximating the oscillatory aerodynamic forces and moments generated on the rotor blade during oscillation of the blade (angle of jet deflection fixed relative to blade chord).

2. The low frequency approximation developed by Spence in Reference 25 adequately describes the unsteady aerodynamic forces and moments developed on the rotor blade during oscillation of the jet relative to the blade chord.

3. The oscillatory forces and moments developed on the rotor blade during oscillation of the mechanical flap (used to control the jet deflection) are adequately predicted by Theodorsen in Reference 26.

The first approximation was briefly discussed in a previous section of the report.

It should be noted that the second assumption is consistent with the quasi-steady approximation for the aerodynamic forces and moments generated by blade oscillations. However, because of the high flutter frequencies obtained, both assumptions 1 and 2 may be questionable. It is well known, however, that theories used beyond their theoretical limits can, in many cases, still yield valid results. Whether or not this is the case with the present theory cannot be stated until experimental verification is obtained.

The use of the unsteady aerodynamic theory developed by Theodorsen to predict the aerodynamic forces and moments acting on the rotor blade during oscillation of the mechanical control flap was questioned because of the flow field in the vicinity of the mechanical control flap. The jet blows over the top surface of the control flap, and the pressure gradient produced by the mechanical flap as it is deflected rotates the jet stream relative to the rotor chord. To determine the importance of the mechanical flap aerodynamics to the instabilities being studied, one analysis was conducted in which these aerodynamic forces were neglected entirely. Figure 15 presents the results of this investigation. As can be seen, the inclusion of the unsteady control flap aerodynamics caused about an 11% reduction in the critical rotor speed but did not alter the variation of the critical rotor speed with advance ratio.

In addition to the limitation that might be imposed on the results because of the aerodynamic approximations, the effects of higher order flapwise bending modes on the results should be considered. A brief study was made in which the first bending mode was replaced by the second bending mode. The instability boundaries were affected only slightly. Hence, it was concluded that, since the instability is predominantly a torsion-control flap and since the second mode did not alter the boundaries significantly, the inclusion of the higher modes into the analyses would not radically alter the results presented here. It should be noted, however, that the rotor configuration for which the effects of the higher modes were investigated was that for which the effective mass center was nearly coincident with the elastic axis and, thus, the intermodal mass coupling is almost zero. For configurations that have significant intermodal coupling, the effects of higher order bending modes may be significant.

BIBLIOGRAPHY

1. Dorand, R., Boehler, F. D. "Application of the Jet-Flap Principle to Helicopters" Paper presented before the American Helicopter Society Fifteenth Annual National Forum Washington, D. C. 7-9 May 1959

2. Dorand, R., Tararine, S. "Design Study of the Feasibility of Flying-Crane Type Helicopters Incorporating the Jet-Flap Control System" Giravions-Dorand, Engineering Division for the European Research Office U. S. Department of the Army Report No. 1088 Volumes I and II 30 April 1959

3. DuWaldt, F. A., Gates, C. A., Piziali, R. A. "Investigation of Helicopter Rotor Blade Flutter and Flapwise Bending Response in Hovering" WADC TR-59-403 August 1959

4. Daughaday, H., DuWaldt, F., Gates, C. "Investigation of Helicopter Rotor Flutter and Load Amplification Problems" Journal of the American Helicopter Society, Vol. 2, No. 3 July 1957

5. Daughaday, H. "Flutter Analysis of the H-5 Rotor with a Pitch-Cone Coupling Linkage" Cornell Aeronautical Laboratory Report No. BB-538-S-3 July 1952

6. Brooks, G., Becker, H. "An Experimental Investigation of the Effects of Various Parameters Including Tip Mach Number on the Flutter of Some Model Helicopter Rotor Blades" NACA RM L53D24 June 1953

7. Miller, R., Ellis, C. "Helicopter Blade Vibration and Flutter" Institute of the Aeronautical Sciences Preprint No. 635 January 1956

8. Chan, P. "Pitch-Lag Instability of Helicopter Rotors" Journal of the American Helicopter Society, Vol. 3, No. 3 July 1958

9. Zvara, J. "The Aeroelastic Stability of Helicopter Rotors in Hovering Flight" M.I.T. Aeroelastic and Structures Research Laboratory TR 61-1 September 1956

10. Timan, R., Van de Vooren, A. "Flutter of a Helicopter Rotor Rotating in its Own Wake" Nationaal Luchtvaartlaboratorium Report No. F187 April 1956

11. Brooks, G.W., Sylvester, M. A. "The Effect of Control Stiffness and Forward Speed on the Flutter of a 1/10-Scale Dynamic Model of a Two-Bladed Jet-Driven Helicopter Rotor" NACA TN 3376 April 1955

12. Hohenemser, K. H. "Remarks on the Unloaded Type of Convertiplane" Proceedings of the Eleventh Annual Forum, American Helicopter Society April 1955

13. Hohenemser, K. H. "On a Type of Low-Advance-Ratio Blade Flapping Instability of Three-or-More-Bladed Rotors Without Drag Hinges" Proceedings of the Thirteenth Annual Forum, American Helicopter Society May 1957

14. Hohenemser, K. H., Perisho, C. H. "Analysis of the Vertical Flight Dynamic Characteristics of the Lifting Rotor with Floating Hub and Off-Set Coning Hinges" Journal of the American Helicopter Society, Vol. 3, No. 4 October 1958

15. Chou, P. C. "Pitch Lag-Instability of Helicopter Rotors" Journal of the American Helicopter Society, Vol. 3, No. 3 July 1958

16. McKee, J. W. "Pitch-Lag Instability as Encountered During Tests of a Model Rotor" Institute of the Aeronautical Sciences Preprint No. 807 June 1958

17. Perisho, C. H. "Analysis of the Stability of a Flexible Rotor Blade at High Advance Ratio" Journal of the American Helicopter Society, Vol. 4, No. 2 April 1959

18. DuWaldt, F. A., Gates, C. A., Piziali, R. A. "Investigation of the Flutter of a Model Helicopter Rotor Blade in Forward Flight" WADD TR-60-479 July 1960

19. DuWaldt, F. A., Gates, C. A. "Experimental and Theoretical Investigation of the Flutter Characteristics of a Model Helicopter Rotor Blade in Forward Flight" ASD TR-61-712 February 1962

20. White, R. P., Jr. and Crimi, P. "Theoretical Investigation of the Flutter Characteristics of a Jet-Flap Rotor System in Hovering Flight" Cornell Aeronautical Laboratory Report No. BB-1493-S-1 TCREC TR-61-142 November 1961 Institute of the Aeronautical Sciences Preprint No. 62-35 22-24 January 1962

21. Targoff, W. P.   "The Bending Vibrations of a Twisted Rotating Beam"
    WADC TR-56-27   December 1955

22. Daughaday, H., DuWaldt, F., Gates, C.   "Investigation of Helicopter
    Rotor Flutter and Load Amplification Problems"   Cornell Aeronautical
    Laboratory Report No. SB-862-S-4   August 1956

23. Spence, D. A.   "A Treatment of the Jet-Flap by Thin Aerofoil Theory"
    RAE Report Aero. 2568   November 1955

24. Hough, G. R.   "Cambered Jet-Flap Airfoil Theory"   Master Thesis
    Cornell University   September 1959

25. Spence, D. A.   "The Theory of the Jet-Flap for Unsteady Motion"
    Journal of Fluid Mechanics, Vol. 10, Pt. 2   March 1961   pp. 237-258

26. Theodorsen, T.   "General Theory of Aerodynamic Instability and the
    Mechanism of Flutter"   NACA Report 496   1935

27. Theodorsen, T., Garrick, I. E.   "Mechanism of Flutter —
    A Theoretical and Experimental Investigation of the Flutter Problem"
    NACA Report 685   1940
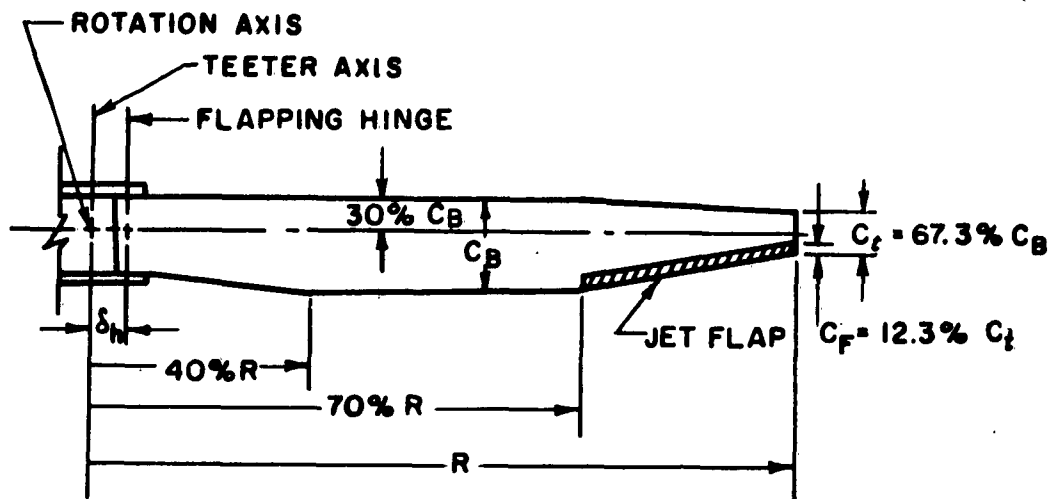
Figure 1 PLANFORM GEOMETRY OF BLADE ANALYZED
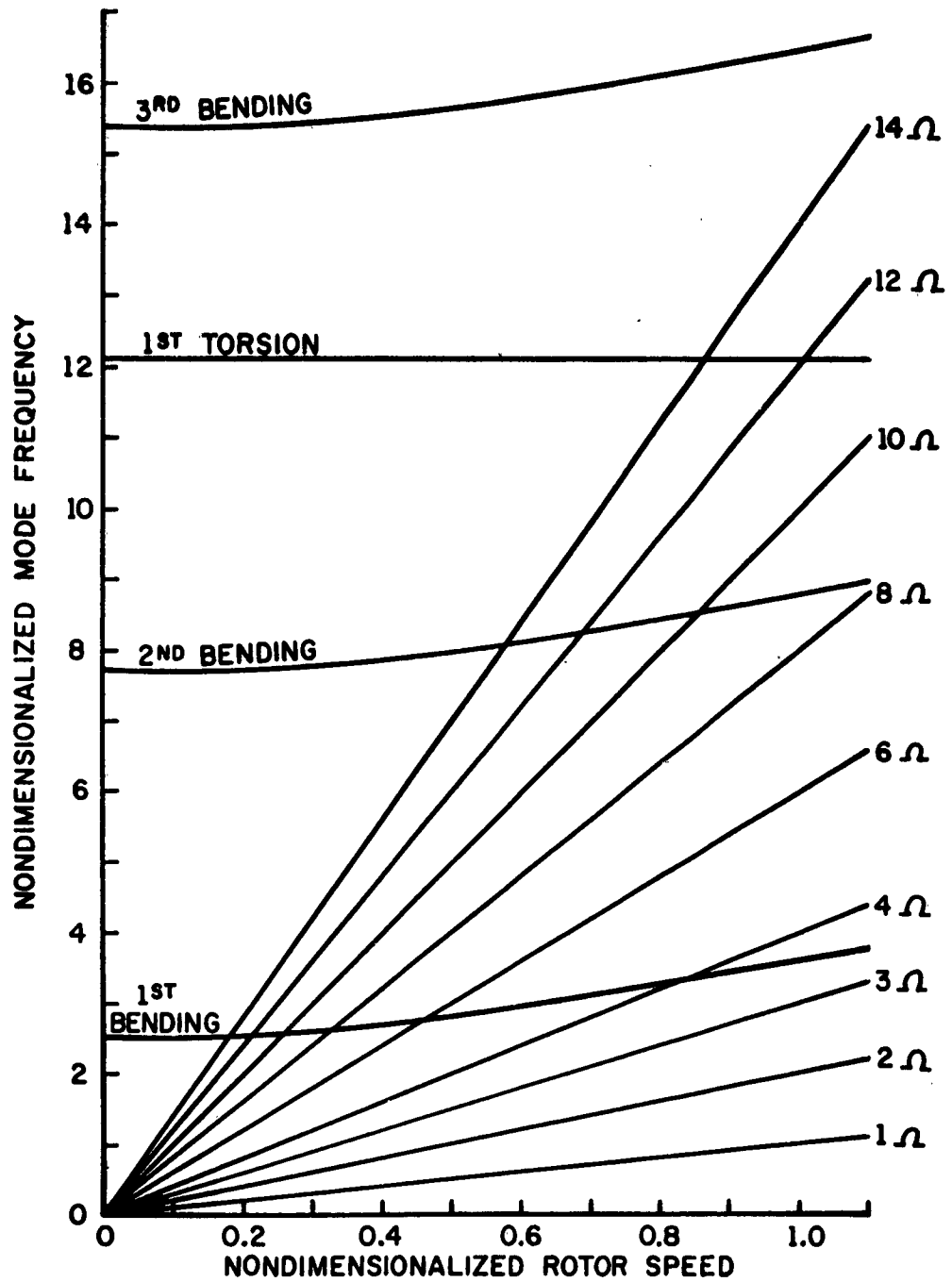
Figure 2 NONDIMENSIONALIZED MODE FREQUENCY
versus NONDIMENSIONALIZED ROTOR SPEED

63-9

SYMBOL		GENERALIZED COORDINATE
$\Delta\beta_1$	—	OSC. FLAPPING
$\Delta\beta_2$	—	OSC. TEETERING
$\Delta\phi_N$	—	OSC. Nth MODE BENDING AT TIP
$\Delta\theta_1$	—	OSC. 1st MODE TORSION AT TIP
$\Delta\tau$	—	OSC. JET-FLAP DEFLECTION
Δu	—	OSC. TEETER PIN DISPLACEMENT IN x-DIRECTION
Δv	—	OSC. TEETER PIN DISPLACEMENT IN y-DIRECTION

$\theta, \beta, \phi \& \tau$ ARE STEADY STATE DEFLECTIONS
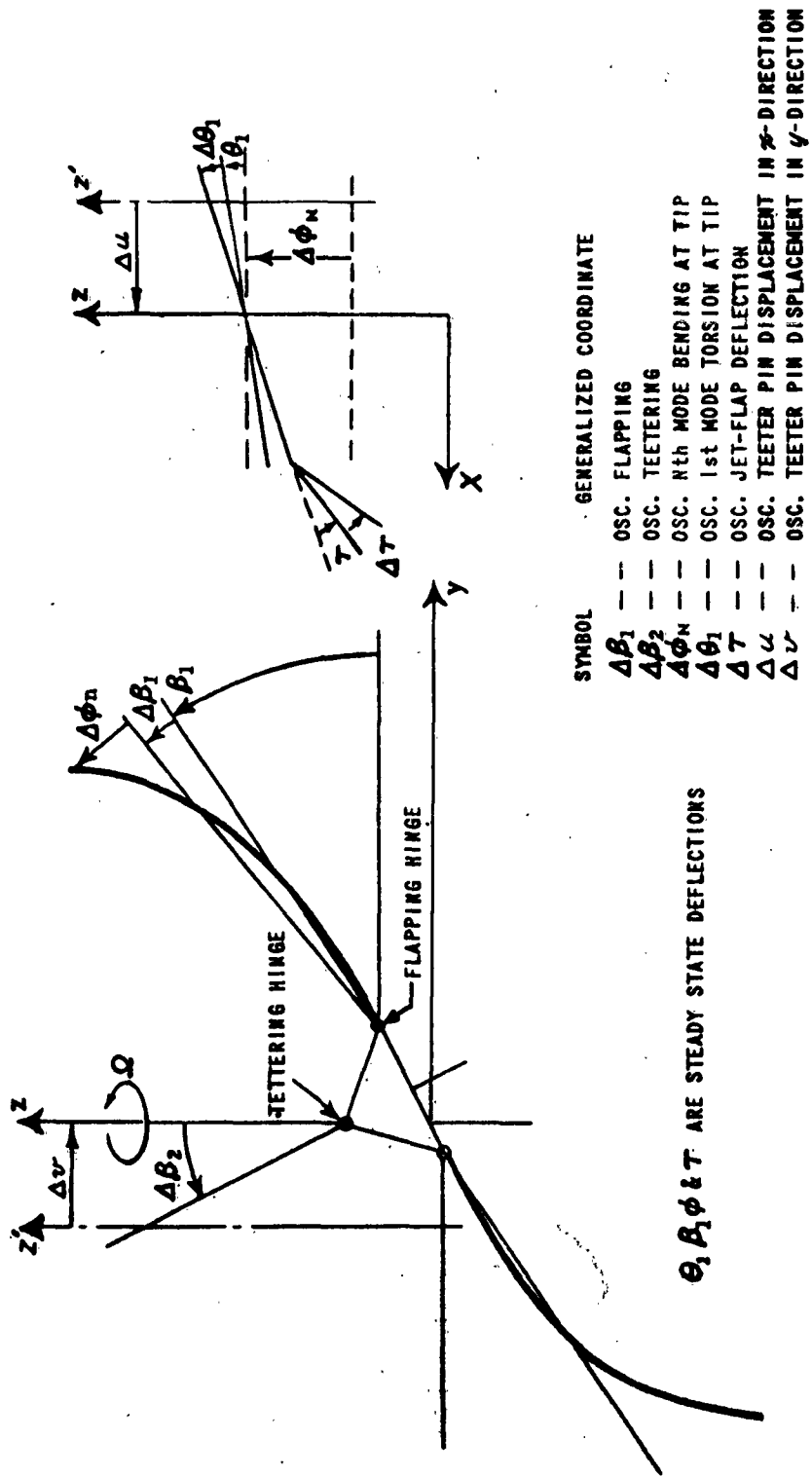
Figure 3   SCHEMATIC REPRESENTATION OF TWO BLADED JET-FLAP ROTOR

33

63-9
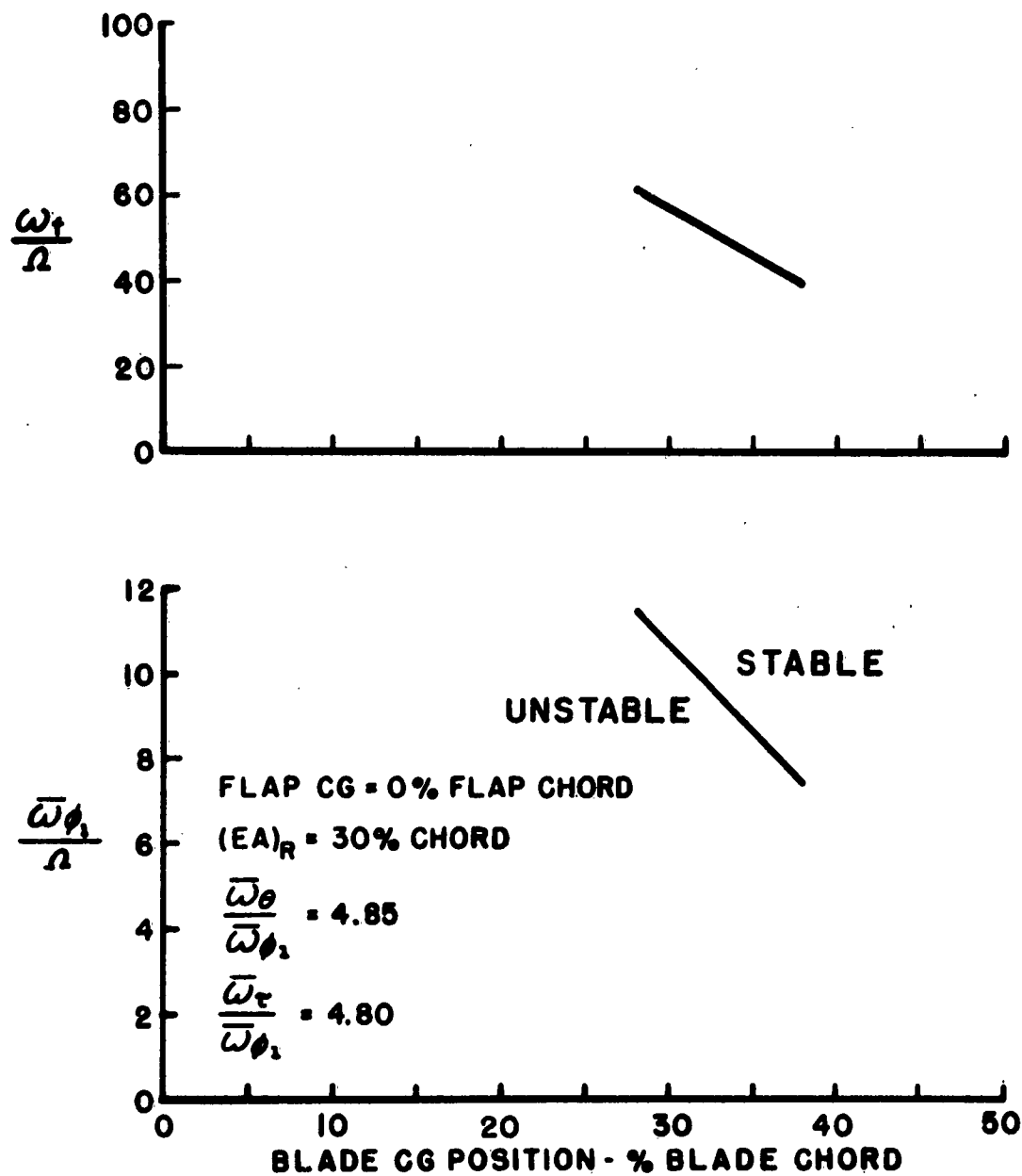
Figure 4 ω_f/Ω AND $\overline{\omega}_{\phi_1}/\Omega$ versus BLADE CG POSITION

34   63-9
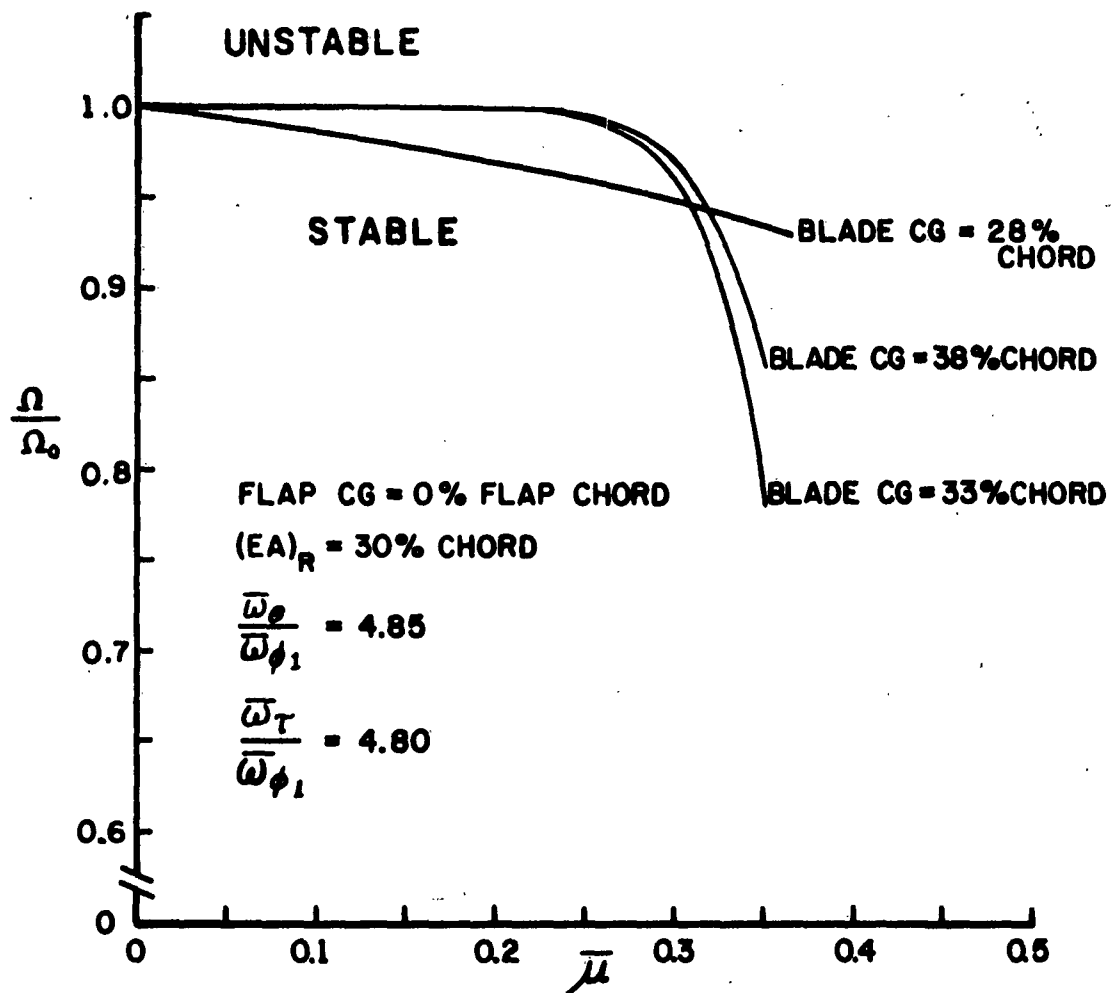
Figure 5 NONDIMENSIONALIZED ROTOR SPEED versus
ADVANCE RATIO FOR VARIOUS BLADE CG POSITIONS

Figure 6 $\dfrac{\omega_{\phi_l}}{\Omega}$ AND $\dfrac{\omega_f}{\Omega}$ versus $\dfrac{\overline{\omega}_\tau}{\overline{\omega}_\theta}$

63-9
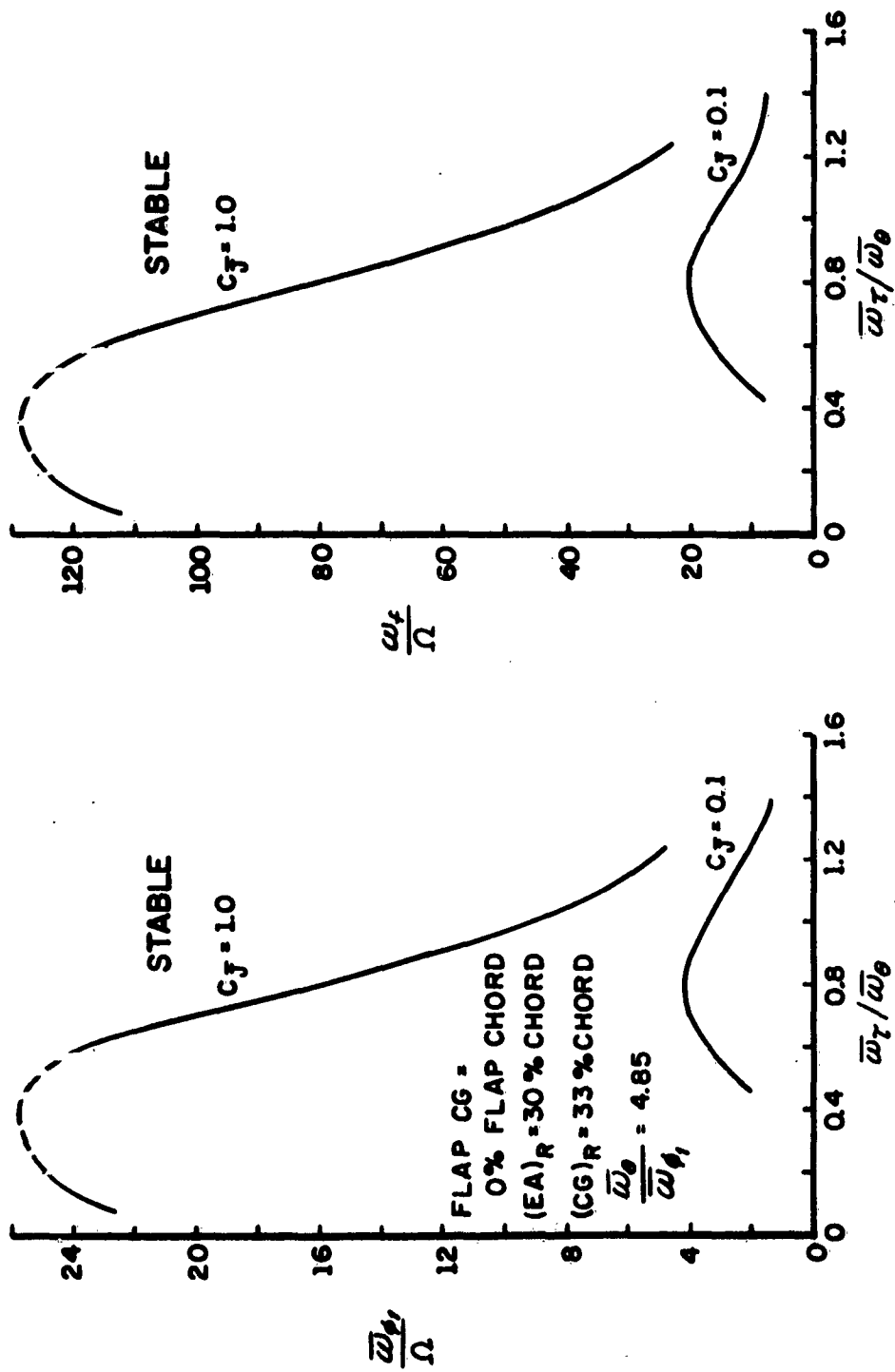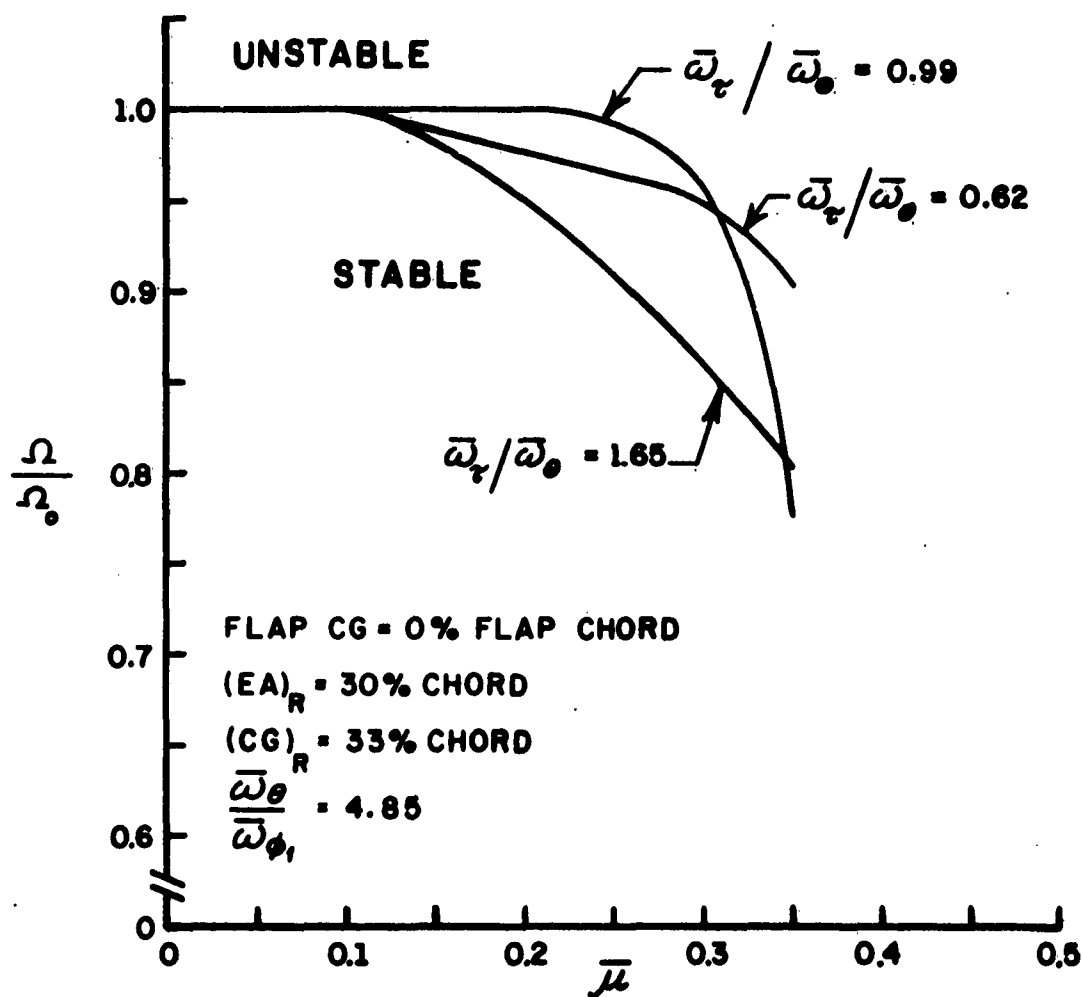
Figure 7 NONDIMENSIONALIZED ROTOR SPEED versus ADVANCE RATIO FOR VARIOUS $\omega_\tau / \bar{\omega}_\theta$
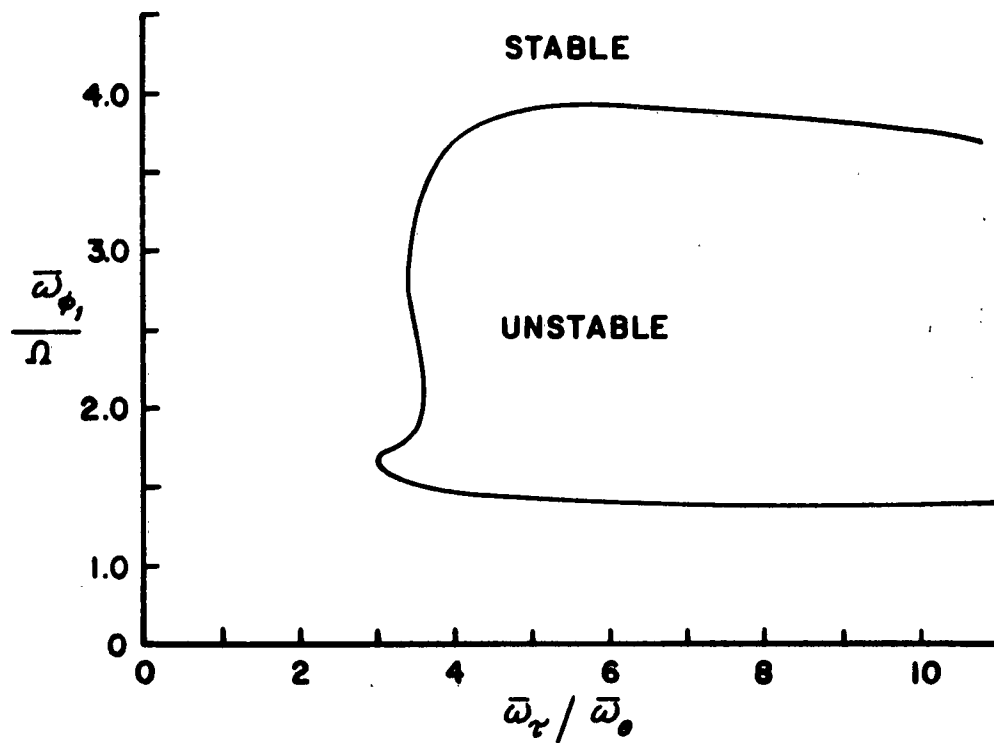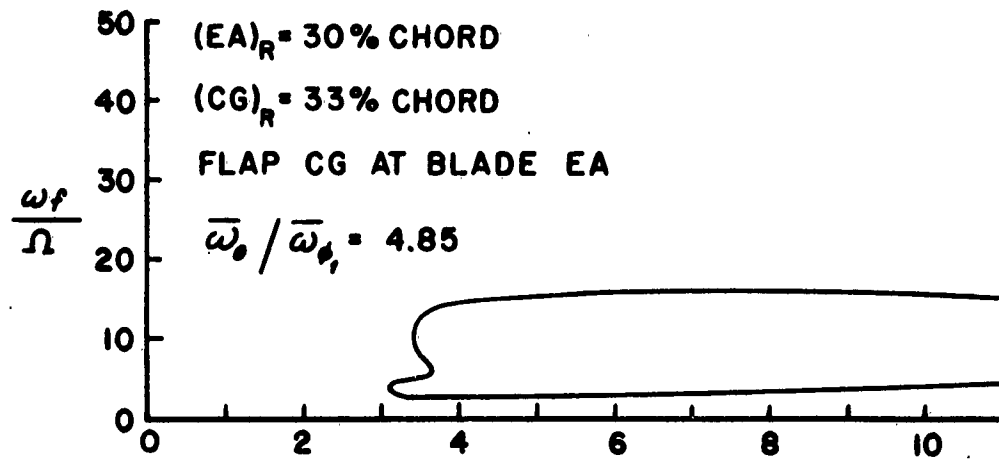
Figure 8 $\frac{\omega_f}{\Omega}$ AND $\frac{\varpi_{\phi_1}}{\Omega}$ versus $\frac{\overline{\omega}_\tau}{\overline{\omega}_\theta}$ FOR HEAVY OVERBALANCE ON CONTROL FLAP

63-9
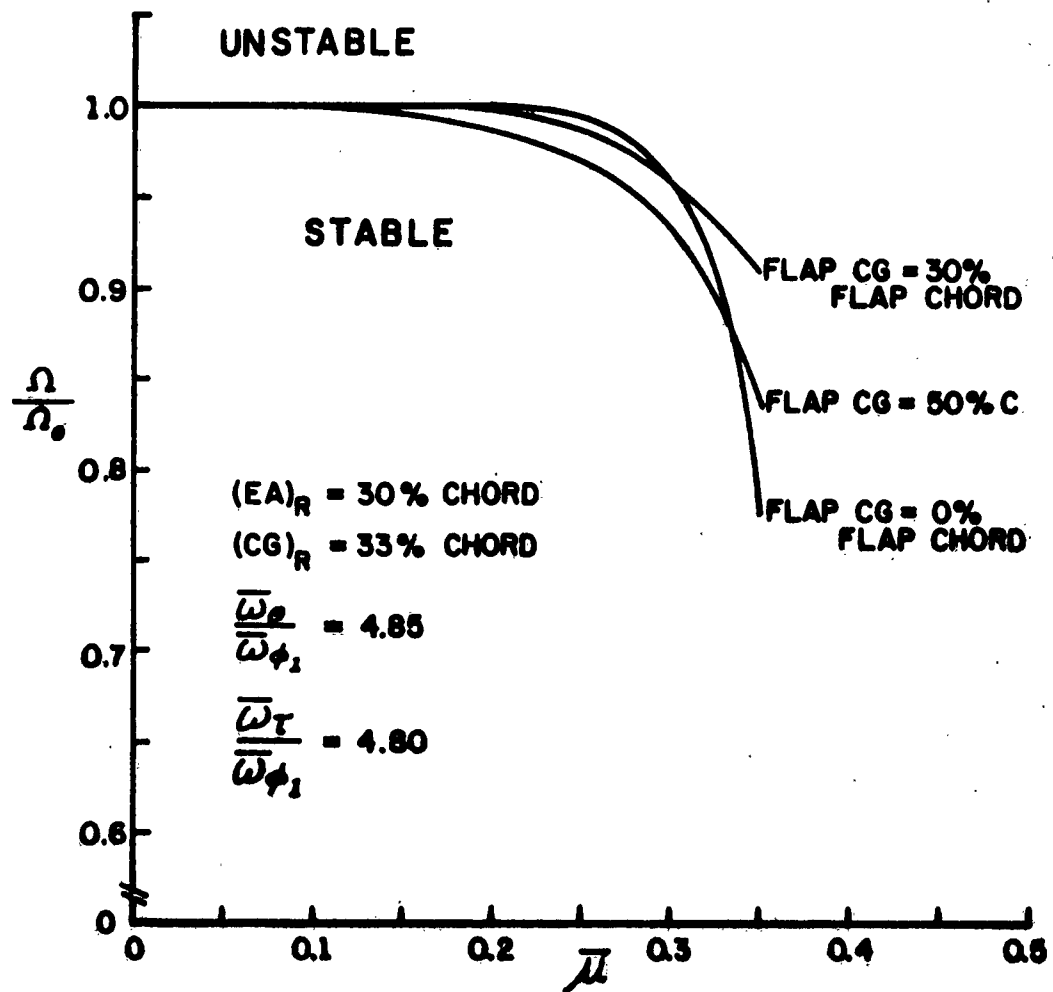
Figure 9 NONDIMENSIONALIZED ROTOR SPEED versus
ADVANCE RATIO FOR VARIOUS FLAP CG POSITIONS
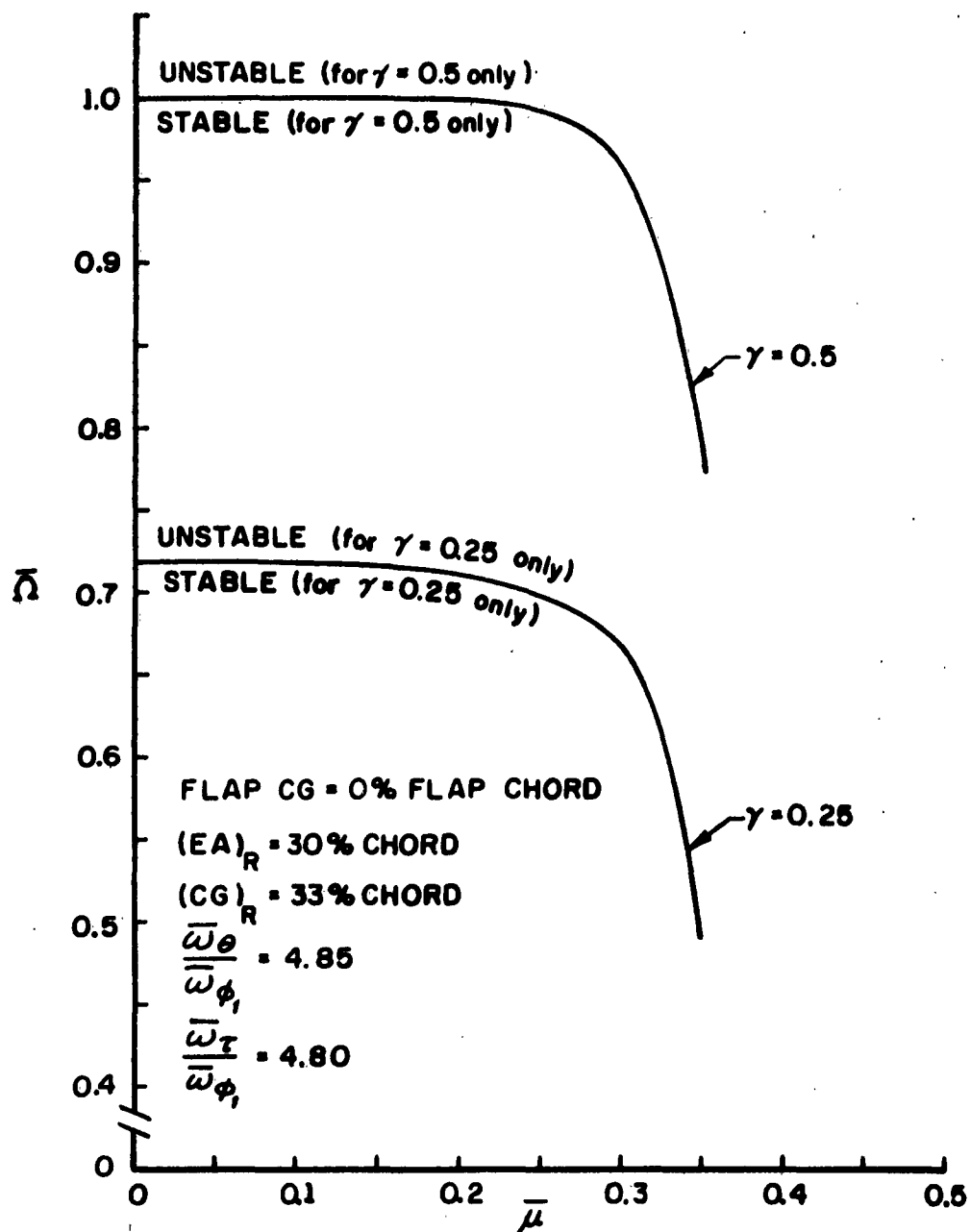
Figure 10 NONDIMENSIONALIZED ROTOR SPEED versus
ADVANCE RATIO FOR VARIOUS CONTROL FLAP
VISCOUS DAMPING COEFFICIENTS

40
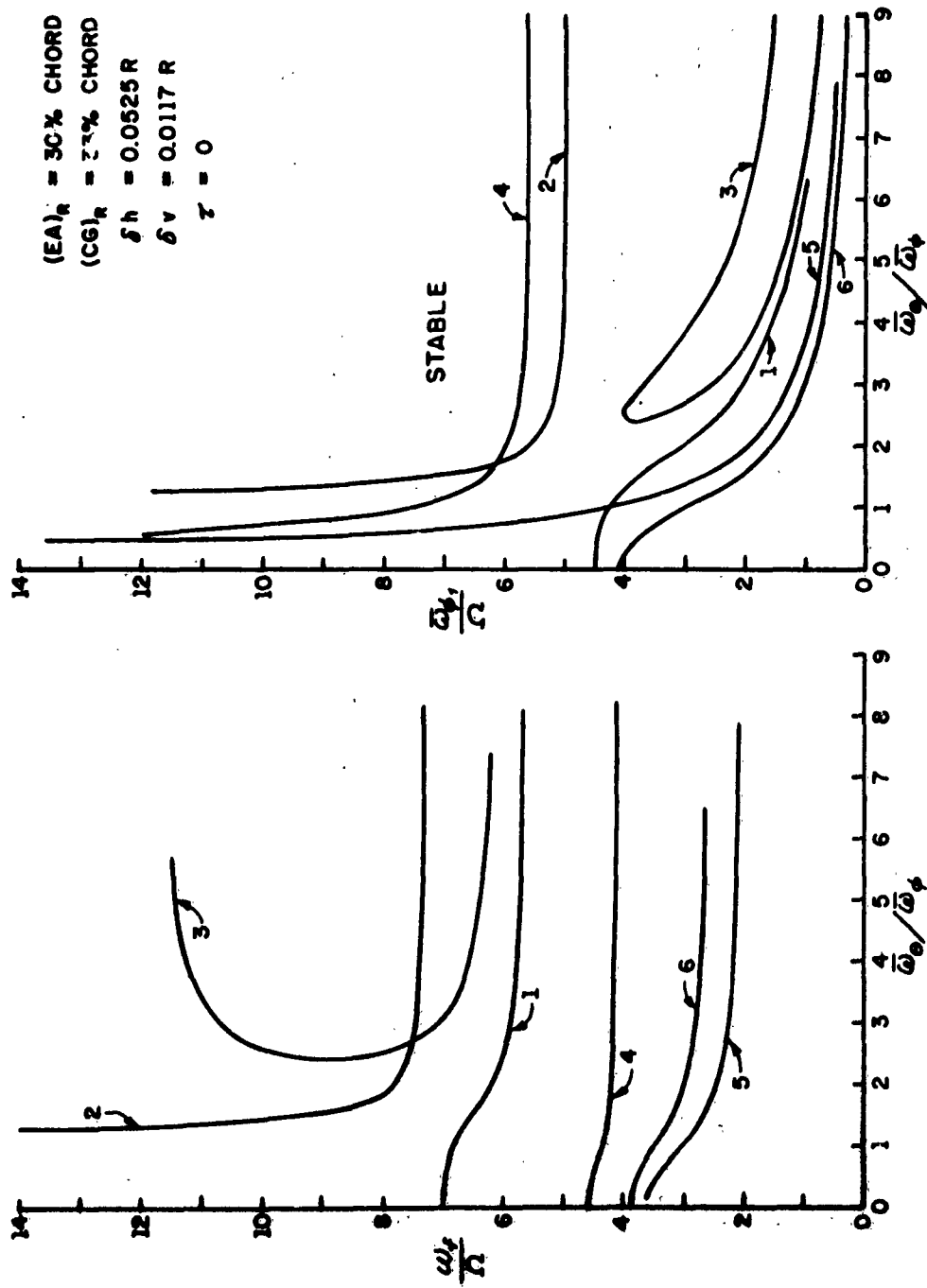
Figure 11 ω_f/Ω AND $\overline{\omega}_{\phi_1}/\Omega$ versus $\overline{\omega}_\theta/\overline{\omega}_\phi$, ANTISYMMETRIC FLUTTER MODES SWIVEL LOCKED
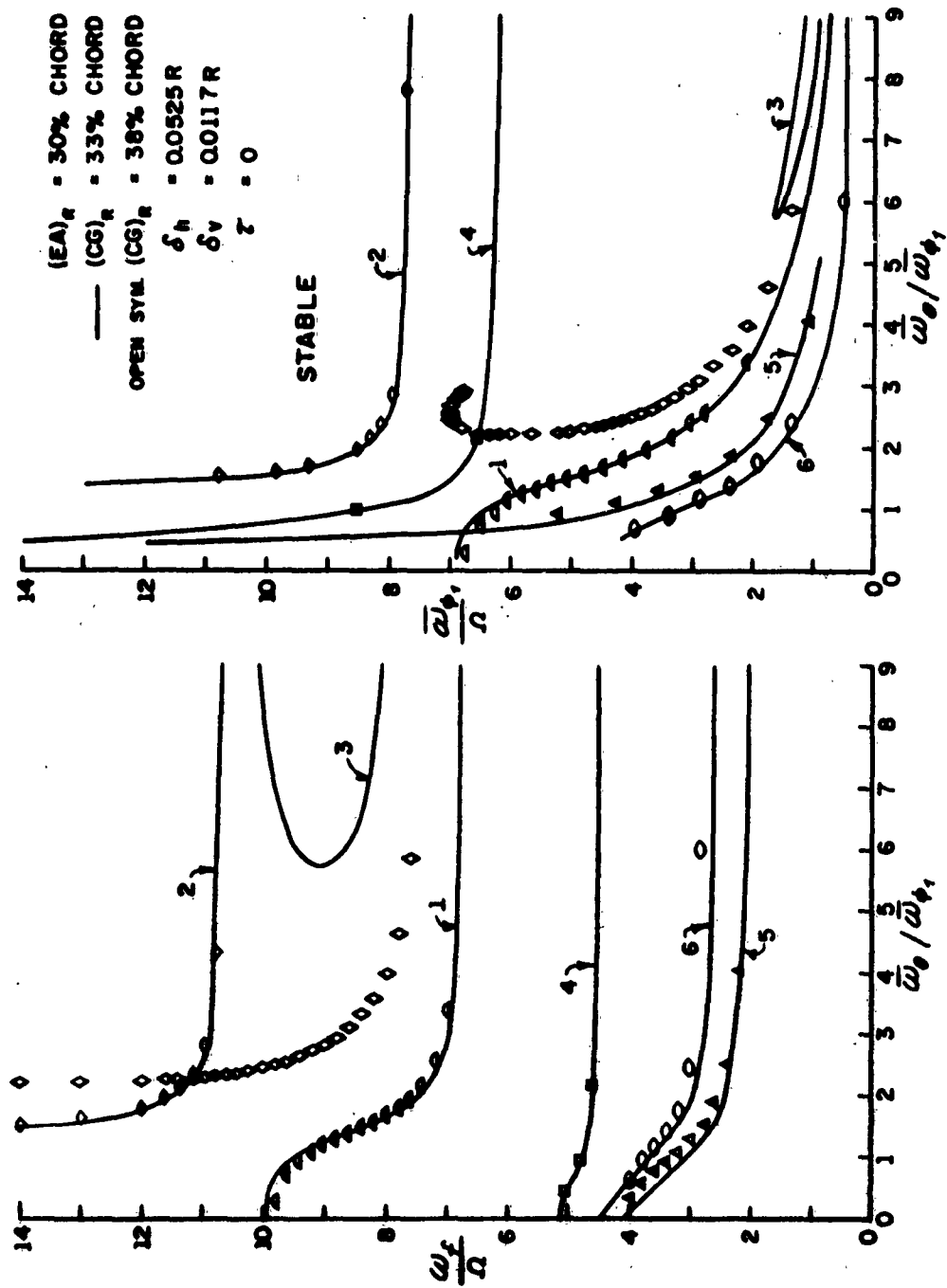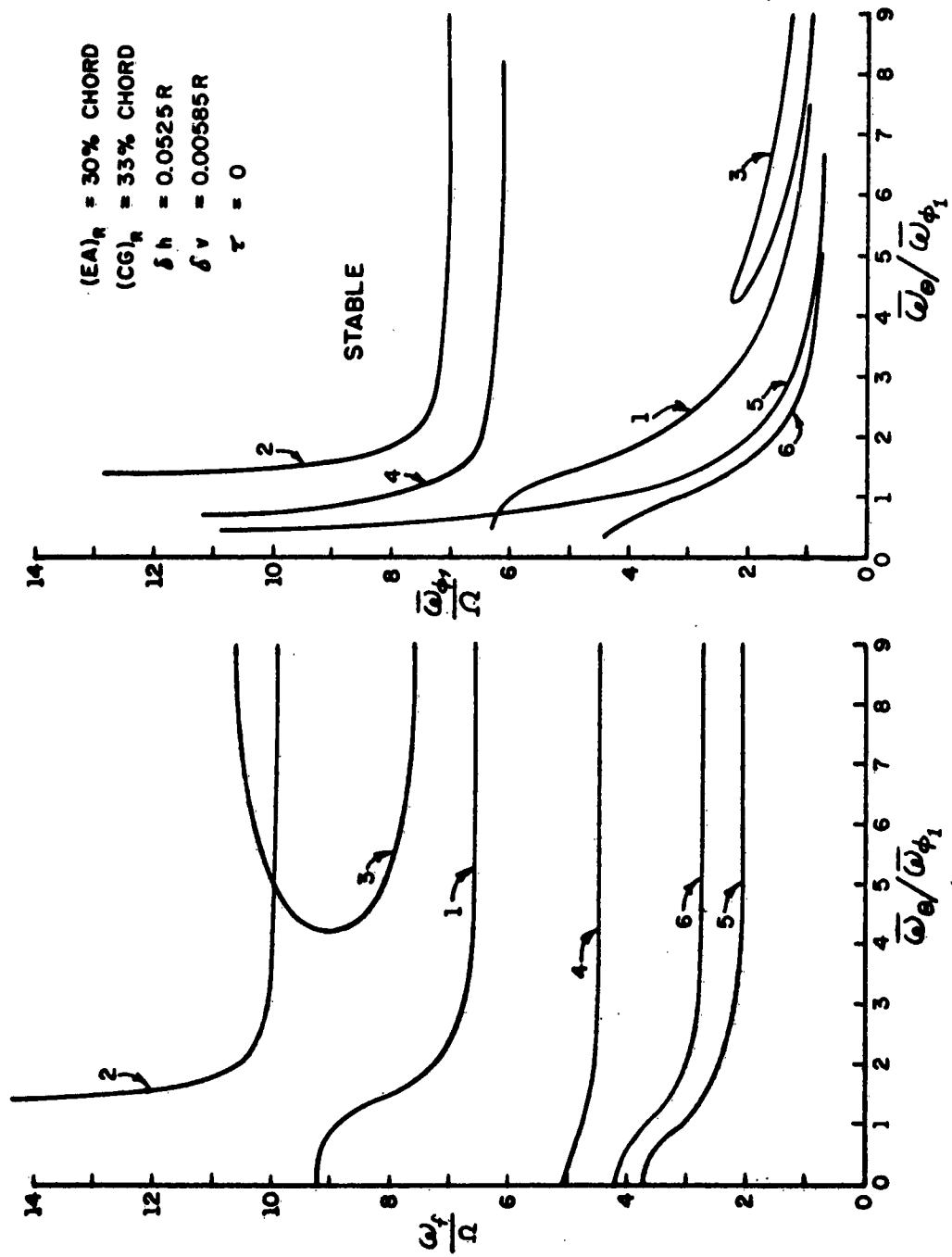
41

Figure 12 ω_f/Ω AND $\overline{\omega}_{\phi_1}/\Omega$ versus $\overline{\omega}_\theta/\overline{\omega}_{\phi_1}$ ASYMMETRIC FLUTTER MODES

SWIVEL FREE

Figure 13 ω_f/Ω AND $\overline{\omega}_\theta/\Omega$ versus $\overline{\omega}_\theta/\overline{\omega}_{\phi_1}$, ASYMMETRIC FLUTTER MODES

SWIVEL FREE

$(EA)_R$ = 30% CHORD
$(CG)_R$ = 33% CHORD
δ_h = 0.0525 R
δ_v = 0.00585 R
τ = 0

STABLE

43
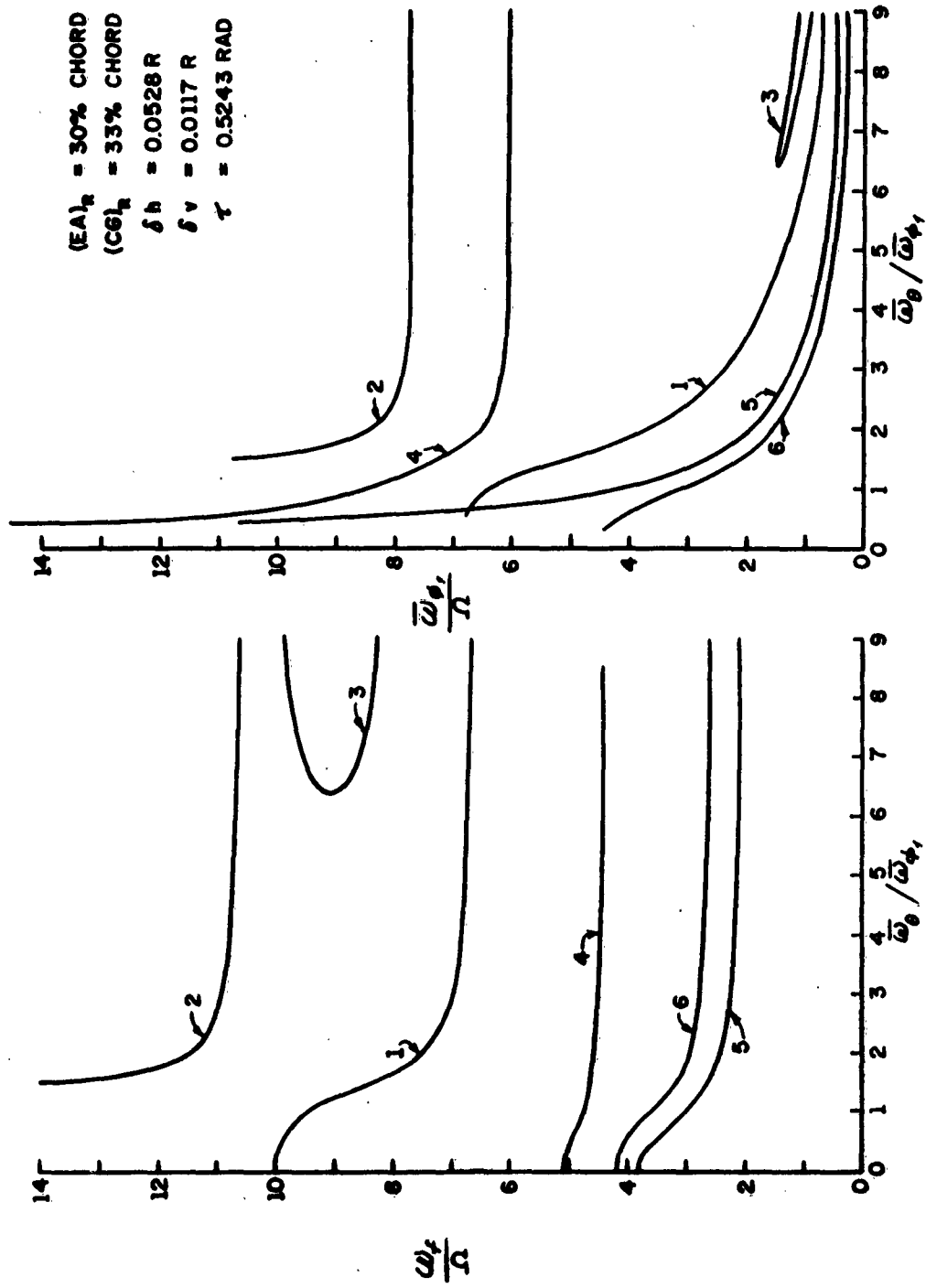
Figure 14 ω_f/Ω AND $\overline{\omega}_{\phi_1}/\Omega$ versus $\overline{\omega}_\theta/\overline{\omega}_{\phi_1}$, ASYMMETRIC FLUTTER MODES

SWIVEL FREE
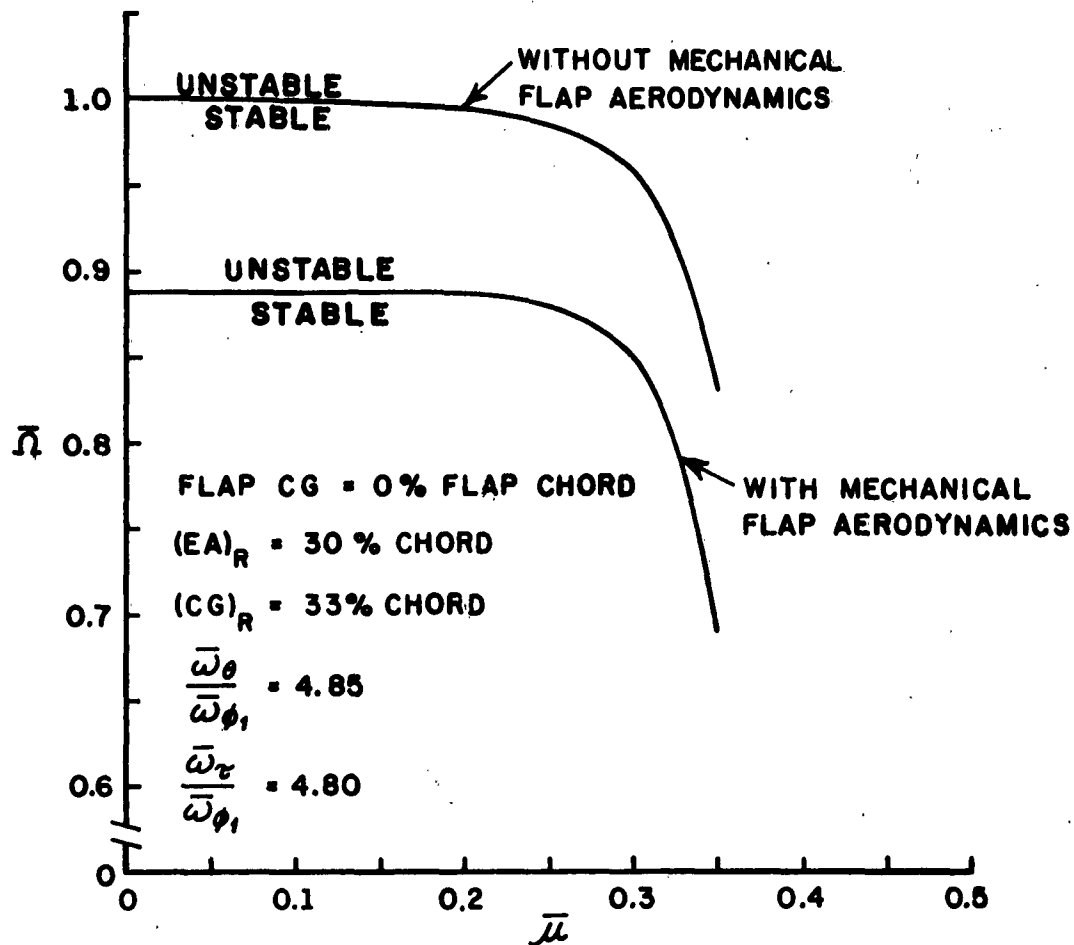
Figure 15 NONDIMENSIONALIZED ROTOR SPEED versus ADVANCE RATIO WITH AND WITHOUT MECHANICAL FLAP AERODYNAMICS

LIST OF SYMBOLS FOR APPENDICES

A_{ij} generalized aerodynamic force coefficient

a_{ij} real part of flutter determinant element

B tip loss factor

b_{ij} imaginary part of flutter determinant element

b local semichord

b_{ref} reference length — maximum semichord length

$\bar{b}_f$ nondimensional local flap semichord

C_L two-dimensional lift coefficient

C_M two-dimensional moment coefficient, referred to the aerodynamic moment about the leading edge, positive nose down

C_{L_i} or C_{M_i} partial derivative of C_L or C_M with respect to i where $i = \alpha, \tau, t$

C_J jet coefficient $C_J = \dfrac{\rho_J V_J^2 \delta_J}{\rho U^2 b}$

$\bar{C}_J$ value of C_J at $\xi = 1$

$\bar{C}_X$ nondimensional distance of section c.g. position aft of elastic axis
$\bar{C}_X = \bar{x}_1 / b$

$\bar{C}_z$ nondimensional distance of section c.g. position above chord plane
$\bar{C}_z = \bar{z}_1 / b$

$\bar{C}_{f_x}$ nondimensional distance from blade elastic axis to flap c.g. $\bar{C}_{f_x} = \bar{X}_{f_1}/b$

f_{ϕ_N} bending deflection shape — n^{th} mode, unit tip deflection

$f_{\phi_N}^* \Delta\phi_N$ perturbation bending displacement referred to root chord plane —

$$f_{\phi_N}^* \Delta\phi_N = f_{\phi_N} \Delta\phi_N - r\left(\frac{df_{\phi_N}}{dr}\right)_{r=0} \Delta\phi_N$$

f_{θ_1} first cantilever torsional mode shape — unit tip deflection

G_{ij} generalized gyroscopic coupling coefficient

g_i structural damping coefficient for i^{th} degree of freedom

$\bar{g}, \bar{h}$ correction terms to account for warping of elastic axis in chord plane —

$$\bar{g} = 2\int_0^{\xi} f_{\theta_1}(\xi_1) \, F(\xi_1) \, d\xi_1$$

$$\bar{h} = \int_0^{\xi} F(\xi_1) \, d\xi_1$$

<div align="center">where</div>

$$F(\xi_1) = \frac{df_{\theta_1}}{d\xi_1}\left[\bar{I}(\xi) - \frac{\epsilon_b(\xi_1)}{\epsilon_b(\xi)}\bar{I}(\xi_1) - \frac{(\xi-\xi_1)}{\epsilon_b(\xi)}\frac{d(\epsilon_b\bar{l})}{d\xi_1}\right]$$

$\bar{I}_{x_1}$ nondimensional moment of inertia about elastic axis due to chordwise mass distribution — $\bar{I}_{x_1} = I_{x_1}/M_b R^2$

$\bar{I}_{z_1}$ nondimensional moment of inertia about elastic axis due to mass distribution normal to chord plane — $\bar{I}_{z_1} = I_{z_1}/M_b R^2$

$\bar{I}_{z_1 (root)}$ contribution to I_{z_1} from part of root fitting which flaps

<div align="center">47</div>

$\bar{I}_{f_x}$ nondimensional moment of inertia of control flap about its leading edge due to chordwise mass distribution – $\bar{I}_{f_x} = I_{f_x}/M_b R^2$

I_{f_z} nondimensional moment of inertia of control flap about its leading edge due to mass distribution normal to chord plane – $\bar{I}_{f_z} = I_{f_z}/M_b R^2$

$I_{i,j}^k$ nondimensional aerodynamic integrals for forward flight case

$\bar{I}_H$ nondimensional hub moment of inertia about teetering hinge – $\bar{I}_H = I_H/M_b R^2$

$K_{i,j}$ generalized stiffness coefficient

$\left. \begin{matrix} K_\alpha \\ K_{\dot\alpha} \end{matrix} \right\}$ flap moment coefficient derivatives

$$M_f \quad \text{(flap leading edge)} = 2b_f^2 \, \Gamma U^2 \left[K_\alpha \, \alpha_f + K_{\dot\alpha}\left(\frac{b_f \, \dot\alpha_f}{U}\right) \right]$$

    where α_f is flap local angle-of-attack

$\left. \begin{matrix} K_{L_\tau} \\ K_{L_{\dot\tau}} \\ K_{M_\tau} \\ K_{M_{\dot\tau}} \end{matrix} \right\}$ flap lift and moment coefficients per Reference 27

$\bar{\ell}$ nondimensional distance of elastic axis aft of pitching (reference) axis $\bar{\ell} = \ell/b$

$\bar{\ell}_H$ nondimensional distance below the teeter pin of the hub center of gravity $\bar{\ell}_H = \ell_H/R$

M_b total mass of one blade

$M_{i,j}$ generalized mass coefficient

M' aerodynamic moment per unit span

$\overline{M}_H$ nondimensional hub mass $\overline{M}_H = M_H / M_b$

$\overline{m}$ nondimensional mass per unit spanwise length $\overline{m} = mR / M_b$

$\overline{m}_f$ nondimensional mass per unit spanwise length of the mechanical flap — $\overline{m}_f = m_f R / M_b$

$\overline{Q}$ nondimensional distance of aerodynamic reference axis (midchord) aft of elastic axis — $\overline{Q} = Q / b$

q_i the ith generalized coordinate

R blade radius

r spanwise distance from flapping hinge

r_0 inboard spanwise limit on integration of aerodynamic forces

$\overline{r}_0$ nondimensional lower limit on aerodynamic spanwise integrals — $\overline{r}_0 = r_0 / R$

T_{ij} generalized centrifugal force coefficient

t maximum camber

U local free stream velocity

$\Delta \overline{u}$ nondimensional teeter pin displacement in X-direction

$\Delta \overline{v}$ nondimensional teeter pin displacement in Y-direction

LIST OF SYMBOLS FOR APPENDICES (Continued)

V_J magnitude of jet velocity relative to airfoil

W_0 average downwash velocity

$X'Y'Z'$ components of aerodynamic force per unit span in the x , y and z directions, respectively

(x,y,z) coordinate system rotating at angular speed Ω , z axis aligned with Ω , positive y axis directed outward along blade

$\bar{x}_f$ nondimensional distance from control flap leading edge to elastic axis — $\bar{x}_f = x_f / b$

α local angle of attack

α_0 inclination of rotor axis with vertical

β_I initial flapping angle

$\Delta\beta_I$ perturbation flapping angle with respect to y axis

$\Delta\beta_2$ perturbation teetering angle of hub with respect to z axis

γ viscous damping in τ mode

$\bar{\delta}_h$ nondimensional distance from center of rotation to flapping hinge — $\bar{\delta}_h = \delta_h / R$

$\bar{\delta}_v$ nondimensional vertical distance of teetering hinge above the flapping hinge — $\bar{\delta}_v = \delta_v / R$

δ_J jet thickness

ϵ_b ratio of local semichord to reference semichord length

θ_0 pitch angle with respect to x-y plane

θ_1 initial blade twist about elastic axis

$\Delta\theta_1$ perturbation torsional deflection at the blade tip about the elastic axis

μ mass ratio, $\mu = M_b / \rho b_{ref} R^2$

ν ratio of oscillation frequency to shaft rotational speed, $\nu = \omega/\Omega$

ξ nondimensional spanwise coordinate, $\xi = r/R$

ξ_0 value of ξ defining length of jet-flap, flap is $(1-\xi)R$ long

ρ density of the free stream

ρ_J air density of the jet

τ steady state jet angle with respect to mean chord line

$\Delta\tau$ perturbation jet deflection angle

$\bar{\phi}_1$ nondimensional initial bending deflection $\bar{\phi}_1 = \phi_1/R$

$\Delta\bar{\phi}_N$ nondimensional perturbation bending displacement at blade tip in n^{th} nation mode — $\Delta\bar{\phi}_N = \Delta\phi_N/R$

Ω rotational speed of the rotor

ω oscillation frequency

$\bar{\omega}_i$ uncoupled, undamped, nonrotating, natural frequency of ith degree of freedom

$\bar{\mu}$ advance ratio, $\bar{\mu} = U\cos\alpha_0 / R\Omega$

ψ azimuthal position

APPENDIX I

DERIVATION OF FLUTTER DETERMINANT ELEMENTS

A. GENERAL EQUATIONS OF MOTION

The general equations of motion for a helicopter blade are derived, using the Lagrangian approach, as in Appendix I of Reference 13. The resulting relationship for the ith degree of freedom (i = 1, 2 . . ., N) assuming the system is undergoing sinusoidal motions at a frequency ω , may be written as follows:

$$(I.1) \qquad \sum_{j=1}^{N} \left(-\omega^2 M_{ij} + K_{ij} - \Omega^2 T_{ij} - 2i\omega\Omega G_{ij} - \Omega^2 A_{ij} \right) q_j = 0$$

The q_j 's are the generalized coordinates, and the quantities M_{ij} , T_{ij}

and G_{ij} may be identified as the generalized mass, centrifugal force, and

gyroscopic coupling coefficients, respectively. These coefficients are given by the following integrals over the entire system.

$$M_{ij} = \iiint \left[\left(\frac{\partial x}{\partial q_i} \right)_0 \left(\frac{\partial x}{\partial q_j} \right)_0 + \left(\frac{\partial y}{\partial q_i} \right)_0 \left(\frac{\partial y}{\partial q_j} \right)_0 + \left(\frac{\partial z}{\partial q_i} \right)_0 \left(\frac{\partial z}{\partial q_j} \right)_0 \right] dm$$

$$T_{ij} = \iiint \left[\left(\frac{\partial x}{\partial q_i} \right)_0 \left(\frac{\partial x}{\partial q_j} \right)_0 + \left(\frac{\partial y}{\partial q_i} \right)_0 \left(\frac{\partial y}{\partial q_j} \right)_0 + x_0 \left(\frac{\partial^2 x}{\partial q_i \partial q_j} \right)_0 + y_0 \left(\frac{\partial^2 y}{\partial q_i \partial q_j} \right)_0 \right] dm$$

$$G_{ij} = \iiint \left[\left(\frac{\partial x}{\partial q_i} \right)_0 \left(\frac{\partial y}{\partial q_j} \right)_0 - \left(\frac{\partial y}{\partial q_i} \right)_0 \left(\frac{\partial x}{\partial q_j} \right)_0 \right] dm$$

where (x , y , z) are the coordinates of the differential mass dm , referred to a rotating orthogonal coordinate system having the z – axis aligned with the angular velocity Ω and the positive y axis directed outward along the blade. The subscript (0) refers to the value of that quantity when all perturbations on the generalized coordinates are zero. The generalized spring forces K_{ij} are given by

$$K_{ij} = \left(\frac{\partial^2 \mu}{\partial q_i \partial q_j} \right)_0$$

APPENDIX I (Continued)

where μ is the total potential energy of the system. The generalized aerodynamic force coefficients A_{ij} were derived from consideration of the generalized (nonconservative) forces acting on the system and are given by the following integrals over the spanwise variable r .

$$A_{ij} = \frac{1}{\Omega^2}\int_{r_0}^{B}\left[\left(\frac{\partial x}{\partial q_i}\right)_0\left(\frac{\partial \Delta X'}{\partial q_j}\right)+\left(\frac{\partial y}{\partial q_i}\right)_0\left(\frac{\partial \Delta Y'}{\partial q_j}\right)+\left(\frac{\partial z}{\partial q_i}\right)_0\left(\frac{\partial \Delta Z'}{\partial q_j}\right)+\left(\frac{\partial \eta}{\partial q_i}\right)_0\left(\frac{\partial \Delta M'}{\partial q_j}\right)\right.$$
$$\left.+ (X')_0\left(\frac{\partial^2 x}{\partial q_i \partial q_j}\right)_0+(Y')_0\left(\frac{\partial^2 y}{\partial q_i \partial q_j}\right)_0+(Z')_0\left(\frac{\partial^2 z}{\partial q_i \partial q_j}\right)_0+(M')_0\left(\frac{\partial^2 \eta}{\partial q_i \partial q_j}\right)_0\right]dr$$

where $\left[(X')_0 + \Delta X'\right]$, etc., are the aerodynamic forces per unit span in the x , y and z directions, respectively. $\left[(M')_0 + \Delta M'\right]$ is the aerodynamic moment per unit span corresponding to the angular displacement η , and B is the tip correction factor.

B. FORMULATION OF THE ELEMENTS OF THE FLUTTER DETERMINANT

Each of the generalized coefficients appearing in the equations of motion was computed, in a manner analogous to the one described in Reference 13, using the aerodynamic coefficients derived in APPENDIX I where applicable. The generalized coordinates considered in the generation of these coefficients are:

β_1 - blade flapping angle with respect to y -axis

β_2 - hub teetering angle with respect to z -axis

$\bar{\phi}_n = \frac{\phi_n}{R}$ - nondimensionalized n^{th} mode bending displacement at blade tip

θ_1 - first mode torsional deflection at blade tip

τ - jet angle with respect to mean chord line

$\bar{u} = u/R$ - nondimensionalized teeter pin displacement in x direction

$\bar{v} = v/R$ - nondimensionalized teeter pin displacement in y direction

So that the formulation of the problem would be more general, the equations of motion were nondimensionalized by dividing through by the quantity $\rho b_{ref}. \Omega^2 R^4$. The nondimensionalized coefficients are given by

54

63-9

$$\overline{M}_{ij} = \frac{M_{ij}}{\rho\, b_{ref}\, R^4} \qquad \overline{A}_{ij} = \frac{A_{ij}}{\rho\, b_{ref}\, R^4}$$

$$\overline{T}_{ij} = \frac{T_{ij}}{\rho\, b_{ref}\, R^4} \qquad \overline{K}_{ij} = \frac{K_{ij}}{\rho\, b_{ref}\, R^4 \Omega^2}$$

$$\overline{G}_{ij} = \frac{G_{ij}}{\rho\, b_{ref}\, R^4}$$

The ij^{th} element of the flutter determinant, with real and imaginary parts designated by a_{ij} and b_{ij}, respectively, are therefore given by:

$$\left\{ \begin{array}{l} a_{ij} = -\nu^2 \overline{M}_{ij} + \overline{K}_{ij} - \overline{T}_{ij} - \mathcal{R}\left\{\overline{A}_{ij}\right\} \\[2ex] b_{ij} = -2\nu\, \overline{G}_{ij} - \mathcal{I}\left\{\overline{A}_{ij}\right\} \end{array} \right\} \quad i \neq j$$

$$\left\{ \begin{array}{l} a_{ii} = \left(-\nu^2 + \dfrac{\overline{\omega}_i^{\,2}}{\Omega^2}\right) M_{ii} - T_{ii} - \mathcal{R}\left\{\overline{A}_{ii}\right\} \\[2ex] b_{ii} = -2\nu\, G_{ii} + q_i\, \dfrac{\omega_i^{\,2}}{\Omega^2}\, M_{ii} - \mathcal{I}\left\{\overline{A}_{ii}\right\} \end{array} \right\} \quad i = j$$

The expressions for the nondimensional coefficients making up these elements are given on the following pages. It should be noted that an additional factor of 2 is applied to all $i\,\beta_2$ coefficients. This factor actually should be included in the definition of the determinant elements $i\,\beta_2$, because the teetering vibrations are excited only when the two blades of the rotor exhibit antisymmetric oscillations. The factor of 2 thus appears when the seven-degree-of-freedom system is reduced to one with four degrees of freedom. The factor was applied to the coefficients instead, however, to simplify the definition of the determinant elements. A similar argument applies to the $i\,u$ and $i\,\nu$ coefficients.

55

63-9

C. FORMULATION OF THE EQUATIONS OF MOTION FOR FORWARD FLIGHT

Again following the lead of Reference 22 we may write the equations of motion for forward flight as

$$(I.2) \qquad \sum_j \left[M_{ij} \, \ddot{q}_{ij} + (D_{ij} - 2\Omega \, G_{ij}) \, \dot{q}_{ij} + (K_{ij} - \Omega^2 T_{ij}) \, q_{ij} \right] = \Delta Q_i$$

where

$$i, j = \beta_1, \, \phi_N, \, \theta_1, \, \tau$$

$$D_{ij} = \text{damping coefficient}$$

$$\Delta Q_i = \text{generalized force due to perturbation displacements, velocities and forces.}$$

Nondimensionalizing as in Section B above and employing the same definitions for $\overline{M}_{ij}$, $\overline{T}_{ij}$, $\overline{G}_{ij}$, and $\overline{K}_{ij}$ Equation (I.2) may be written:

FLAP DEGREE OF FREEDOM EQUATION

$$\left[\bar{M}_{\beta,\beta}\right]\frac{\Delta\ddot{\beta}}{\Omega^2} + \left[-2\bar{G}_{\beta,\beta} + \left\{2\pi I^{\infty}_{\beta,\beta} + (C_{\ell_\alpha}-C_{\ell})I'_{\beta,\beta}\right\}\bar{\mu}\sin\psi\right]\frac{\Delta\dot{\beta}}{\Omega} + \left[-\bar{J}_{\beta,\beta} + \left\{2\pi I^{\infty}_{\beta,\beta} + (C_{\ell_\alpha}-C_{\ell})I'_{\beta,\beta}\right\}\right.$$
$$+ \left\{2\pi I^{\infty}_{\beta,\beta} + C_{\ell}I'_{\beta,\beta} - C_{\ell}I^2_{\beta,\beta}\right\}\bar{\mu}\sin\psi$$
$$+ \left\{2\pi I^{\infty}_{\beta,\beta} + (C_{\ell_\alpha}-C_{\ell})I'_{\beta,\beta}\right\}\bar{\mu}^2\sin 2\psi\right]\Delta\beta_i$$

$$\left[\bar{M}_{\beta,\theta}\right]\frac{\Delta\ddot{\theta}}{\Omega^2} + \left[-2\bar{G}_{\beta,\theta} + \left\{2\pi I^{\infty}_{\beta,\theta} + (C_{\ell_\alpha}-C_{\ell})I'_{\beta,\theta}\right\}\bar{\mu}\sin\psi\right.$$
$$\left. + \left\{\left(\frac{C_{\ell}}{r+\bar{\mu}\sin\psi}\right)I'_{\beta,\theta}\right\}\bar{\mu}\cos\psi\right]\frac{\Delta\dot{\theta}}{\Omega} + \left[-\bar{J}_{\beta,\theta} + \left\{2\pi I^{\infty}_{\beta,\theta} + C_{\ell}I'_{\beta,\theta} - C_{\ell}I^2_{\beta,\theta}\right\}\right.$$
$$+ \left\{2\pi I^{\infty}_{\beta,\theta} + C_{\ell}I'_{\beta,\theta} - C_{\ell}I^2_{\beta,\theta}\right\}\bar{\mu}\sin\psi$$
$$+ \left\{2\pi I^{\infty}_{\beta,\theta} + (C_{\ell_\alpha}-C_{\ell})I'_{\beta,\theta}\right\}\right]\Delta\theta_M$$

$$\left[\bar{M}_{\beta,\theta}\right]\frac{\Delta\ddot{\theta}}{\Omega^2} + \left[-2\bar{G}_{\beta,\theta} + \left\{2\pi I^{\infty}_{\beta,\theta} + C_{\ell}I'_{\beta,\theta} - C_{\ell}I^2_{\beta,\theta}\right\}\bar{\mu}\sin\psi\right.$$
$$\left. + \left\{2\pi I^{\infty}_{\beta,\theta} + C_{\ell}I'_{\beta,\theta} - C_{\ell}I^2_{\beta,\theta}\right\}\bar{\mu}\sin\psi\right]\frac{\Delta\dot{\theta}}{\Omega} + \left[-\bar{J}_{\beta,\theta} - \left\{2\pi(I^{\infty}_{\beta,\theta} + \bar{\mu}^2 I^{\infty}_{\beta,\theta}) + C_{\ell}(I'_{\beta,\theta} + \bar{\mu}^2 I'_{\beta,\theta})\right\}\right.$$
$$- \left\{2\pi I^{\infty}_{\beta,\theta} + C_{\ell}I'_{\beta,\theta}\right\}\bar{\mu}\sin\psi$$
$$- \left\{\left(\frac{C_{\ell}}{r+\bar{\mu}\sin\psi}\right)I'_{\beta,\theta}\right\}\bar{\mu}\cos\psi + \left\{2\pi I^{\infty}_{\beta,\theta} + C_{\ell}I'_{\beta,\theta}\right\}\bar{\mu}^2\cos 2\psi\right]\Delta\theta$$

$$\left[\bar{M}_{\beta,\tau}\right]\frac{\Delta\ddot{\tau}}{\Omega^2} + \left[-2\bar{G}_{\beta,\tau} - \left\{(-K_{\ell_\tau} + C_{\ell_\tau})I'_{\beta,\tau}\right\}\right]$$
$$- \left\{(-K_{\ell_\tau} + C_{\ell_\tau})I'_{\beta,\tau}\right\}\bar{\mu}\sin\psi\right]\frac{\Delta\dot{\tau}}{\Omega} + \left[-\bar{J}_{\beta,\tau} - \left\{(-K_{\ell_\tau}+C_{\ell_\tau})(I'_{\beta,\tau}+\bar{\mu}^2 I^2_{\beta,\tau})\right\} - \left\{(-K_{\ell_\tau}+C_{\ell_\tau})I'_{\beta,\tau}\right\}\bar{\mu}\sin\psi + \left\{(-K_{\ell_\tau}+C_{\ell_\tau})I'_{\beta,\tau}\right\}\bar{\mu}^2\cos 2\psi\right]\Delta\tau = 0$$

BENDING DEGREE OF FREEDOM EQUATION

$$\left[\bar{M}_{\beta_N \beta_N}\right]\frac{\Delta \dot\beta_N}{\Omega^2} + \left[-2\bar{G}_{\beta_N \phi_N} + \left\{g_{\phi_N} \bar{M}_{\phi\phi}\right\}\frac{\omega_{\phi_N}}{\Omega} + \left\{2\pi I_{\beta_N \beta_N}^{10} + (C_{l_\alpha} - C_J)I_{\beta_N \beta_N}^{\prime}\right\}\right.$$

$$\left. + \left\{\bar\mu \sin\psi\right\}\right]\frac{\Delta \dot\beta_N}{\Omega} + \left[\bar{M}_{\beta_N}\frac{\omega_{\beta_N}^2}{\Omega^2} - \tau_{\beta_N} + \left\{2\pi I_{\beta_N \beta_N}^{20} + C_J I_{\beta_N \beta_N}^{\prime} - C_{l_\xi}I_{\beta_N \beta_N}^{\delta}\right\}\right.$$

$$+ \left\{2\pi I_{\beta_N \beta_N}^{30} + C_{l_\alpha}I_{\beta_N \beta_N}^{\prime} - C_{l_J}I_{\beta_N \beta_N}^{\delta}\right\}\bar\mu \sin\psi$$

$$+ \left\{2\pi I_{\beta_N \beta_N}^{60} + (C_{l_\alpha} - C_J)I_{\beta_N \beta_N}^{\phi}\right\}\bar\mu \cos\psi$$

$$\left. + \left\{2\pi I_{\beta_N \beta_N}^{50} + (C_{l_\xi} - C_J)I_{\beta_N \beta_N}^{\delta}\right\}\bar\mu^2 \sin 2\psi\right]\Delta\Phi_N$$

$$\left[\bar{M}_{\theta_N \theta}\right]\frac{\Delta\dot\theta}{\Omega^2} + \left[-2\bar{G}_{\theta_N \theta}\right.$$

$$+ \left\{2\pi I_{\theta_N \theta}^{10} + C_{l_\alpha}I_{\theta_N \theta}^{\prime} - C_{l_\xi}I_{\theta_N \theta}^{\delta}\right\}$$

$$\left. + \left\{2\pi I_{\theta_N \theta}^{40} + (C_{l_\alpha} - C_J)I_{\theta_N \theta}^{\delta}\right\}\bar\mu \sin\psi\right]\frac{\Delta\dot\theta}{\Omega} + \left[\right.$$

$$-\tau_{\theta\theta} - \left\{2\pi\left[I_{\theta_N \theta}^{10} + \bar\mu^2 I_{\theta_N \theta}^{20}\right] + C_{l_\alpha}\left[I_{\theta_N \theta}^{\prime} + \bar\mu^2 I_{\theta_N \theta}^{\delta}\right]\right\}$$

$$- \left\{\left(\frac{C_J}{r + \bar\mu \sin\psi}\right)I_{\theta_N \theta}^{\delta}\right\}\bar\mu \sin\psi$$

$$- \left\{\left(\frac{C_J}{r + \bar\mu \sin\psi}\right)I_{\theta_N \theta}^{\delta}\right\}\bar\mu \cos\psi$$

$$\left. + \left\{2\pi I_{\theta_N \theta}^{50} + C_J I_{\theta_N \theta}^{\delta}\right\}\bar\mu^2 \cos 2\psi\right]\Delta\theta$$

$$\left[\bar{M}_{\beta_N \beta_i}\right]\frac{\Delta\dot\beta_i}{\Omega^2} + \left[-2\bar{G}_{\beta_N \beta_i}\right.$$

$$+ \left\{2\pi I_{\beta_N \beta_i}^{10} + (C_{l_\alpha} - C_J)I_{\beta_N \beta_i}^{\prime}\right\}$$

$$\left. + \left\{2\pi I_{\beta_N \beta_i}^{20} + (C_{l_\alpha} - C_J)I_{\beta_N \beta_i}^{\delta}\right\}\bar\mu \sin\psi\right]\frac{\Delta\dot\beta_i}{\Omega} + \left[\right.$$

$$-\tau_{\beta_N \beta_i} + \left\{2\pi I_{\beta_N \beta_i}^{30} + C_{l_\alpha}I_{\beta_N \beta_i}^{\prime} - C_{l_\xi}I_{\beta_N \beta_i}^{\delta}\right\}$$

$$+ \left\{2\pi I_{\beta_N \beta_i}^{40} + C_{l_\alpha}I_{\beta_N \beta_i}^{\delta} - C_{l_\xi}I_{\beta_N \beta_i}^{\theta}\right\}\bar\mu \cos\psi$$

$$+ \left\{2\pi I_{\beta_N \beta_i}^{60} + (C_{l_\alpha} - C_J)I_{\beta_N \beta_i}^{\delta}\right\}\bar\mu \cos\psi$$

$$\left. + \left\{2\pi I_{\beta_N \beta_i}^{50} + (C_{l_\alpha} - C_J)I_{\beta_N \beta_i}^{\delta}\right\}\bar\mu^2 \sin 2\psi\right]\Delta\beta_i$$

$$\left[\bar{M}_{\phi_N \tau}\right]\frac{\Delta\ddot\tau}{\Omega^2} + \left[-2\bar{G}_{\phi_N \tau}\right.$$

$$- \left\{(-K_{l_\xi} + C_{l_\tau})I_{\phi_N \tau}^{\prime}\right\}$$

$$\left. - \left\{(-K_{l_\xi} + C_{l_\tau})I_{\phi_N \tau}^{\delta}\right\}\bar\mu \sin\psi\right]\frac{\Delta\dot\tau}{\Omega} + \left[\right.$$

$$-\tau_{\phi_N \tau} - \left\{(-K_{l_\xi} + C_{l_\tau})\left(I_{\phi_N \tau}^{\prime} + \bar\mu^2 I_{\phi_N \tau}^{\delta}\right)\right\}$$

$$- \left\{(-K_{l_\xi} + C_{l_\tau})I_{\phi_N \tau}^{\delta}\right\}\bar\mu \sin\psi$$

$$\left. + \left\{(-K_{l_\xi} + C_{l_\tau})I_{\phi_N \tau}^{\delta}\right\}\bar\mu^2 \cos 2\psi\right]\Delta\tau = 0$$

58

63-9

TORSION DEGREE OF FREEDOM EQUATION

$$
[\bar{M}_{\theta\theta}]\frac{\Delta\ddot{\theta}}{\Omega^2} + \left[-2\bar{G}_{\theta\theta}\dot{\theta} + \left\{g_{\theta\theta}\bar{M}_{\theta\theta}\right\}\frac{\omega_\theta}{\Omega} - \right\}
$$

$$
\left(\frac{\pi}{2}-\left(\frac{\bar{b}-\bar{a}}{2\bar{b}}\right)2\pi\right)I^{s\theta}_{\theta\dot{\theta}} + \left(c_{M_{\bar{a}}}-\left(\frac{\bar{b}-\bar{a}}{2\bar{b}}\right)c_{L_{\bar{a}}}\right)I^s_{\theta\dot{\theta}} - \left(c_{M_{\bar{a}}}-\left(\frac{\bar{b}-\bar{a}}{2\bar{b}}\right)c_{L_{\bar{a}}}\right)I^c_{\theta\dot{\theta}}
$$

$$
-\left[\left(\frac{\pi}{2}-\left(\frac{\bar{b}-\bar{a}}{2\bar{b}}\right)2\pi\right)I^{s\theta}_{\theta\dot{\theta}} + \left(c_{M_{\bar{a}}}-\left(\frac{\bar{b}-\bar{a}}{2\bar{b}}\right)c_{L_{\bar{a}}}\right)I^s_{\theta\dot{\theta}}\right\}\left|\bar{\mu}\sin\psi\right]\frac{\Delta\dot{\theta}}{\Omega} +
$$

$$
\left[\bar{M}_{\theta\theta}\frac{\omega^2_\theta}{\Omega^2} - \mathcal{T}_{\theta\theta} + \left\{\left(\frac{\pi}{2}-\left(\frac{\bar{b}-\bar{a}}{2\bar{b}}\right)2\pi\right)\left(I^{s\theta}_{\theta\theta} + \bar{\mu}^2 I^{2\theta}_{\theta\theta}\right) + \left(c_{M_{\bar{a}}}-\left(\frac{\bar{b}-\bar{a}}{2\bar{b}}\right)c_{L_{\bar{a}}}\right)\left(I^s_{\theta\theta} + \bar{\mu}^2 I^2_{\theta\theta}\right)\right\}
$$

$$
+ \left\{\left(\frac{\pi}{2}-\left(\frac{\bar{b}-\bar{a}}{2\bar{b}}\right)2\pi\right)I^{s\theta}_{\theta\theta} + \left(c_{M_{\bar{a}}}-\left(\frac{\bar{b}-\bar{a}}{2\bar{b}}\right)c_{L_{\bar{a}}}\right)I^c_{\theta\theta}\right\}\bar{\mu}\cos 2\psi\right]\Delta\theta
$$

$$
[\bar{M}_{\theta\beta_1}]\frac{\Delta\ddot{\beta}_1}{\Omega^2} + \left[-2\bar{G}_{\theta}\dot{\beta}_1
$$

$$
-\left[\left(\frac{\pi}{2}-\left(\frac{\bar{b}-\bar{a}}{2\bar{b}}\right)2\pi\right)I^{s\theta}_{\theta\dot{\beta}_1} + \left(c_{M_{\bar{a}}}-\left(\frac{\bar{b}-\bar{a}}{2\bar{b}}\right)c_{L_{\bar{a}}}\right)I^s_{\theta\dot{\beta}_1}\right\} - \left\{\left(\frac{\pi}{2}-\left(\frac{\bar{b}-\bar{a}}{2\bar{b}}\right)c_{L_{\bar{a}}}\right)I^c_{\theta\dot{\beta}_1}\right\}\bar{\mu}\sin\psi\right]\frac{\Delta\dot{\beta}_1}{\Omega} +
$$

$$
\left[-\mathcal{T}_{\theta\beta_1} - \left\{\left(\frac{\pi}{2}-\left(\frac{\bar{b}-\bar{a}}{2\bar{b}}\right)2\pi\right)I^{s\theta}_{\theta\beta_1}\left(c_{M_{\bar{a}}}+\left(\frac{\bar{b}-\bar{a}}{2\bar{b}}\right)c_{L_{\bar{a}}}\right)I^s_{\theta\beta_1} - \left(c_{M_{\bar{a}}}+\left(\frac{\bar{b}-\bar{a}}{2\bar{b}}\right)c_{L_{\bar{a}}}\right)I^c_{\theta\beta_1}\right\}
$$

$$
- \left\{\left(\frac{\pi}{2}-\left(\frac{\bar{b}-\bar{a}}{2\bar{b}}\right)2\pi\right)I^{s\theta}_{\theta\beta_1} + \left(c_{M_{\bar{a}}}-\left(\frac{\bar{b}-\bar{a}}{2\bar{b}}\right)c_{L_{\bar{a}}}\right)I^c_{\theta\beta_1}\right\}\bar{\mu}^2\sin 2\psi\right]\Delta\beta_1
$$

$$
[\bar{M}_{\theta\beta_N}]\frac{\Delta\ddot{\beta}_N}{\Omega^2} + \left[-2\bar{G}_{\theta}\dot{\beta}_N
$$

$$
-\left[\left(\frac{\pi}{2}-\left(\frac{\bar{b}-\bar{a}}{2\bar{b}}\right)2\pi\right)I^{s\theta}_{\theta\dot{\beta}_N} + \left(c_{M_{\bar{a}}}-\left(\frac{\bar{b}-\bar{a}}{2\bar{b}}\right)c_{L_{\bar{a}}}\right)I^s_{\theta\dot{\beta}_N}\right] - \left\{\left(c_{M_{\bar{a}}}-\left(\frac{\bar{b}-\bar{a}}{2\bar{b}}\right)c_{L_{\bar{a}}}\right)I^c_{\theta\dot{\beta}_N}\right\}\bar{\mu}\sin\psi\right]\frac{\Delta\dot{\beta}_N}{\Omega} +
$$

$$
\left[-\mathcal{T}_{\theta\beta_N} - \left\{\left(\frac{\pi}{2}-\left(\frac{\bar{b}-\bar{a}}{2\bar{b}}\right)2\pi\right)I^{s\theta}_{\theta\beta_N} + \left(c_{M_{\bar{a}}}-\left(\frac{\bar{b}-\bar{a}}{2\bar{b}}\right)c_{L_{\bar{a}}}\right)I^c_{\theta\beta_N}\right\}\bar{\mu}^2\sin 2\psi\right]\Delta\beta_N
$$

$$
[\bar{M}_{\theta\zeta}]\frac{\Delta\ddot{\zeta}}{\Omega^2} + \left[-2\bar{G}_{\theta}\dot{\zeta}
$$

$$
-\left\{\left(c_{M_{\bar{\zeta}}}-c_{M_{\bar{\zeta}}}+\left(\frac{\bar{b}-\bar{a}}{2\bar{b}}\right)c_{L_{\bar{\zeta}}}\right)I^s_{\theta\zeta}\right\} - \left\{\left(c_{M_{\bar{\zeta}}}-c_{M_{\bar{\zeta}}}+\left(\frac{\bar{b}-\bar{a}}{2\bar{b}}\right)c_{L_{\bar{\zeta}}}\right)I^c_{\theta\zeta}\right\}\bar{\mu}\sin\psi\right]\frac{\Delta\dot{\zeta}}{\Omega} +
$$

$$
\left[-\mathcal{T}_{\theta\zeta} - \left\{\left(c_{M_{\bar{\zeta}}}-c_{M_{\bar{\zeta}}}+\left(\frac{\bar{b}-\bar{a}}{2\bar{b}}\right)c_{L_{\bar{\zeta}}}\right)\left(I^c_{\theta\zeta}+\bar{\mu}^2 I^2_{\theta\zeta}\right)\right\}
$$

$$
- \left\{\left(c_{M_{\bar{\zeta}}}-c_{M_{\bar{\zeta}}}+\left(\frac{\bar{b}-\bar{a}}{2\bar{b}}\right)c_{L_{\bar{\zeta}}}\right)I^s_{\theta\zeta}\right\}\bar{\mu}\sin\psi + \left(c_{M_{\bar{\zeta}}}-c_{M_{\bar{\zeta}}}+\left(\frac{\bar{b}-\bar{a}}{2\bar{b}}\right)c_{L_{\bar{\zeta}}}\right)I^c_{\theta\zeta}\right\}\bar{\mu}^2\cos 2\psi\right]\Delta\zeta = 0
$$

CONTROL FLAP DEGREE OF FREEDOM

$$\left[\bar{M}_{\tau\tau}\right]\frac{\Delta\ddot{\tau}}{\Omega^2} + \left[-2\bar{G}_{\tau\tau} + \left\{\,2\gamma\bar{M}_{\tau\tau}\,\right\}\frac{\omega_\tau}{\Omega}\right]\frac{\Delta\dot{\tau}}{\Omega} + \left[\bar{M}_{\tau\tau}\frac{\omega_\tau^2}{\Omega^2} - \bar{T}_{\tau\tau}\right]\Delta\tau$$

$$+ \left[\bar{M}_{\tau\phi_N}\right]\frac{\Delta\ddot{\phi}_N}{\Omega^2} + \left[-2\bar{G}_{\tau\phi_N}\right]\frac{\Delta\dot{\phi}_N}{\Omega} + \left[\quad\right] - \bar{T}_{\tau\phi_N}\,\Delta\phi_N$$

$$+ \left[\bar{M}_{\tau\theta}\right]\frac{\Delta\ddot{\theta}}{\Omega^2} + \left[-2\bar{G}_{\tau\theta}\right]\frac{\Delta\dot{\theta}}{\Omega} + \left[\quad\right] - \bar{T}_{\tau\theta}\,\Delta\theta$$

$$+ \left[\bar{M}_{\tau\beta_1}\right]\frac{\Delta\ddot{\beta}_1}{\Omega^2} + \left[-2\bar{G}_{\tau\beta_1}\right]\frac{\Delta\dot{\beta}_1}{\Omega} + \left[\quad\right] - \bar{T}_{\tau\beta_1}\,\Delta\beta_1 = 0$$

60

In order to make the forward flight problem tractable several additional assumptions concerning the aerodynamics were made which do not apply to the hovering case except in those cases where the hovering results were obtained on the analog.

(a) Terms of order greater than $\bar{\mu}^2$ were neglected.

(b) Since the jet coefficient varies along the span as well as around the azimuth,

$$C_J = \frac{\rho_J V_J^2 \delta_J}{\rho_0 R^2 \Omega^2 b} \frac{1}{(\bar{\xi} + \mu \sin \psi)^2}$$

it was necessary to choose a representative station at which to compute C_J . The station chosen was the 72% span.

(c) The only control flap aerodynamics considered were those of the flap acting in the other degrees of freedom. No aerodynamic effects of other modes into the control flap were allowed.

For the forward flight case the aerodynamic coefficients are denoted by $I_{i,j}^{no}$ or $I_{i,j}^{n}$ where

$$I_{i,j}^{no} = \int_{r_0}^{\xi_0} [\ ] \, d\xi \qquad \begin{array}{l} n = 1, 2, \ldots \\ i = \beta_1, \phi_N, \theta_1, \tau \\ j = \beta_1, \phi_N, \theta_1, \tau \end{array}$$

$$I_{i,j}^{n} = \int_{\xi_0}^{B} [\ ] \, d\xi$$

Generalized Mass Coefficients

$$\overline{M}_{\phi_n \, \phi_n} = \mu \left[\int_0^1 (f_{\phi_n})^2 \, \overline{m} \, d\xi + \left(\frac{df_{\phi_n}}{d\xi} \right)_{\xi=0}^2 \overline{I}_{z_i \, (root)} \right]$$

$$\overline{M}_{\phi_n \, \theta_n} = -\mu \, \frac{b_{ref}}{R} \int_0^1 \epsilon_b \, f_{\phi_n} \, \overline{m} \left(f_{\theta_i} \overline{C}_x + \overline{h} \right) d\xi$$

$$\overline{M}_{\phi_n \, \beta_1} = +\mu \int_0^1 \xi \, f_{\phi_n} \, \overline{m} \, d\xi$$

$$\overline{M}_{\phi_n \, \beta_2} = 2\mu \, \overline{\delta}_h \int_0^1 f_{\phi_n} \, \overline{m} \, d\xi$$

$$\overline{M}_{\phi_n \, \tau} = -\mu \, \frac{b_{ref}}{R} \int_{\xi_0}^1 \epsilon_b \, f_{\phi_n} \left(\overline{C}_{f_x} - \overline{x}_f \right) \overline{m}_f \, d\xi$$

$$\overline{M}_{\theta_i \, \phi_n} = \overline{M}_{\phi_n \, \theta_n}$$

$$\overline{M}_{\theta_i \, \theta_i} = \mu \int_0^1 \left\{ f_{\theta_i}^2 \left[\frac{d\overline{I}_z}{d\xi} + \frac{d\overline{I}_{x_i}}{d\xi} \right] + \overline{m} \, \epsilon_b^2 \left(\frac{b_{ref}}{R} \right)^2 \overline{h} \left[\overline{h} + 2\overline{C}_x f_{\theta_i} \right] \right\} d\xi$$

$$\overline{M}_{\theta_i \, \beta_1} = -\mu \, \frac{b_{ref}}{R} \int_0^1 \epsilon_b \, \xi \, \overline{m} \left(f_{\theta_i} \overline{C}_x + \overline{h} \right) d\xi$$

$$\overline{M}_{\theta_i \, \beta_2} = -2\mu \, \overline{\delta}_h \, \frac{b_{ref}}{R} \int_0^1 \epsilon_b \, \overline{m} \left(f_{\theta_i} \overline{C}_x + \overline{h} \right) d\xi$$

$$M_{\theta_i \, \tau} = \mu \int_{\xi_0}^1 f_{\theta_i} \left[\frac{d\overline{I}_{fx}}{d\xi} + \frac{d\overline{I}_{fz}}{d\xi} + \overline{m}_f \, \epsilon_b^2 \left(\frac{\overline{b}_{ref}}{R} \right)^2 \overline{x}_f \left(\overline{C}_{f_x} - \overline{x}_f \right) \right] d\xi$$

63-9

Generalized Mass Coefficients (continued)

$$\overline{M}_{\beta_1 \phi_n} = \overline{M}_{\phi_n \beta_1}$$

$$\overline{M}_{\beta_1 \theta_1} = \overline{M}_{\theta_1 \beta_1}$$

$$\overline{M}_{\beta_1 \beta_1} = \mu \left[\int_0^1 m \, \xi^2 \, d\xi + I_{\mathbb{Z}_1 (root)} \right]$$

$$\overline{M}_{\beta_1 \beta_2} = 2\mu \, \overline{\delta}_h \int_0^1 \xi \, \overline{m} \, d\xi$$

$$\overline{M}_{\beta_1 \tau} = -\mu \, \frac{b_{ref}}{R} \int_{\xi_0}^1 \epsilon_b \, \xi \left(\overline{C}_{f\mathbb{Z}} - \overline{\mathbb{Z}}_f \right) \overline{m}_f \, d\xi$$

$$\overline{M}_{\beta_2 \phi_n} = \frac{1}{2} \overline{M}_{\phi_n \beta_2}$$

$$\overline{M}_{\beta_2 \theta_1} = \frac{1}{2} \overline{M}_{\theta_1 \beta_2}$$

$$\overline{M}_{\beta_2 \beta_1} = \frac{1}{2} \overline{M}_{\beta_1 \beta_2}$$

$$\overline{M}_{\beta_2 \beta_2} = \mu \left[\overline{I}_H + 2\left(\overline{\delta}_v^2 + \overline{\delta}_h^2 \right) \right]$$

$$\overline{M}_{\beta_2 \tau} = -\mu \, \overline{\delta}_h \, \frac{b_{ref}}{R} \int_{\xi_0}^1 \epsilon_b \left(\overline{C}_{f\mathbb{Z}} - \overline{\mathbb{Z}}_f \right) \overline{m}_f \, d\xi$$

Generalized Mass Coefficients (continued)

$$\overline{M}_{\tau\phi_n} = \overline{M}_{\phi_n\tau}$$

$$\overline{M}_{\tau\theta_1} = \overline{M}_{\theta_1\tau}$$

$$\overline{M}_{\tau\beta_1} = \overline{M}_{\beta_1\tau}$$

$$\overline{M}_{\tau\beta_2} = 2\overline{M}_{\beta_2\tau}$$

$$\overline{M}_{\tau\tau} = \mu\int_{\xi_o}^{1}\left(\frac{d\overline{I}_{fx}}{d\xi} + \frac{d\overline{I}_{fz}}{d\xi}\right) d\xi$$

$$\overline{M}_{\phi_n u} = 2\mu\int_{0}^{1} f_{\phi_n}^{*}\,\theta_o\,\overline{m}\,d\xi$$

$$\overline{M}_{\phi_n v} = -2\mu\int_{0}^{1}\left\{\int_{0}^{\xi}\frac{d\overline{\phi}_1}{d\xi_1}\,\frac{df_{\phi_n}}{d\xi}\,d\xi + \epsilon_b\frac{b_1}{R}\,\overline{C}_z\,\frac{df_{\phi_n}}{d\xi} + f_{\phi_n}\beta_{10}\right\}\overline{m}\,d\xi$$

$$\overline{M}_{\beta_1 u} = 0$$

$$\overline{M}_{\beta_1 v} = -2\mu\int_{0}^{1}\left(\beta_{10}\,\xi + \epsilon_b\frac{b_1}{R}\,\overline{C}_z + \overline{\phi}_1\right)\overline{m}\,d\xi$$

$$\overline{M}_{\theta_1 u} = 2\mu\frac{b_1}{R}\int_{0}^{1}\epsilon_b f_{\theta_1}\left[\overline{C}_z - (\theta_o + \theta_1)\,\overline{C}_x\right]\overline{m}\,d\xi$$

$$\overline{M}_{\theta_1 v} = 2\mu\frac{b_1}{R}\int_{0}^{1}\epsilon_b\,\overline{C}_x f_{\theta_1}\left(\beta_{10} + \frac{d\overline{\phi}_1}{d\xi}\right)\overline{m}\,d\xi$$

Generalized Mass Coefficients (continued)

$$\overline{M}_{\beta_2 u} = 0$$

$$\overline{M}_{\beta_2 v} = \mu(\overline{M}_H \bar{l}_H + 2\bar{\delta}_v)$$

$$\overline{M}_{u\beta_1} = 0$$

$$\overline{M}_{u\phi_N} = \frac{1}{2}\overline{M}_{\phi_n u}$$

$$\overline{M}_{u\theta_1} = \frac{1}{2}\overline{M}_{\theta_1 u}$$

$$\overline{M}_{u\beta_2} = 0$$

$$\overline{M}_{uu} = \mu(M_H + 2)$$

$$\overline{M}_{uv} = 0$$

$$\overline{M}_{v\phi_n} = \frac{1}{2}\overline{M}_{\phi_n v}$$

$$\overline{M}_{v\theta_1} = \frac{1}{2}\overline{M}_{\theta_1 v}$$

$$\overline{M}_{v\beta_1} = \frac{1}{2}\overline{M}_{\beta_1 v}$$

$$\overline{M}_{v\beta_2} = \overline{M}_{\beta_2 v}$$

$$\overline{M}_{vu} = 0$$

$$\overline{M}_{vv} = \overline{M}_{uu}$$

Generalized Centrifugal Force Coefficients

$$\overline{T}_{\phi_n \phi_n} = \mu \left[-\int_0^{'} \left(\frac{df_{\phi_n}}{d\xi}\right)^2 \left(\int_{\xi}^{'} \xi_1 \, \overline{m} \, d\xi_1 \right) d\xi + \left(\frac{df_{\phi_n}}{d\xi}\right)^2_{\xi=0} \overline{I}_{\Xi(root)} \right]$$

$$\overline{T}_{\phi_n \theta_1} = \mu \, \frac{b_{ref}}{R} \int_0^{'} \epsilon_b \, \xi \, \frac{df_{\phi_n}}{d\xi} \, \overline{m} (f_{\theta_1} \overline{C}_x + \overline{h}) \, d\xi$$

$$\overline{T}_{\phi_n \beta_1} = -\mu \int_0^{'} f_{\phi_n} (\xi + \overline{\delta}_n) \, \overline{m} \, d\xi$$

$$\overline{T}_{\phi_n \beta_2} = -2\mu \, \overline{\delta}_v \int_0^{'} \left[\int_0^{\xi} \frac{d\overline{\phi}_1}{d\xi_1} \frac{df_{\phi_n}}{d\xi_1} + \epsilon_b \, \frac{b_{ref}}{R} \, \overline{C}_{\Xi} \, \frac{df_{\phi_n}}{d\xi} + f_{\phi_n} \beta_1 \right] \overline{m} \, d\xi$$

$$\overline{T}_{\phi_n \tau} = \mu \, \frac{b_{ref}}{R} \int_{\xi_0}^{'} \epsilon_b \, \xi \, \frac{df_{\phi_n}}{d\xi} (\overline{C}_{fx} - \overline{x}_f) \, \overline{m}_f \, d\xi$$

$$\overline{T}_{\theta_n \theta_1} = \overline{T}_{\phi_n \theta_1}$$

$$\overline{T}_{\theta_1 \theta_1} = \mu \int_0^{'} \left\{ f_{\theta_1}^2 \left[\frac{d\overline{I}_{\Xi_1}}{d\xi} - \frac{d\overline{I}_{x_1}}{d\xi} \right] - \epsilon_b^2 \left(\frac{b_{ref}}{R}\right)^2 \overline{m} \left[f_{\theta_1}^2 \overline{C}_x \overline{l} + (\overline{l} + \overline{C}_x) \overline{q} \right] \right\} d\xi$$

$$\overline{T}_{\theta_1 \beta_1} = \mu \, \frac{b_{ref}}{R} \int_0^{'} \epsilon_b \, \xi \, \overline{m} (f_{\theta_1} \overline{C}_x + \overline{h}) \, d\xi$$

$$\overline{T}_{\theta_1 \beta_2} = 2\mu \, \overline{\delta}_v \, \frac{b_{ref}}{R} \int_0^{'} \left(\frac{d\overline{\phi}_1}{d\xi} + \beta_1\right) \left(f_{\theta_1} \overline{C}_x + \overline{h}\right) \overline{m} \, d\xi$$

$$\overline{T}_{\theta_1 \tau} = \mu \int_{\xi_0}^{'} f_{\theta_1} \left\{ \frac{d\overline{I}_{f\Xi}}{d\xi} - \frac{d\overline{I}_{fx}}{d\xi} + \overline{m}_f \left(\frac{b_{ref}}{R}\right)^2 \epsilon_b^2 \left[\overline{x}_f (\overline{x}_f + \overline{l} - \overline{C}_{fx}) - \overline{l} \, \overline{C}_{fx} \right] \right\} d\xi$$

$$\overline{T}_{\beta_1 \phi_n} = \overline{T}_{\phi_n \beta_1}$$

$$\overline{T}_{\beta_1 \theta} = \overline{T}_{\theta_1 \beta_1}$$

Generalized Centrifugal Force Coefficients (continued)

$$\overline{T}_{\beta_1\beta_1} = \mu\left[\overline{I}_{z_1(root)} - \int_0^1 \xi(\xi + \overline{\delta}_h)\,\overline{m}\,d\xi\right]$$

$$\overline{T}_{\beta_1\beta_2} = -2\mu\overline{\delta}_v\int_0^1\left(\beta_1\xi + \frac{b_{ref}}{R}\epsilon_b\overline{C}_z + \overline{\phi}_1\right)\overline{m}\,d\xi$$

$$\overline{T}_{\beta_1\tau} = \mu\,\frac{b_{ref}}{R}\int_0^1 \epsilon_b\xi\,(\overline{C}_{fx} - \overline{x}_f)\,\overline{m}_f\,d\xi$$

$$\overline{T}_{\beta_2\phi_n} = \frac{1}{2}\,\overline{T}_{\phi_n\beta_2}$$

$$T_{\beta_2\theta_1} = \frac{1}{2}\,\overline{T}_{\theta_1\beta_2}$$

$$T_{\beta_2\beta_1} = \frac{1}{2}\,\overline{T}_{\beta_1\beta_2}$$

$$\overline{T}_{\beta_2\beta_2} = \mu\left\{\frac{1}{M_bR^2}\int_{HUb}\left[(\overline{\delta}_v - z)^2 - y^2\right]d\overline{m} + 2\left(\overline{\delta}_v^2 - \overline{\delta}_h^2\right) - 2\overline{\delta}_h\int_0^1\xi\overline{m}\,d\xi\right\}$$

$$T_{\beta_2\tau} = \mu\overline{\delta}_v\frac{b_{ref}}{R}\int_{\xi_0}^1 \epsilon_b\left(\frac{d\overline{\phi}_1}{d\xi} + \beta_1\right)\left(\overline{C}_{fx} - \overline{x}_f\right)\overline{m}_f\,d\xi$$

$$\overline{T}_{\tau\phi_n} = \overline{T}_{\phi_n\tau}$$

$$\overline{T}_{\tau\theta_1} = \overline{T}_{\theta_1\tau}$$

$$\overline{T}_{\tau\beta_1} = \overline{T}_{\beta_1\tau}$$

$$\overline{T}_{\tau\beta_2} = 2\overline{T}_{\beta_2\tau}$$

$$\overline{T}_{\tau\tau} = \mu\int_{\xi_0}^1\left\{\frac{d\overline{I}_{fz}}{d\xi} - \frac{d\overline{I}_{fx}}{d\xi} + \overline{m}_f\left(\frac{b_{ref}}{R}\right)^2\epsilon_b^2\left[\overline{x}_f(\overline{x}_f + l - \overline{C}_{fx}) - l\overline{C}_{fx}\right]\right\}d\xi$$

$$\overline{T}_{\phi_n u} = \overline{M}_{\phi_n u}$$

Generalized Centrifugal Force Coefficients (continued)

$$\overline{T}_{\phi_n v} = \overline{M}_{\phi_n v}$$

$$\overline{T}_{\beta_1 u} = 0$$

$$\overline{T}_{\beta_1 v} = \overline{M}_{\beta_1 v}$$

$$\overline{T}_{\theta_1 u} = \overline{M}_{\theta_1 u}$$

$$\overline{T}_{\theta_1 v} = \overline{M}_{\theta_1 v}$$

$$\overline{T}_{\beta_2 u} = 0$$

$$\overline{T}_{\beta_2 v} = \overline{M}_{\beta_2 v}$$

$$\overline{T}_{u\beta_1} = 0$$

$$\overline{T}_{u\phi_n} = \overline{M}_{u\phi_n}$$

$$\overline{T}_{u\theta_1} = \overline{M}_{u\theta_1}$$

$$\overline{T}_{u\beta_2} = 0$$

$$\overline{T}_{uu} = \overline{M}_{uu}$$

$$\overline{T}_{uv} = 0$$

$$\overline{T}_{v\phi_n} = \overline{M}_{v\phi_n}$$

$$\overline{T}_{v\theta_1} = \overline{M}_{v\theta_1}$$

$$\overline{T}_{v\beta_1} = \overline{M}_{v\beta_1}$$

$$\overline{T}_{v\beta_2} = \overline{M}_{v\beta_2}$$

$$\overline{T}_{vu} = 0$$

$$\overline{T}_{vv} = \overline{M}_{vv}$$

Generalized Gyroscopic Coupling Coefficients

$$G_{i,j} \equiv 0, \quad i = j$$

$$G_{\phi_n \theta_1} = 0$$

$$\bar{G}_{\phi_n \beta_1} = -\mu \int_0^1 (\bar{\phi}_1 + \beta_1 \xi) f_{\phi_n}^* \theta_0 \bar{m} \, d\xi$$

$$\bar{G}_{\phi_n \beta_2} = 2\mu \bar{\delta}_v \int_0^1 f_{\phi_n}^* \theta_0 \bar{m} \, d\xi$$

$$\bar{G}_{\phi_n \tau} = 0$$

$$\bar{G}_{\theta_1 \phi_n} = 0$$

$$\bar{G}_{\theta_1 \beta_1} = +\mu \int_0^1 f_{\theta_1} \frac{d\bar{I}_{z_1}}{d\xi} \, d\xi$$

$$\bar{G}_{\theta_1 \beta_2} = -2\mu \bar{\delta}_v \frac{b_{ref}}{R} \int_0^1 \epsilon_b f_{\theta_1} \bar{C}_z (\theta_0 + \theta_1) \bar{m} \, d\xi$$

Generalized Gyroscopic Coupling Coefficients (continued)

$$\bar{G}_{\theta_1 \tau} = 0$$

$$\bar{G}_{\beta_1 \phi_n} = -\bar{G}_{\phi_n \beta_1}$$

$$\bar{G}_{\beta_1 \theta_1} = -\bar{G}_{\theta_1 \beta_1}$$

$$\bar{G}_{\beta_1 \beta_2} = 0$$

$$\bar{G}_{\beta_1 \tau} = 0$$

$$\bar{G}_{\beta_2 \phi_n} = -\frac{1}{2} \bar{G}_{\phi_n \beta_2}$$

$$\bar{G}_{\beta_2 \theta_1} = -\frac{1}{2} \bar{G}_{\theta_1 \beta_2}$$

$$\bar{G}_{\beta_2 \beta_1} = 0$$

$$\bar{G}_{\beta_2 \tau} = 0$$

$$\bar{G}_{\tau \phi_n} = 0$$

Generalized Gyroscopic Coupling Coefficients (continued)

$$\bar{G}_{\tau\theta_1} = 0$$

$$\bar{G}_{\tau\beta_1} = 0$$

$$\bar{G}_{\tau\beta_2} = 0$$

$$\bar{G}_{\phi_n u} = -\bar{M}_{\phi_n v}$$

$$\bar{G}_{\phi_n v} = \bar{M}_{\phi_n u}$$

$$\bar{G}_{\theta_1 u} = -M_{\theta_1 v}$$

$$\bar{G}_{\theta_1 v} = \bar{M}_{\theta_1 u}$$

$$\bar{G}_{\beta_1 u} = -\bar{M}_{\beta_1 v}$$

$$\bar{G}_{\beta_1 v} = 0$$

$$\bar{G}_{\beta_2 u} = -\bar{M}_{\beta_2 v}$$

$$\bar{G}_{\beta_2 v} = 0$$

$$\bar{G}_{u\phi_n} = \bar{M}_{v\phi_n}$$

$$\bar{G}_{u\theta_1} = \bar{M}_{v\theta_1}$$

$$\bar{G}_{u\beta_1} = \bar{M}_{v\beta_1}$$

$$\bar{G}_{u\beta_2} = \bar{M}_{v\beta_2}$$

$$\bar{G}_{uu} = 0$$

$$\bar{G}_{uv} = \bar{M}_{uu}$$

$$\bar{G}_{v\phi_n} = -M_{u\phi_n}$$

$$\bar{G}_{v\theta_1} = -M_{u\theta_1}$$

71

63-9

APPENDIX I (Continued)

Generalized Gyroscopic Coupling Coefficients (continued)

$$\bar{G}_{v\beta_1} = 0$$

$$\bar{G}_{v\beta_2} = 0$$

$$\bar{G}_{vu} = -\bar{M}_{uu}$$

$$\bar{G}_{vv} = 0$$

APPENDIX I (Continued)

Generalized Stiffness Coefficients

$$\overline{K}_{ij} = 0, \quad i \neq j$$

$$\overline{K}_{\phi_n \phi_n} = \frac{1}{\rho\, b_{ref}\, R^5 \Omega^2} \int_0^1 EI\left(\frac{d^2 f_{\phi_n}}{d\xi^2}\right)^2 d\xi \equiv \overline{M}_{\phi_n \phi_n} \frac{\bar{\omega}_{\phi_n}^2}{\Omega^2}$$

$$\overline{K}_{\theta_1 \theta_1} = \frac{1}{\rho\, b_{ref}\, R \Omega^2} \int_0^1 GJ\left(\frac{d f_{\theta_1}}{d\xi}\right)^2 d\xi \equiv \overline{M}_{\theta_1 \theta_1} \frac{\bar{\omega}_{\theta_1}^2}{\Omega^2}$$

$$\overline{K}_{\beta_1 \beta_1} = 0$$

$$\overline{K}_{\beta_2 \beta_2} = 0$$

$$\overline{K}_{\tau\tau} \equiv M_{\tau\tau} \frac{\bar{\omega}_{\tau}^2}{\Omega^2}$$

APPENDIX I (Continued)

Generalized Aerodynamic Force Coefficients

$$\overline{A}_{\phi_n \phi_n} = \frac{b_{ref}}{R} \int_{\overline{r}_0}^{B} \epsilon_b^2 \xi f_{\phi_n} \frac{df_{\phi_n}}{d\xi} \left[\frac{1}{4} \frac{\partial C_L}{\partial(t/2b)} + (\overline{I}+\overline{Q})\left(\frac{\partial C_L}{\partial \alpha} - C_L\right) \right] d\xi$$

$$- i\nu \int_{\overline{r}_0}^{B} \epsilon_b \xi f_{\phi_n}^2 \left(\frac{\partial C_L}{\partial \alpha} - C_J\right) d\xi$$

$$\overline{A}_{\phi_n \theta_1} = \int_{\overline{r}_0}^{B} \epsilon_b \xi^2 f_{\phi_n} f_{\theta_1} \frac{\partial C_L}{\partial} d\xi + i\nu \frac{b_{ref}}{R} \int_{\overline{r}_0}^{B} \epsilon_b^2 \xi^2 f_{\phi_n} \left[\frac{f_{\theta_1}}{4} \frac{\partial C_L}{\partial(t/2b)} \right.$$

$$\left. + \left(f_{\theta_1} \overline{Q} + \overline{h}\right)\left(\frac{\partial C_L}{\partial \alpha} - C_J\right) \right] d\xi$$

$$\overline{A}_{\phi_n \beta_1} = \frac{b_{ref}}{R} \int_{\overline{r}_0}^{B} \epsilon_b^2 \xi f_{\phi_n} \left[\frac{1}{4} \frac{\partial C_L}{\partial(t/2b)} + (\overline{I}+\overline{Q})\left(\frac{\partial C_L}{\partial \alpha} - C_J\right) \right] d\xi$$

$$- i\nu \int_{\overline{r}_0}^{B} \epsilon_b \xi^2 f_{\phi_n} \left(\frac{\partial C_L}{\partial \alpha} - C_J\right) d\xi$$

$$\overline{A}_{\phi_n \beta_2} = -2 i\nu \overline{\delta}_n \int_{\overline{r}_0}^{B} \epsilon_b \xi f_{\phi_n} \left(\frac{\partial C_L}{\partial \alpha} - C_J\right) d\xi$$

$$\overline{A}_{\phi_n \tau} = \int_{\overline{r}_0}^{B} \epsilon_b \xi^2 f_{\phi_n} \frac{\partial C_L}{\partial \tau} d\xi + i\nu \frac{b_{ref}}{R} \int_{\overline{r}_0}^{B} \epsilon_b^2 \xi f_{\phi_n} \frac{\partial C_L}{\partial \tau} d\xi$$

$$\overline{A}_{\theta_1 \phi_n} = -\left(\frac{b_{ref}}{R}\right)^2 \int_{\overline{r}_0}^{B} \epsilon_b^3 \xi \frac{df_{\phi_n}}{d\xi} \left\{ 2 f_{\theta_1} \left[\frac{1}{4}\left(\frac{\partial C_M}{\partial(t/2b)} - \frac{1}{2}\frac{\partial C_L}{\partial(t/2b)}\right) + (\overline{I}+Q)\left(\frac{\partial C_M}{\partial \alpha} - \frac{1}{2}\frac{\partial C_L}{\partial \alpha}\right) \right] \right.$$

$$\left. + \left(f_{\theta_1} \overline{Q} + \overline{h}\right)\left[\frac{1}{4}\frac{\partial C_L}{\partial(t/2b)} + (\overline{I}+\overline{Q})\left(\frac{\partial C_L}{\partial \alpha} - C_J\right) \right] \right\} d\xi$$

$$+ i\nu \frac{b_{ref}}{R} \int_{\overline{r}_0}^{B} \epsilon_b^2 \xi f_{\phi_n} \left[2 f_{\theta_1}\left(\frac{\partial C_M}{\partial \alpha} - \frac{1}{2}\frac{\partial C_L}{\partial \alpha}\right) + \left(f_{\theta_1} \overline{Q} + \overline{h}\right)\left(\frac{\partial C_L}{\partial \alpha} - C_J\right) \right] d\xi$$

74

63-9

Generalized Aerodynamic Force Coefficients (continued)

$$\bar{A}_{\theta_1\theta_1} = -\frac{b_{ref}}{R}\int_{\bar{r}_0}^{B}\epsilon_b^2\,\xi^2\left[2f_{\theta_1}^2\left(\frac{\partial C_M}{\partial\alpha}-\frac{1}{2}\frac{\partial C_L}{\partial\alpha}\right)+\left(f_{\theta_1}^2\bar{Q}+\bar{g}\right)\left(\frac{\partial C_L}{\partial\alpha}-C_J\right)\right]d\xi$$

$$-i\nu\left(\frac{b_{ref}}{R}\right)\int_{\bar{r}_0}^{B}\epsilon_b^3\,\xi\left\{2f_{\theta_1}\left[\frac{f_{\theta_1}}{4}\left(\frac{\partial C_M}{\partial(t/2b)}-\frac{1}{2}\frac{\partial C_L}{\partial(t/2b)}\right)+\left(f_{\theta_1}\bar{Q}+\bar{h}\right)\left(\frac{\partial C_M}{\partial\alpha}-\frac{1}{2}\frac{\partial C_L}{\partial\alpha}\right)\right]d\xi\right.$$

$$\left.+\left(f_{\theta_1}\bar{Q}+\bar{h}\right)\left[\frac{f_{\theta_1}}{4}\frac{\partial C_L}{\partial(t/2b)}+\left(f_{\theta_1}\bar{Q}+\bar{h}\right)\left(\frac{\partial C_L}{\partial\alpha}-C_J\right)\right]\right\}d\xi$$

$$\bar{A}_{\theta_1\beta_1} = -\left(\frac{b_{ref}}{R}\right)^2\int_{\bar{r}_0}^{B}\epsilon_b^3\,\xi\left\{2f_{\theta_1}\left[\frac{1}{4}\left(\frac{\partial C_m}{\partial(t/2b)}-\frac{1}{2}\frac{\partial C_L}{\partial(t/2b)}\right)+\left(\bar{l}+\bar{Q}\right)\left(\frac{\partial C_M}{\partial\alpha}-\frac{1}{2}\frac{\partial C_L}{\partial\alpha}\right)\right]\right.$$

$$\left.+\left(f_{\theta_1}\bar{Q}+\bar{h}\right)\left[\frac{1}{4}\frac{\partial C_L}{\partial(t/2b)}+\left(l+Q\right)\left(\frac{\partial C_L}{\partial\alpha}-C_J\right)\right]\right\}d\xi$$

$$+i\nu\frac{b_{ref}}{R}\int_{\bar{r}_0}^{B}\epsilon_b^2\,\xi^2\left[2f_{\theta_1}\left(\frac{\partial C_M}{\partial\alpha}-\frac{1}{2}\frac{\partial C_L}{\partial\alpha}\right)+\left(f_{\theta_1}\bar{Q}+\bar{h}\right)\left(\frac{\partial C_L}{\partial\alpha}-C_J\right)\right]d\xi$$

$$\bar{A}_{\theta_1\beta_2} = -2i\nu\frac{b_{ref}}{R}\delta_h\int_{\bar{r}_0}^{B}\epsilon_b^2\,\xi\left[2f_{\theta_1}\left(\frac{\partial C_M}{\partial\alpha}-\frac{1}{2}\frac{\partial C_L}{\partial\alpha}\right)+\left(f_{\theta_1}\bar{Q}+\bar{h}\right)\left(\frac{\partial C_L}{\partial\alpha}-C_J\right)\right]d\xi$$

$$\bar{A}_{\theta_1\tau} = -\frac{b_{ref}}{R}\int_{\bar{r}_0}^{B}\epsilon_b^2\,\xi^2 f_{\theta_1}\left[2\left(\frac{\partial C_M}{\partial\tau}-\frac{1}{2}\frac{\partial C_L}{\partial\tau}\right)+\bar{Q}\frac{\partial C_L}{\partial\tau}\right]d\xi$$

$$-i\nu\left(\frac{b_{ref}}{R}\right)^2\int_{\bar{r}_0}^{B}\epsilon_b^3\,\xi f_{\theta_1}\left[2\left(\frac{\partial C_M}{\partial\tau}-\frac{1}{2}\frac{\partial C_L}{\partial\tau}\right)+\bar{Q}\frac{\partial C_L}{\partial\tau}\right]$$

$$\bar{A}_{\beta_1\theta_n} = \frac{b_{ref}}{R}\int_{\bar{r}_0}^{B}\epsilon_b^2\,\xi^2\frac{df_{\theta_n}}{d\xi}\left|\frac{1}{4}\frac{\partial C_L}{\partial(t/2b)}+\left(\bar{l}+\bar{Q}\right)\left(\frac{\partial C_L}{\partial\alpha}-C_J\right)\right|d\xi-i\nu\int_{\bar{r}_0}^{B}\epsilon_b\,\xi^2 f_{\theta_n}\left(\frac{\partial C_L}{\partial\alpha}-C_J\right)d\xi$$

Generalized Aerodynamic Force Coefficients (continued)

$$\bar{A}_{\beta,\theta_1} = \int_{\bar{r}_0}^{B} \epsilon_b \xi^3 f_{\theta_1} \frac{\partial C_L}{\partial \alpha} d\xi + i\nu \frac{b_{ref}}{R}\int_{\bar{r}_0}^{B} \epsilon_b^2 \xi^2 \left[\frac{f_{\theta_1}}{4}\frac{\partial C_L}{\partial(t/2b)} + (f_{\theta_1}\bar{Q}+\bar{h})\left(\frac{\partial C_L}{\partial\alpha}-C_J\right)\right]d\xi$$

$$\bar{A}_{\beta,\beta_1} = \frac{b_{ref}}{R}\int_{\bar{r}_0}^{B} \epsilon_b^2 \xi^2 \left|\frac{1}{4}\frac{\partial C_L}{\partial(t/2b)} + (\bar{\ell}+\bar{Q})\left(\frac{\partial C_L}{\partial\alpha}-C_J\right)\right. d\xi - i\nu\int_{\bar{r}_0}^{B}\epsilon_b\xi^3\left(\frac{\partial C_L}{\partial\alpha}-C_J\right)d\xi$$

$$\bar{A}_{\beta,\beta_2} = -2i\nu\bar{\delta}_h\int_{\bar{r}_0}^{B}\epsilon_b\xi^2\left(\frac{\partial C_L}{\partial\alpha}-C_J\right)d\xi$$

$$\bar{A}_{\beta,\tau} = \int_{\bar{r}_0}^{B}\epsilon_b\xi^3\frac{\partial C_L}{\partial\tau}d\xi + i\nu\frac{b_{ref}}{R}\int_{\bar{r}_0}^{B}\epsilon_b^2\xi^2\frac{\partial C_L}{\partial\tau}d\xi$$

$$\bar{A}_{\beta_2,\phi_n} = \int_{\bar{r}_0}^{B}\epsilon_b\xi\frac{df_{\phi_n}}{d\xi}\left\{\bar{\delta}_h\epsilon_b\frac{b_{ref}}{R}\left[\frac{1}{4}\frac{\partial C_L}{\partial(t/2b)}+(\bar{\ell}+\bar{Q})\left(\frac{\partial C_L}{\partial\alpha}-C_J\right)\right]\right.$$

$$-\bar{\delta}_v\xi\left[\frac{\partial C_L}{\partial\alpha}\left(\theta_0+\theta_1-\frac{W_0}{\Omega\xi R}\right)+\frac{\partial C_L}{\partial\tau}\tau+\frac{\partial C_L}{\partial(t/2b)}\left(\frac{t}{2b}\right)\right]\right\}d\xi$$

$$-i\nu\bar{\delta}_h\int_{\bar{r}_0}^{B}\epsilon_b\xi f_{\phi_n}\left(\frac{\partial C_L}{\partial\alpha}-C_J\right)d\xi$$

$$\bar{A}_{\beta_2,\theta_1} = \bar{\delta}_h\int_{\bar{r}_0}^{B}\epsilon_b\xi^2 f_{\theta_1}\frac{\partial C_L}{\partial\alpha}d\xi + i\nu\bar{\delta}_h\frac{b_{ref}}{R}\int_{\bar{r}_0}^{B}\epsilon_b^2\xi\left[\frac{f_{\theta_1}}{4}\frac{\partial C_L}{\partial(t/2b)}+(f_{\theta_1}\bar{Q}+\bar{h})\left(\frac{\partial C_L}{\partial\alpha}-C_J\right)\right]$$

$$\bar{A}_{\beta_2,\beta_1} = \int_{\bar{r}_0}^{B}\epsilon_b\xi\left\{\bar{\delta}_h\epsilon_b\frac{b_{ref}}{R}\left[\frac{1}{4}\frac{\partial C_L}{\partial(t/2b)}+(\bar{\ell}+\bar{Q})\left(\frac{\partial C_L}{\partial\alpha}-C_J\right)\right]\right.$$

$$-\bar{\delta}_v\xi\left[\frac{\partial C_L}{\partial\alpha}\left(\theta_0+\theta_1-\frac{W_0}{\Omega\xi R}\right)+\frac{\partial C_L}{\partial\tau}\tau+\frac{\partial C_L}{\partial(t/2b)}\left(\frac{t}{2b}\right)\right]\right\}d\xi - i\nu\bar{\delta}_h\int_{\bar{r}_0}^{B}\epsilon_b\xi^2\left(\frac{\partial C_L}{\partial\alpha}-C_J\right)d\xi$$

Generalized Aerodynamic Force Coefficients (continued)

$$\bar{A}_{\beta_2 \beta_2} = \bar{\delta}_v \int_{\bar{r}_0}^{B} \epsilon_b \xi^2 \left[\frac{\partial C_L}{\partial \alpha} \left(\Theta_o + \Theta_r - \frac{W_o}{\Omega R \xi} \right) + \frac{\partial C_L}{\partial \tau} \tau + \frac{\partial C_L}{\partial (t/2b)} \left(\frac{t}{2b} \right) + C_J \frac{W_o}{\Omega \xi R} \right] d\xi$$

$$- i \nu \bar{\delta}_h^2 \int_{\bar{r}_0}^{B} \epsilon_b \xi \left(\frac{\partial C_L}{\partial \alpha} - C_J \right) d\xi$$

$$\bar{A}_{\beta_2 \tau} = \bar{\delta}_h \int_{\bar{r}_0}^{B} \epsilon_b \xi^2 \frac{\partial C_L}{\partial \tau} d\xi + i \nu \frac{b_{ref}}{R} \bar{\delta}_h \int_{\bar{r}_0}^{B} \epsilon_b^2 \xi \frac{\partial C_L}{\partial \tau} d\xi$$

$$\bar{A}_{\tau \phi_n} = -2 \left(\frac{b_{ref}}{R} \right)^2 \int_{\xi_0}^{B} \epsilon_b^3 \bar{b}_f^2 \xi \frac{df_{\phi_n}}{d\xi} \left[K_\alpha (\bar{l} + \bar{x}_f) + K_{\dot\alpha} \bar{b}_f \right] d\xi$$

$$+ 2 i \nu \frac{b_{ref}}{R} \int_{\xi_0}^{B} \epsilon_b^2 \bar{b}_f^2 \xi f_{\phi_n} K_\alpha d\xi$$

$$\bar{A}_{\tau \Theta_1} = -2 \frac{b_{ref}}{R} \int_{\xi_0}^{B} \epsilon_b^2 \bar{b}_f^2 \xi^2 f_{\Theta_1} K_\alpha d\xi - 2 i \nu \left(\frac{b_{ref}}{R} \right)^2 \int_{\xi_0}^{B} \epsilon_b^3 \bar{b}_f^2 \xi f_{\Theta_1} \left(K_\alpha \bar{x}_f + K_{\dot\alpha} \bar{b}_f \right) d\xi$$

$$\bar{A}_{\tau \beta_1} = -2 \left(\frac{b_{ref}}{R} \right)^2 \int_{\xi_0}^{'} \epsilon_b^3 \bar{b}_f^2 \xi \left[K_\alpha (\bar{l} + \bar{x}_f) + K_{\dot\alpha} \bar{b}_f \right] d\xi + 2 i \nu \frac{b_{ref}}{R} \int_{\xi_0}^{B} \epsilon_b^2 \bar{b}_f^2 \xi^2 K_\alpha d\xi$$

$$\bar{A}_{\tau \beta_2} = 4 i \nu \bar{\delta}_h \frac{b_{ref}}{R} \int_{\xi_0}^{B} \epsilon_b^2 \bar{b}_f^2 \xi K_\alpha d\xi$$

$$\bar{A}_{\tau \tau} = -2 \frac{b_{ref}}{R} \int_{\xi_0}^{B} \epsilon_b^2 \bar{b}_f^2 \xi^2 K_\alpha d\xi - 2 i \nu \left(\frac{b_{ref}}{R} \right)^2 \int_{\xi_0}^{B} \epsilon_b^3 \bar{b}_f^2 K_{\dot\alpha} d\xi$$

63-9

Generalized Aerodynamic Force Coefficients (continued)

$$\bar{A}_{\phi_n u} = \bar{A}_{\theta, u} = \bar{A}_{\beta, u} = \bar{A}_{\beta_2 u} = \bar{A}_{u u} = \bar{A}_{v u} = 0$$

$$A_{\phi_n v} = 2iv\int_{\bar{r}_0}^{B}\epsilon_b\,\xi f_{\phi_n}\left(\beta_{10}+\frac{d\bar{\phi}_1}{d\xi}\right)\left(\frac{\partial C_L}{\partial\alpha}-C_J\right)\;d\xi$$

$$\bar{A}_{\theta, v} = 2iv\,\frac{b_r}{R}\int_{\bar{r}_0}^{B}\epsilon_b^{2}\,\xi f_\theta\left(\beta_{10}+\frac{d\bar{\phi}_1}{d\xi}\right)\left[2\left(\frac{\partial C_M}{\partial\alpha}-\frac{1}{2}\frac{\partial C_L}{\partial\alpha}\right)-\bar{Q}\left(\frac{\partial C_L}{\partial\alpha}-C_J\right)\right]d\xi$$

$$\bar{A}_{\beta, v} = 2iv\int_{\bar{r}_0}^{B}\epsilon_b\,\xi^{2}\left(\beta_{10}+\frac{d\bar{\phi}_1}{d\xi}\right)\left(\frac{\partial C_L}{\partial\alpha}-C_J\right)d\xi$$

$$\bar{A}_{\beta_2 v} = 2iv\,\bar{\delta}_h\int_{\bar{r}_0}^{B}\epsilon_b\,\xi\left(\beta_{10}+\frac{d\bar{\phi}_1}{d\xi}\right)\left(\frac{\partial C_L}{\partial\alpha}-C_J\right)d\xi$$

$$\bar{A}_{u\phi_n} = \frac{b_r}{R}\int_{\bar{r}_0}^{B}\epsilon_b^{2}\,\frac{df_{\phi_n}}{d\xi}\left\{\left(\frac{W_0}{\Omega R}\right)\left[\frac{1}{4}\frac{\partial C_L}{\partial(t/2b)}+(\bar{\imath}+\bar{Q})\left(\frac{2\partial C_L}{\partial\alpha}-C_J\right)\right]\right.$$
$$\left.+\xi(\bar{\imath}+\bar{Q})\left[C_J(\tau+\theta_0+\theta_1)-\frac{\partial C_L}{\partial\alpha}(\theta_0+\theta_1)-\frac{\partial C_L}{\partial\tau}\dot\tau-\frac{\partial C_L}{\partial(t/2b)}\left(\frac{t}{2b}\right)\right]\right\}d\xi$$

$$+iv\int_{\bar{r}_0}^{B}\epsilon_b f_{\phi_n}\left\{\xi\left[\frac{\partial C_L}{\partial\alpha}(\theta_0+\theta_1)+\frac{\partial C_L}{\partial\tau}\tau+\frac{\partial C_L}{\partial(t/2b)}\left(\frac{t}{2b}\right)-C_J(\tau+\theta_0+\theta_1)\right]\right.$$
$$\left.-\left(\frac{W_0}{\Omega R}\right)\left[\frac{2\partial C_L}{\partial\alpha}-C_J\right]\right\}d\xi$$

$$\bar{A}_{u\theta_1} = \int_{\bar{r}_0}^{B}\epsilon_b\,\xi f_{\theta_1}\left\{\xi C_J(\tau+\theta_0+\theta_1)+\left(\frac{W_0}{\Omega R}\right)\left(\frac{\partial C_L}{\partial\alpha}-C_J\right)\right\}d\xi$$

$$+iv\,\frac{b_r}{R}\int_{\bar{r}_0}^{B}\epsilon_b^{2}f_{\theta_1}\left\{\left(\frac{W_0}{\Omega R}\right)\left[\frac{1}{4}\frac{\partial C_L}{\partial(t/2b)}+\bar{Q}\left(\frac{2\partial C_L}{\partial\alpha}-C_J\right)\right]\right.$$
$$\left.+\xi\bar{Q}\left[C_J(\tau+\theta_0+\theta_1)-\frac{\partial C_L}{\partial\alpha}(\theta_0+\theta_1)-\frac{\partial C_L}{\partial(t/2b)}\left(\frac{t}{2b}\right)-\frac{\partial C_L}{\partial\tau}\,\tau\right]\right\}d\xi$$

Generalized Aerodynamic Force Coefficients (continued)

$$\bar{A}_{u\beta_1} = \frac{b_r}{R}\int_{\bar{r}_0}^{B}\epsilon_b^2\left\{\left(\frac{W_0}{\Omega R}\right)\left[\frac{1}{4}\frac{\partial C_L}{\partial(t/2b)}+(\bar{l}+\bar{Q})\left(\frac{2\partial C_L}{\partial\alpha}-C_J\right)\right]\right.$$

$$\left.+\xi(\bar{l}+\bar{Q})\left[C_J(\tau+\theta_0+\theta_1)-\frac{\partial C_L}{\partial\alpha}(\theta_0+\theta_1)-\frac{\partial C_L}{\partial\tau}\tau-\frac{\partial C_L}{\partial(t/2b)}\left(\frac{t}{2b}\right)\right]\right\}d\xi$$

$$+i\upsilon\int_{\bar{r}_0}^{B}\epsilon_b\xi\left\{\xi\left[\frac{\partial C_L}{\partial\alpha}(\theta_0+\theta_1)+\frac{\partial C_L}{\partial\tau}\tau+\frac{\partial C_L}{\partial(t/2b)}\left(\frac{t}{2b}\right)-C_J(\tau+\theta_0+\theta_1)\right]\right.$$

$$\left.-\left(\frac{W_0}{\Omega R}\right)\left[\frac{2\partial C_L}{\partial\alpha}-C_J\right]\right\}d\xi$$

$$\bar{A}_{u\beta_2} = 2i\upsilon\bar{\delta}_h\int_{\bar{r}_0}^{B}\epsilon_b\left\{\xi\left[\frac{\partial C_L}{\partial\alpha}(\theta_0+\theta_1)+\frac{\partial C_L}{\partial(t/2b)}\left(\frac{t}{2b}\right)+\frac{\partial C_L}{\partial\tau}\tau-C_J(\tau+\theta_0+\theta_1)\right]\right.$$

$$\left.-\left(\frac{W_0}{\Omega R}\right)\left[\frac{2\partial C_L}{\partial\alpha}-C_J\right]\right\}d\xi$$

$$\bar{A}_{u\upsilon} = 2i\upsilon\int_{\bar{r}_0}^{B}\epsilon_b\left(\beta_{10}+\frac{d\bar{\phi}_1}{d\xi}\right)\left\{\left(\frac{W_0}{\Omega R}\right)\left(\frac{2\partial C_L}{\partial\alpha}-C_J\right)\right.$$

$$\left.+\xi\left[C_J(\tau+\theta_0+\theta_1)-\frac{\partial C_L}{\partial\alpha}(\theta_0+\theta_1)-\frac{\partial C_L}{\partial(t/2b)}\left(\frac{t}{2b}\right)-\frac{\partial C_L}{\partial\tau}\tau\right]\right\}d\xi$$

$$\bar{A}_{\upsilon\phi_n} = -\int_{\bar{r}_0}^{B}\epsilon_b\xi\frac{df_{\phi_n}}{d\xi}\left\{\xi\left[\frac{\partial C_L}{\partial\alpha}(\theta_0+\theta_1)+\frac{\partial C_L}{\partial\tau}\tau+\frac{\partial C_L}{\partial(t/2b)}\left(\frac{t}{2b}\right)\right]-\frac{W_0}{\Omega R}\frac{\partial C_L}{\partial\alpha}\right\}d\xi$$

$$+i\upsilon\int_{\bar{r}_0}^{B}\epsilon_b\xi f_{\phi_n}\left(\beta_{10}+\frac{d\phi_1}{d\xi}\right)\frac{\partial C_L}{\partial\alpha}\ d\xi$$

$$\bar{A}_{\upsilon\theta_1} = -\int_{\bar{r}_0}^{B}\epsilon_b\xi^2 f_{\theta_1}\left(\beta_{10}+\frac{d\bar{\phi}_1}{d\xi}\right)\frac{\partial C_L}{\partial\alpha}\ d\xi$$

$$-i\upsilon\frac{b_r}{R}\int_{\bar{r}_0}^{B}\epsilon_b^2\xi f_{\theta_1}\left(\beta_{10}+\frac{d\bar{\phi}_1}{d\xi}\right)\left[\frac{1}{4}\frac{\partial C_L}{\partial(t/2b)}+\bar{Q}\frac{\partial C_L}{\partial\alpha}\right]d\xi$$

$$\bar{A}_{\upsilon\beta_1} = -\int_{\bar{r}_0}^{B}\epsilon_b\xi\left\{\xi\left[\frac{\partial C_L}{\partial\alpha}(\theta_0+\theta_1)+\frac{\partial C_L}{\partial\tau}\tau+\frac{\partial C_L}{\partial(t/2b)}\left(\frac{t}{2b}\right)\right]-\frac{W_0}{\Omega R}\frac{\partial C_L}{\partial\alpha}\right\}d\xi$$

$$+i\upsilon\int_{\bar{r}_0}^{B}\epsilon_b\xi^2\left(\beta_{10}+\frac{d\bar{\phi}_1}{d\xi}\right)\frac{\partial C_L}{\partial\alpha}\ d\xi$$

79

63-9

Generalized Aerodynamic Force Coefficients (continued)

$$\bar{A}_{\upsilon\beta_3} = 2i\upsilon\delta_h\int_{\bar{r}_0}^{B}\epsilon_b\zeta\left(\beta_{10}+\frac{d\bar{\phi}_1}{d\xi}\right)\frac{\partial C_L}{\partial\alpha}\,d\xi$$

$$\bar{A}_{\upsilon\upsilon} = -2i\upsilon\int_{\bar{r}_0}^{B}\epsilon_b\zeta\left(\beta_{10}+\frac{d\bar{\phi}_1}{d\xi}\right)^2\frac{\partial C_L}{\partial\alpha}\,d\xi$$

$$I_{\beta_1\beta_1}^{1} = \left(\frac{b_r}{R}\right)^2\int\epsilon_b^2\xi^2\bar{Q}\,d\xi$$

$$I_{\beta_1\beta_1}^{2} = \frac{1}{4}\left(\frac{b_r}{R}\right)^2\int\epsilon_b^2\xi^2\,d\xi$$

$$I_{\beta_1\beta_1}^{3} = \left(\frac{b_r}{R}\right)^2\int\epsilon_b^2\xi\bar{Q}\,d\xi$$

$$I_{\beta_1\beta_1}^{4} = \frac{1}{4}\left(\frac{b_r}{R}\right)^2\int\epsilon_b^2\xi\,d\xi$$

$$I_{\beta_1\beta_1}^{5} = \left(\frac{b_r}{R}\right)\int\epsilon_b\xi^2\,d\xi$$

$$I_{\beta_1\beta_1}^{6} = \frac{1}{2}\left(\frac{b_r}{R}\right)\int\epsilon_b\xi\,d\xi$$

$$I_{\beta_1\dot{\beta}_1}^{1} = \left(\frac{b_r}{R}\right)\int\epsilon_b\xi^3\,d\xi$$

$$I_{\beta_1\dot{\beta}_1}^{2} = I_{\beta_1\beta_1}^{5}$$

$$I_{\beta_1\phi_N}^{1} = \left(\frac{b_r}{R}\right)^2\int\epsilon_b^2\xi^2\bar{Q}\,\frac{df_{\phi_N}}{d\xi}\,d\xi$$

$$I_{\beta_1\phi_N}^{2} = \frac{1}{4}\left(\frac{b_r}{R}\right)^2\int\epsilon_b^2\xi^2\frac{df_{\phi_N}}{d\xi}\,d\xi$$

$$I_{\beta_1\phi_N}^{3} = \left(\frac{b_r}{R}\right)^2\int\epsilon_b^2\xi\bar{Q}\,\frac{df_{\phi_N}}{d\xi}\,d\xi$$

Generalized Aerodynamic Force Coefficients (continued)

$$I_{\beta,\phi_N}^4 = \frac{1}{4}\left(\frac{b_r}{R}\right)^2 \int \epsilon_b^2 \, \zeta \, \frac{df_{\phi_N}}{d\zeta} \, d\zeta$$

$$I_{\beta,\phi_N}^5 = \frac{1}{2}\left(\frac{b_r}{R}\right) \int \epsilon_b \, \zeta \, \frac{df_{\phi_N}}{d\zeta} \, d\zeta$$

$$I_{\beta,\phi_N}^6 = \left(\frac{b_r}{R}\right) \int \epsilon_b \, \zeta^2 \frac{df_{\phi_N}}{d\zeta} \, d\zeta$$

$$I_{\beta,\dot{\phi}_N}^1 = \left(\frac{b_r}{R}\right) \int \epsilon_b \, \zeta^2 f_{\phi_N} \, d\zeta$$

$$I_{\beta,\dot{\phi}_N}^2 = \left(\frac{b_r}{R}\right) \int \epsilon_b \, \zeta \, f_{\phi_N} \, d\zeta$$

$$I_{\beta,\dot{\phi}_N}^3 = \left(\frac{b_r}{R}\right) \int \epsilon_b \left(\beta_1 + \frac{d\bar{\phi}_N}{d\zeta}\right) \zeta f_{\phi_N} \left[2(\overline{W}_0 + \bar{\mu}\tan\alpha_s) - \zeta(\theta_0 + \theta_s + \tau)\right] d\zeta$$

$$I_{\beta,\theta_1}^1 = \left(\frac{b_r}{R}\right) \int \epsilon_b \, \zeta^3 f_{\theta_1} \, d\zeta$$

$$I_{\beta,\theta_1}^2 = \frac{1}{2}\left(\frac{b_r}{R}\right) \int \epsilon_b \, \zeta \, f_{\theta_1} \, d\zeta$$

$$I_{\beta,\theta_1}^3 = 2\left(\frac{b_r}{R}\right) \int \epsilon_b \, \zeta^2 f_{\theta_1} \, d\zeta$$

$$I_{\beta,\theta_1}^4 = \left(\frac{b_r}{R}\right) \int \epsilon_b \, \zeta^2 f_{\theta_1} \left[1 + \frac{df_{\phi_N}}{d\zeta}\right]\left[2(\overline{W}_0 + \bar{\mu}\tan\alpha_s) - \zeta(\theta_0 + \theta_1 + \tau)\right] d\zeta$$

$$I_{\beta,\theta_1}^5 = \frac{1}{2}\left(\frac{b_r}{R}\right) \int \epsilon_b \, \zeta \, f_{\theta_1} \, d\zeta$$

$$I_{\beta,\dot{\theta}_1}^1 = \left(\frac{b_r}{R}\right) \int \epsilon_b^2 \, \zeta^2 \bar{Q} \, f_{\theta_1} \, d\zeta$$

$$I_{\beta,\dot{\theta}_1}^2 = \frac{1}{4}\left(\frac{b_r}{R}\right) \int \epsilon_b^2 \, \zeta^2 f_{\theta_1} \, d\zeta$$

Generalized Aerodynamic Force Coefficients (continued)

$$I^3_{\beta_1 \dot\theta_1} = \left(\frac{b_r}{R}\right)\int \epsilon_b \xi \bar{Q} f_{\theta_1} d\xi$$

$$I^4_{\beta_1 \dot\theta_1} = \left(\frac{b_r}{R}\right)^2 \int \epsilon_b^2 \xi f_{\theta_1} d\xi$$

$$I^1_{\theta_1 \theta_1} = 2\left(\frac{b_r}{R}\right)^2 \int \epsilon_b^2 \xi^2 f_{\theta_1} d\xi$$

$$I^2_{\theta_1 \theta_1} = \left(\frac{b_r}{R}\right)^2 \int \epsilon_b f_{\theta_1} d\xi$$

$$I^3_{\theta_1 \theta_1} = 4\left(\frac{b_r}{R}\right)^2 \int \epsilon_b^2 \xi f_{\theta_1}^2 d\xi$$

$$I^4_{\theta_1 \theta_1} = I^2_{\theta_1 \theta_1}$$

$$I^1_{\theta_1 \dot\theta_1} = \frac{1}{2}\left(\frac{b_r}{R}\right)^3 \int \epsilon_b^3 \xi f_{\theta_1}^2 d\xi$$

$$I^2_{\theta_1 \dot\theta_1} = 2\left(\frac{b_r}{R}\right)^3 \int \epsilon_b^3 \xi \bar{Q} f_{\theta_1}^2 d\xi$$

$$I^3_{\theta_1 \dot\theta_1} = \frac{1}{2}\left(\frac{b_r}{R}\right)^3 \int \epsilon_b^3 f_{\theta_1}^2 d\xi$$

$$I^4_{\theta_1 \dot\theta_1} = 2\left(\frac{b_r}{R}\right)^3 \int \epsilon_b^3 \bar{Q} f_{\theta_1}^2 d\xi$$

$$I^1_{\theta_1 \beta_1} = 2\left(\frac{b_r}{R}\right)^3 \int \epsilon_b^3 \xi \bar{Q} f_{\theta_1} d\xi$$

$$I^2_{\theta_1 \beta_1} = \frac{1}{2}\left(\frac{b_r}{R}\right)^3 \int \epsilon_b^3 \xi f_{\theta_1} d\xi$$

$$I^3_{\theta_1 \beta_1} = 2\left(\frac{b_r}{R}\right)^3 \int \epsilon_b^3 \bar{Q} f_{\theta_1} d\xi$$

Generalized Aerodynamic Force Coefficients (continued)

$$I_{\theta_1 \beta_1}^4 = \frac{1}{2}\left(\frac{b_r}{R}\right)^3 \int \epsilon_b^3 f_{\theta_1} d\xi$$

$$I_{\theta_1 \beta_1}^5 = \left(\frac{b_r}{R}\right)^2 \int \epsilon_b^2 f_{\theta_1} d\xi$$

$$I_{\theta_1 \beta_1}^6 = 8 I_{\beta_1 \dot\theta_1}^4$$

$$I_{\theta_1 \dot\beta_1}^1 = 8 I_{\beta_1 \dot\theta_1}^2$$

$$I_{\theta_1 \dot\beta_1}^2 = 8 I_{\beta_1 \dot\theta_1}^4$$

$$I_{\theta_1 \phi_N}^1 = 2\left(\frac{b_r}{R}\right)^3 \int \epsilon_b^3 \xi \bar{Q} f_{\theta_1} \frac{df_{\phi_N}}{d\xi} d\xi$$

$$I_{\theta_1 \phi_N}^2 = \frac{1}{2}\left(\frac{b_r}{R}\right)^3 \int \epsilon_b^3 \xi f_{\theta_1} \frac{df_{\phi_N}}{d\xi} d\xi$$

$$I_{\theta_1 \phi_N}^3 = 2\left(\frac{b_r}{R}\right)^3 \int \epsilon_b^3 \bar{Q} f_{\theta_1} \frac{df_{\phi_N}}{d\xi} d\xi$$

$$I_{\theta_1 \phi_N}^4 = \frac{1}{2}\left(\frac{b_r}{R}\right)^3 \int \epsilon_b^3 f_{\theta_1} \frac{df_{\phi_N}}{d\xi} d\xi$$

$$I_{\theta_1 \phi_N}^5 = \left(\frac{b_r}{R}\right)^2 \int \epsilon_b^2 f_{\theta_1} \frac{df_{\phi_N}}{d\xi} d\xi$$

$$I_{\theta_1 \phi_N}^6 = 2\left(\frac{b_r}{R}\right)^2 \int \epsilon_b^2 \xi f_{\theta_1} \frac{df_{\phi_N}}{d\xi} d\xi$$

$$I_{\theta_1 \dot\phi_N}^1 = 2\left(\frac{b_r}{R}\right)^2 \int \epsilon_b^2 \xi f_{\theta_1} f_{\phi_N} d\xi$$

$$I_{\theta_1 \dot\phi_N}^2 = 2\left(\frac{b_r}{R}\right)^2 \int \epsilon_b^2 f_{\phi_N} f_{\theta_1} d\xi$$

$$I_{\phi_N \phi_N}^1 = \left(\frac{b_r}{R}\right)^2 \int \epsilon_b^2 \xi \bar{Q} f_{\phi_N} \frac{df_{\phi_N}}{d\xi} d\xi$$

Generalized Aerodynamic Force Coefficients (continued)

$$I^2_{\phi_N \phi_N} = \frac{1}{4}\left(\frac{b_r}{R}\right)^2 \int \epsilon_b^2 \, \xi f_{\phi_N} \frac{df_{\phi_N}}{d\xi} \, d\xi$$

$$I^3_{\phi_N \phi_N} = \left(\frac{b_r}{R}\right) \int \epsilon_b \, \bar{Q} \, f_{\phi_N} \frac{df_{\phi_N}}{d\xi} \, d\xi$$

$$I^4_{\phi_N \phi_N} = \frac{1}{4}\left(\frac{b_r}{R}\right)^2 \int \epsilon_b^2 \, f_{\phi_N} \frac{df_{\phi_N}}{d\xi} \, d\xi$$

$$I^5_{\phi_N \phi_N} = \frac{1}{2}\left(\frac{b_r}{R}\right)^2 \int \epsilon_b \, f_{\phi_N} \frac{df_{\phi_N}}{d\xi} \, d\xi$$

$$I^6_{\phi_N \phi_N} = \left(\frac{b_r}{R}\right) \int \epsilon_b \, \zeta f_{\phi_N} \frac{df_{\phi_N}}{d\xi} \, d\xi$$

$$I^1_{\phi_N \dot{\phi}_N} = \left(\frac{b_r}{R}\right) \int \epsilon_b \, \xi f_{\phi_N}^2 \, d\xi$$

$$I^2_{\phi_N \dot{\phi}_N} = \left(\frac{b_r}{R}\right) \int \epsilon_b \, f_{\phi_N}^2 \, d\xi$$

$$I^1_{\phi_N \theta_1} = \left(\frac{b_r}{R}\right) \int \epsilon_b \, \zeta^2 f_{\theta_1} f_{\phi_N} \, d\xi$$

$$I^2_{\phi_N \theta_1} = \frac{1}{2}\left(\frac{b_r}{R}\right) \int \epsilon_b \, f_{\phi_N} f_{\theta_1} \, d\xi$$

$$I^3_{\phi_N \theta_1} = 2\left(\frac{b_r}{R}\right) \int \epsilon_b \, \xi f_{\phi_N} f_{\theta_1} \, d\xi$$

$$I^4_{\phi_N \theta_1} = \left(\frac{b_r}{R}\right) \int \epsilon_b \, \zeta f_{\phi_N} f_{\theta_1} \left(\beta_1 + \frac{d\bar{\phi}}{d\xi}\right)\left(2\left[\bar{W}_0 + \bar{\mu} \tan \alpha_s\right] - \zeta\left[\theta_0 + \theta_1 + \tau\right]\right) d\xi$$

$$I^5_{\phi_N \theta_1} = I^2_{\phi_N \theta_1}$$

$$I^1_{\phi_N \dot{\theta}_1} = \frac{1}{8} I^1_{\theta_1 \dot{\phi}_N}$$

Generalized Aerodynamic Force Coefficients (continued)

$$I^2_{\phi_N \dot{\theta}_1} = \left(\frac{b_r}{R}\right)^2 \int \epsilon_b^2 \, \xi \, \bar{Q} \, f_{\phi_N} \, f_{\theta_1} \, d\xi$$

$$I^3_{\phi_N \dot{\theta}_1} = \frac{1}{4}\left(\frac{b_r}{R}\right)^2 \int \epsilon_b^2 \, f_{\phi_N} \, f_{\theta_1} \, d\xi$$

$$I^4_{\phi_N \dot{\theta}_1} = \left(\frac{b_r}{R}\right)^2 \int \epsilon_b^2 \, \bar{Q} \, f_{\phi_N} \, f_{\theta_1} \, d\xi$$

$$I^1_{\phi_N \beta_1} = \left(\frac{b_r}{R}\right) \int \epsilon_b \, \xi \, \bar{Q} \, f_{\phi_N} \, d\xi$$

$$I^2_{\phi_N \beta_1} = \frac{1}{4}\left(\frac{b_r}{R}\right)^2 \int \epsilon_b^2 \, \xi \, f_{\phi_N} \, d\xi$$

$$I^3_{\phi_N \beta_1} = \left(\frac{b_r}{R}\right)^2 \int \epsilon_b^2 \, \bar{Q} \, f_{\phi_N} \, d\xi$$

$$I^4_{\phi_N \beta_1} = \frac{1}{4}\left(\frac{b_r}{R}\right) \int \epsilon_b^2 \, f_{\phi_N} \, d\xi$$

$$I^5_{\phi_N \beta_1} = \frac{1}{2}\left(\frac{b_r}{R}\right) \int \epsilon_b \, f_{\phi_N} \, d\xi$$

$$I^6_{\phi_N \beta_1} = I^2_{\beta_1 \dot{\phi}_N}$$

$$I^1_{\phi_N \dot{\beta}_1} = I^1_{\beta_1 \dot{\phi}_N}$$

$$I^2_{\phi_N \dot{\beta}_1} = I^2_{\beta_1 \dot{\phi}_N}$$

$$I^3_{\phi_N \dot{\beta}_1} = I^3_{\beta_1 \dot{\phi}_N}$$

$$I^1_{\beta_1 \tau} = \left(\frac{b_r}{R}\right) \int \epsilon_b \, (\xi + \bar{\delta}_h)^2 \, \xi \, d\xi$$

$$I^2_{\beta_1 \tau} = \frac{1}{2}\left(\frac{b_r}{R}\right) \int \epsilon_b \, \xi \, d\xi$$

APPENDIX I (Continued)

Generalized Aerodynamic Force Coefficients (continued)

$$I_{\beta,\tau}^{3} = 2\left(\frac{b_r}{R}\right)\int \epsilon_b(\xi + \bar{\delta}_h)\xi \, d\xi$$

$$I_{\beta,\tau}^{4} = I_{\beta,\tau}^{2}$$

$$I_{\beta,\dot{\tau}}^{\prime} = \left(\frac{b_r}{R}\right)^{2}\int \epsilon_b^{2}(\xi + \bar{\delta}_h)\,\xi \, d\xi$$

$$I_{\beta,\dot{\tau}}^{2} = \left(\frac{b_r}{R}\right)\int \epsilon_b^{2}\,\xi \, d\xi$$

$$I_{\phi\tau}^{\prime} = \left(\frac{b_r}{R}\right)\int \epsilon_b(\xi + \delta_h)^{2} f_{\phi_N} \, d\xi$$

$$I_{\phi_N\tau}^{2} = \frac{1}{2}\left(\frac{b_r}{R}\right)\int \epsilon_b f_{\phi_N} \, d\xi$$

$$I_{\phi_N\tau}^{3} = 2\left(\frac{b_r}{R}\right)\int \epsilon_b(\xi + \bar{\delta}_h)\, f_{\phi_N} \, d\xi$$

$$I_{\phi_N\tau}^{4} = I_{\phi_N\tau}^{2}$$

$$I_{\phi_N\dot{\tau}}^{\prime} = \left(\frac{b_r}{R}\right)^{2}\int \epsilon_b^{2}(\xi + \bar{\delta}_h)\, f_{\phi_N} \, d\xi$$

$$I_{\phi_N\dot{\tau}}^{2} = \left(\frac{b_r}{R}\right)^{2}\int \epsilon_b^{2}\, f_{\phi_N} \, d\xi$$

$$I_{\theta,\tau}^{\prime} = 2\left(\frac{b_r}{R}\right)^{2}\int \epsilon_b^{2}(\xi + \bar{\delta}_h)^{2} f_{\theta_1} \, d\xi$$

$$I_{\theta,\tau}^{2} = \left(\frac{b_r}{R}\right)^{2}\int \epsilon_b^{2}\, f_{\theta_1} \, d\xi$$

86

63-9

Generalized Aerodynamic Force Coefficients (continued)

$$I_{\theta,\tau}^{3} = 4\left(\frac{b_r}{R}\right)^{2}\int \epsilon_b^{2}(\xi + \bar{\delta}_h)\, f_{\theta_1}\, d\xi$$

$$I_{\theta,\tau}^{4} = \left(\frac{b_r}{R}\right)\int \epsilon_b\, f_{\theta_1}\, d\xi$$

$$I_{\theta,\tau}^{1} = 2\left(\frac{b_r}{R}\right)^{3}\int \epsilon_b^{3}(\xi + \bar{\delta}_h)\, f_{\theta_1}\, d\xi$$

$$I_{\theta,\dot{\tau}}^{2} = 2\left(\frac{b_r}{R}\right)^{3}\int \epsilon_b^{3}\, f_{\theta_1}\, d\xi$$

APPENDIX II

DERIVATION OF QUASI-STEADY AERODYNAMIC COEFFICIENTS

FOR A TWO-DIMENSIONAL JET-FLAP AIRFOIL

A. CONSTANT JET ANGLE

In Reference 14, the lift and moment coefficients for a zero-thickness two-dimensional jet-flap airfoil with parabolic camber are derived for the steady case. These coefficients may be expressed as in Equations (II. 1) and (II. 2) below.

$$(\text{II. 1}) \qquad C_L = \frac{\partial C_L}{\partial \tau} \tau + \frac{\partial C_L}{\partial \alpha} \alpha + \frac{\partial C_L}{\partial (t/2b)} \left(\frac{t}{2b} \right)$$

$$(\text{II. 2}) \qquad C_M = \frac{\partial C_M}{\partial \tau} \tau + \frac{\partial C_M}{\partial \alpha} \alpha + \frac{\partial C_M}{\partial (t/2b)} \left(\frac{t}{2b} \right)$$

where τ, α, t and b are, respectively, the angle of the jet with respect to the airfoil chordline, angle of attack, maximum camber and the airfoil semichord. The moment coefficient C_M is defined to be positive for a nose-down moment about the leading edge. The derivatives

$$\frac{\partial C_L}{\partial \alpha} \quad , \quad \frac{\partial C_M}{\partial \alpha} \quad , \text{ etc., are functions only of the jet coefficient } C_J ,$$

the latter quantity being defined by

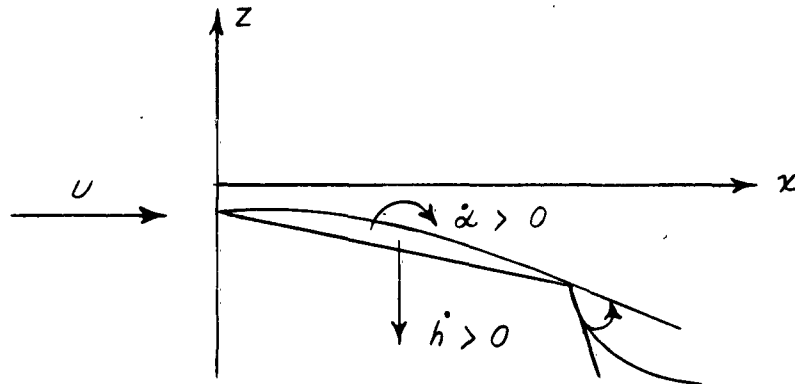$$C_J \equiv \frac{\rho_J V_J^2 \delta_J}{\frac{1}{2} \rho U^2 (2b)}$$

where $\rho_J V_J^2 \delta_J$ is the momentum flux of the jet per unit span and $\frac{1}{2} \rho U^2$

is the free stream dynamic pressure.

Consider the airfoil to be plunging at a rate $\dot{h}$, and pitching about midchord

A. CONSTANT JET ANGLE (continued)

at a rate $\dot{\alpha}$, as sketched below

The plunging motion gives rise to a constant downwash across the airfoil which is equivalent under the quasi-steady assumption to an increase in angle of attack. The resulting total angle of attack is, thus, given by

$$\hat{\alpha} = \alpha + \frac{\dot{h}}{U}$$

Similarly, the pitching motion produces a linearly varying downwash distribution over the airfoil, which is equivalent to a parabolic camber of the airfoil. It is easily shown that the effective camber is given by

$$\hat{t} = t + \frac{b^2}{2U}\dot{\alpha}$$

The quasi-static approximations for the lift and moment coefficients are, therefore, given by the following expressions:

(II. 3) $$\hat{C}_L = \frac{\partial C_L}{\partial \tau}\tau + \frac{\partial C_L}{\partial \alpha}\left(\alpha + \frac{\dot{h}}{U}\right) + \frac{\partial C_L}{\partial(t/2b)}\left(\frac{t}{2b} + \frac{b}{4U}\dot{\alpha}\right)$$

A. CONSTANT JET ANGLE (continued)

$$(\text{II.4}) \quad \hat{C}_M = \frac{\partial C_M}{\partial \tau}\, \tau + \frac{\partial C_M}{\partial \alpha}\left(\alpha + \frac{\dot{h}}{U}\right) + \frac{\partial C_M}{\partial (t/2b)}\left(\frac{t}{2b} + \frac{b}{4U}\,\dot{\alpha}\right)$$

the above expressions were utilized in the flutter analysis by obtaining α, $\dot{\alpha}$ and $\dot{h}$ in terms of the generalized coordinates chosen for the analysis and substituting these relationships into Equations (I.3) and (I.4). Total lift and moment were then computed and applied to the calculation of generalized forces, as discussed in Appendix I.

For the forward flight case only, the aerodynamic reference station was chosen to be the elastic axis. This resulted in a slight modification to Equations (II.3) and (II.4) since the pitching rate is referenced to the elastic axis position. It can be shown that this shift changes only the quasi-steady total angle of attack from that given above to

$$\hat{\alpha} = \alpha + \frac{\dot{h}}{U} - Q\frac{\dot{\alpha}}{U}$$

B. OSCILLATING JET ANGLE

In Reference 15 Spence analyzes the case of unsteady motion of the jet angle with respect to the airfoil chord line. He finds that if the reduced frequency is of order one or less and that $\frac{1}{4}\, C_t$ is much less than unity, the lift coefficient resulting from the jet is, in the first approximation, modified by a factor $\left(1 + i\frac{b}{R}\nu\right)$ where ν is the frequency of oscillation divided by the rotational speed. This factor was applied to the lift and moment derivatives with respect to τ when deriving the coefficients involving jet deflection.

The application of this factor to the moment coefficient is not strictly correct. It was learned through communication with Mr. J. Erickson that this factor applied to the moment coefficient should be $\left(1 + i\frac{5}{4}\frac{b}{R}\nu\right)$.

It was felt, however, that the error introduced by applying the same factor to both lift and moment coefficients could be tolerated to simplify computations.

DISTRIBUTION

U. S. Army Aviation Test Board	1
Aviation Test Office, Edwards AFB, Calif.	1
The Research Analysis Corporation	1
Army Research Office, Durham, N. C.	2
U. S. Army Aviation and Surface Materiel Command	1
U. S. Army Transportation Research Command	71
U. S. Army Tri-Service Project Officer	1
Air University Library	1
Air Force Systems Command	2
Office of Naval Research	3
Bureau of Supplies and Accounts, Navy Dept.	1
U. S. Naval Postgraduate School	1
David Taylor Model Basin	1
National Aviation Facilities Experimental Center	3
Langley Research Center, NASA	2
George C. Marshall Space Flight Center, NASA	1
Manned Spacecraft Center, NASA	1
Ames Research Center, NASA	2
Lewis Research Center, NASA	1
Scientific and Technical Information Facility	1
U. S. Government Printing Office	1
Armed Services Technical Information Agency	10
U. S. Army Materiel Command	1
U. S. Army Mobility Command	1

AD

Cornell Aeronautical Laboratory, Inc., Buffalo, N.Y. THEORETICAL INVESTIGATION OF THE FLUTTER CHARACTERISTICS OF A JET-FLAP HELICOPTER ROTOR IN HOVERING AND FORWARD FLIGHT - Andrew R. Trenka and Richard P. White, Jr., TRECOM Technical Rept. 63-9, CAL Rept. BB-1493-S-2, April 1963, 90 p., incl., illus., 27 refs. (Contract DA 44-177-TC-699) USATRECOM Task 9R38-13-014-03.

Unclassified Report

A theoretical study of the aeroelastic characteristics of a jet-flap rotor system in hovering and forward flight was made. The effects of bending-to-torsion frequency ratio, center-of-gravity location, elastic-axis position, and advance ratio on the aeroelastic stability of the system were obtained. Also investigated were the effects of control flap frequency and damping and jet blowing coefficient.

UNCLASSIFIED

1. Helicopter Rotors
2. Jet-Flap Rotors

I   U.S. Army Transportation Research Command, Ft. Eustis, Va.
II Cornell Aeronautical Laboratory, Inc., Buffalo, N.Y.
III Contract DA 44-177-TC-699
IV Trenka, Andrew R.
V   White, Richard P., Jr.

AD

Cornell Aeronautical Laboratory, Inc., Buffalo, N.Y. THEORETICAL INVESTIGATION OF THE FLUTTER CHARACTERISTICS OF A JET-FLAP HELICOPTER ROTOR IN HOVERING AND FORWARD FLIGHT - Andrew R. Trenka and Richard P. White, Jr., TRECOM Technical Rept. 63-9, CAL Rept. BB-1493-S-2, April 1963, 90 p., incl., illus., 27 refs. (Contract DA 44-177-TC-699) USATRECOM Task 9R38-13-014-03.

Unclassified Report

A theoretical study of the aeroelastic characteristics of a jet-flap rotor system in hovering and forward flight was made. The effects of bending-to-torsion frequency ratio, center-of-gravity location, elastic-axis position, and advance ratio on the aeroelastic stability of the system were obtained. Also investigated were the effects of control flap frequency and damping and jet blowing coefficient.

UNCLASSIFIED

1. Helicopter Rotors
2. Jet-Flap Rotors

I   U.S. Army Transportation Research Command, Ft. Eustis, Va.
II Cornell Aeronautical Laboratory, Inc., Buffalo, N.Y.
III Contract DA 44-177-TC-699
IV Trenka, Andrew R.
V   White, Richard P., Jr.

AD

Cornell Aeronautical Laboratory, Inc., Buffalo, N.Y. THEORETICAL INVESTIGATION OF THE FLUTTER CHARACTERISTICS OF A JET-FLAP HELICOPTER ROTOR IN HOVERING AND FORWARD FLIGHT - Andrew R. Trenka and Richard P. White, Jr., TRECOM Technical Rept. 63-9, CAL Rept. BB-1493-S-2, April 1963, 90 p., incl., illus., 27 refs. (Contract DA 44-177-TC-699) USATRECOM Task 9R38-13-014-03.

Unclassified Report

A theoretical study of the aeroelastic characteristics of a jet-flap rotor system in hovering and forward flight was made. The effects of bending-to-torsion frequency ratio, center-of-gravity location, elastic-axis position, and advance ratio on the aeroelastic stability of the system were obtained. Also investigated were the effects of control flap frequency and damping and jet blowing coefficient.

UNCLASSIFIED

1. Helicopter Rotors
2. Jet-Flap Rotors

I   U.S. Army Transportation Research Command, Ft. Eustis, Va.
II Cornell Aeronautical Laboratory, Inc., Buffalo, N.Y.
III Contract DA 44-177-TC-699
IV Trenka, Andrew R.
V   White, Richard P., Jr.

AD

Cornell Aeronautical Laboratory, Inc., Buffalo, N.Y. THEORETICAL INVESTIGATION OF THE FLUTTER CHARACTERISTICS OF A JET-FLAP HELICOPTER ROTOR IN HOVERING AND FORWARD FLIGHT - Andrew R. Trenka and Richard P. White, Jr., TRECOM Technical Rept. 63-9, CAL Rept. BB-1493-S-2, April 1963, 90 p., incl., illus., 27 refs. (Contract DA 44-177-TC-699) USATRECOM Task 9R38-13-014-03.

Unclassified Report

A theoretical study of the aeroelastic characteristics of a jet-flap rotor system in hovering and forward flight was made. The effects of bending-to-torsion frequency ratio, center-of-gravity location, elastic-axis position, and advance ratio on the aeroelastic stability of the system were obtained. Also investigated were the effects of control flap frequency and damping and jet blowing coefficient.

UNCLASSIFIED

1. Helicopter Rotors
2. Jet-Flap Rotors

I   U.S. Army Transportation Research Command, Ft. Eustis, Va.
II Cornell Aeronautical Laboratory, Inc., Buffalo, N.Y.
III Contract DA 44-177-TC-699
IV Trenka, Andrew R.
V   White, Richard P., Jr.